Urban Transportation Network Design Problem with Sustainability Considerations

By

Narges Shahraki

Urban Transportation Network Design Problem with Sustainability Considerations

By

Narges Shahraki

Submitted to the Graduate School of Sciences and Engineering in partial fulfillment of the requirements for the degree of

Doctor of Philosophy

In

Industrial Engineering and Operations Management

Koç University

August 2015

Koç University

Graduate School of Sciences and Engineering

This is to certify that I have examined this copy of a doctoral dissertation by

Narges Shahraki

and have found that it is complete and satisfactory in all respects,

and that any and all revisions required by the final

examining committee have been made.

Committee Members:

Prof. Metin Türkay (Advisor)

Assoc. Prof. Emre Alper Yildirim

Assoc. Prof. Alper T. Erdogan

Prof. Kuban Altınel

Assist. Prof. Murat Kaya

Date:

Acknowledgements

My deepest gratitude goes to my supervisor Professor Metin Türkay for his endless support and enormous encouragement. Thank you for allowing me to explore my curiosity while at the same time providing me timely nudges. This project would not have been possible without your support. Thanks for everything!

I am extremely grateful to my Ph.D. committee members, Professor Emre Alper Yıldırım and Professor Alper Erdoğan for all their scientific guidance, invaluable support and excellent feedback.

I would like to thank Professor Murat Kaya and Professor Kuban Altınel for participating in my thesis committee.

Special thanks to Professor Ming Xu for his invaluable guidance and advice during my time at the University of Michigan (UM). Additionally, thanks to Hua Cai at UM for her collaboration and exchange of ideas. I would like to express my gratitude to the Department of Energy at UM for supporting the material of the project partially under Award Number DE-PI0000012.

I would like to express my gratitude to the European Commission LOG4GREEN Project Grant #287091 under FP7 program for financially supporting my Ph.D. dissertation. I also gratefully acknowledge the support of Koç University.

I acknowledge the logistical and administrative support of Metropolitan Planning & Urban Design Center of Istanbul Metropolitan Municipality, BIMTAS. Mr. Metin Cancı and Mr. Serdar Bayburt were incredibly helping in providing me with data about Istanbul's transportation network. And special thanks to Dr. Ulas Akın for his collaboration and exchange of ideas.

I thank my friend Meng Xu, a PhD candidate at Hong Kong University of Science and Technology, for helping me with the ArcGIS analyses. And special thanks to my friend Ozturk Saracoglu for translating the abstract into Turkish.

With a deep sense of gratitude, I would like to thank my oldest sister, Mina, and my husband, Behrooz for encouraging me to do my Ph.D. abroad. Without their attempts I would not be here. Thanks for changing my life.

Special thanks to my lovely flatmates and my friends for their enormous support throughout this journey. And special thanks to my American friend Lauren Davis for helping me to edit some parts of my dissertation.

I thank my husband, my brother, and my sisters for supporting me in ways too valuable and numerous to list. More than anything, I would like to thank my father and mother for their endless love. They gave me courage to follow my interests and passions, to move to Turkey, to finish this project, and to build a life. To them I dedicate this dissertation.

Urban Transportation Network Design Problem with Sustainability Considerations

Narges Shahraki

Industrial Engineering and Operations Management, Ph.D. 's Thesis, 2015

Thesis Supervisor: Prof. Dr. Metin Türkay

Keywords: Sustainability, Optimization, Transportation, Urban region

ABSTRACT

Traffic congestion and environmental issues associated with transportation are considered to be serious problems faced by modern cities because of their negative effects on productivity, health and living conditions. Half a million people in developing countries die each year from transport-related air emissions, with a similar death toll from traffic accidents. Therefore, designing sustainable land use transportation systems is considered one of the most pressing issues faced by modern cities.

In this dissertation, I develop optimization models and solution algorithms to design sustainable land use and transportation systems for urban regions to improve sustainability.

In this study, two novel stochastic bi-objective land use and transportation optimization models are formulated to design a sustainable transportation network to minimize carbon monoxide emissions, traffic congestion, and travel costs: covering environmental, social, and economic aspects of sustainability. The goal is identifying the residential areas and roads in a city that should be expanded. Travel demand is considered as a random variable which affects the probability of traffic congestion and the travel cost. I formulate a closed form expression to calculate the Cholesky factorization matrix that is implemented as a set of constraints in the optimization model, to estimate the probability of traffic congestion by multivariate normal distribution. ϵ-constraint method is implemented to solve the multi-objective optimization problems. In addition, some useful insights on the relationship among land use, transportation network and environmental impact associated with them are found.

The presented models are developed by considering a multi-modal assumption. The problem is formulated as a bi-level optimization problem. In the lower level, the transportation design problem is formulated to minimize traveler transportation costs and in the upper level I consider minimizing carbon monoxide emission and minimizing the probability of traffic congestion as the objective functions. I formulate the closed form optimality expressions of the lower level problem using Karush–Kuhn–Tucker (KKT) conditions. These optimality conditions are incorporated in the upper level problem as a set of constraints, and a single level model is obtained. The formulated single stage model is a Mixed Integer Non-linear Programming (MINLP) problem with two objective functions. An exact solution algorithm based on outer approximation and ϵ-constraint method is implemented to solve the bi-objective MINLP problem.

The developed models are applied for Istanbul, Turkey to minimize emissions and overloading flows. The amount of emissions is calculated as a function of the real average speed in each road based on traffic congestion. In this study, the travel production and attraction of 38 districts and detail information of 17,663 Istanbul main roads such as numbers of lanes, length and maximum speed limit in each main road are implemented as the input to the optimization model. The large data set is successfully handled and the formulated models are solved optimally. The optimal results show the selected roads for capacity expansion and installing additional shared public vehicles. The result shows specific roads have significant effect on emission production and traffic congestion in Istanbul metropolitan area. Furthermore, I analyze the reason of traffic congestion and pollution in these roads. In addition, in this study I analyze the effect of different fuel types on different emission production. This work presents the first optimization framework at micro scale level to analyze traffic emission problem in the Istanbul metropolitan area.

In addition, in this dissertation I explore the problem of selecting the optimal locations of electric vehicle charging stations in urban regions. I propose an optimization model based on vehicle travel patterns to capture public charging demand and select the locations of public charging stations to maximize the amount of vehicle miles traveled (VMT) being electrified. The formulated model is applied to Beijing, China as a case study using vehicle trajectory data of 11,880 taxis over a period of three weeks. The mathematical problem is formulated in GAMS modeling environment and Cplex optimizer is used to find the optimal solutions. Formulating the mathematical model properly, inputting data transformation, and adjusting the Cplex options are considered for accommodating large-scale data. I show that, compared to the 40 existing public charging stations, the 40 optimal ones selected by the model can increase electrified fleet VMT by 59% and 88% for slow and fast charging, respectively.

ÖZETÇE

Trafik sıkışıklığı ve şehir içi ulaşımdan kaynaklanan çevresel etkenler verimlilik, sağlık ve yaşam standardları üzerinde yarattıkları olumsuz etkiden dolayı günümüzde şehirlerde en önemli sorunlardan biri olarak kabul ediliyor. Gelişmekte olan ülkelerde senede yaklaşık olarak yarım milyon insan ulaşımdan kaynaklanan gaz salımını sebebiyle hayatlarını kaybetmekte, aynı zamanda trafik kazalarından da bir o kadar insan hayatını kaybetmektedir. Bu sebeplerden dolayı sürdürebilir bir ulaşım sistemi yaratılması günümüz şehirlerinde en önemli sorunlardan biri haline gelmiştir.

Tezimde, şehirlerde daha sürdürebilir bir arazi kullanımı ve ulaşım sistemi için optimizasyon modeli ve çözüm algoritması geliştirmiş bulunmaktayım.

Bu çalışmada, iki adet özgün stokastik iki amaçlı arazi kullanımı ve ulaşım optimizasyon modellemesi sürdürebilir bir ulaşım ağı yaratmak için sosyal, çevresel ve ekonomik etkenleri kapsayarak karbon monoksit salımını, trafik sıkışıklığı ve ulaşım masrafını minimuma indirmek amacıyla formule edilmiştir. Bu modellemede amaç, şehirde genişleyecek olan yerleşim alanlarını ve yolları belirlemektir. Şehirdeki ulaşım talebi trafik sıkışıklığı ve ulaşım masrafını belirleyen rastlantısal değişken olarak ele alınmaktadır. Trafik sıkışıklığının olasılığını çok değişkenli normal dağılım olarak hesaplamak için, kapalı formda bir ifade olarak Cholesky çarpanlara ayırma matrisi optimizasyon modeline kısıt olarak eklenerek formule edilmiştir. ϵ- kısıt metodu çok amaçlı optimizasyon probleminin çözülmesi için modele eklenmiştir. Bunlara ek olarak; arazi kullanımı, ulaşım ağı ve çevresel etkenler arasındaki ilişkiyi gösteren bazı yararlı kavramlar bulunmuştur.

Önerilen modeller çok türlü varsayımlar düşünülerek geliştirilmiştir. Problem iki katmanlı optimizasyon modeli olarak formule edilmiştir. Alt katmanda, ulaşım modellemesi ulaşım masrafını minimuma inderme amacıyla modellenmiş ve üst katmanda karbon monoksit salımını ve trafik sıkışıklığını minimuma indirme amacıyla model geliştirilmiştir. Alt katmanda kapalı yapıda en iyileme ifadeleri Karush-Kuhn-Tucker (KKT) koşulları kullanılarak formule edilmiştir. Bu en iyileme koşulları üst katman probleminde kısıtlama olarak birleştirilerek tek katmanlı modelleme elde edilmiştir. Tek katmanlı bu model, iki amaçlı doğrusal olmayan karışık tam sayı programlama problemi (MINLP) olarak formule edilmiştir. Dışsal yakınsama ve ϵ-kısıt metodu temel alınarak oluşturulan kesin çözüm algoritması iki amaçlı MINLP problemini çözmek için uygulanmıştır.

Geliştirilen modeller İstanbul, Türkiye için gaz salınımını ve aşırı akışı minimuma indirmek amacıyla uygulanmıştır. Gaz salınım miktarları her yoldaki trafik sıkışıklığının etkisinin gerçek ortalama hız değerleri üzerindeki etkisi dikkate alınarak fonksiyon olarak hesaplanmıştır. Bu çalışmada, 38 ayrı bölgenin ulaşım yapımı ve cazibesi ve 17663 ana yol her yoldaki şerit sayısı, uzunluk ve maksimum hız limiti şeklinde veriler modelleme için veri olarak kullanılmıştır. Tüm bu veriler başarılı bir şekilde işlenmiş ve modeller en iyilemeye uygun bir şekilde çözülmüştür. Optimizasyon modelinin sonuçları kapasite artırımına uygun seçilen yolları ve

eklenmesi gereken toplu taşıma taşıtlarını göstermektedir. Sonuçlar belli yolların gaz salınımı ve trafik sıkışıklığı üzerinde İstanbul için önemli etkisi olduğunu göstermektedir. Bunlara ek olarak bu yollardaki trafik sıkışıklığının ve kirliliğinin sebepleri analiz edilmiştir. Ayrıca, değişik akaryakıt tiplerinin gaz salınımı üzerindeki etkisi analiz edilmiştir. Bu çalışma İstanbul için mikro ölçekli ve trafikten doğan gaz salınımını analiz eden ilk optimizasyon modeli durumundadır.

Ayrıca, bu tezde elektrikli araçlar için şarj istasyonlarının nereye konulması gerektiği ortaya çıkarılmıştır. Elektrikli araçların kattettiği mesafeyi (VMT) maksimuma çıkarmak ve elektrikli araç şarj talebini karşılamak için ulaşım modelleri dikkate alınarak optimizasyon modeli önerilmiştir. Formule edilmiş olan bu model Beijing, Çin için üç haftalık 11880 taksinin araç yörüngesi üzerine uygulanmıştır. Matematiksel modelleme GAMS ve Cplex programları kullanırak en iyi sonucu bulmak için formule edilmiştir. Matematiksel modellemeye uygun şekilde yapılması, veri dönüşümünün girilmesi ve Cplex ayarları büyük ölçekli veri dikkate alınarak yapılmıştır. 40 adet halka açık şarj istasyonunun yeri, model tarafından ortaya çıkan yeni en iyi yerleri ile değiştirildiği zaman yavaş ve hızlı şarj seçeneklerine göre elektrikli araçların kattettiği mesafe sırasıyla %59 ve %88 olarak artmıştır.

TABLE OF CONTENTS

LIST OF FIGURES

LIST OF TABLES

1 Chapter I

General Introduction

Introduction

The concept of sustainability and sustainable development crystallized in 1987 with the publishing of the United Nations report entitled "Our Common Future – Report of the World Commission on Environment and Development" also known as "The Brundtland Report." The Commission defined sustainable development as "development that meets the needs of the present without compromising the ability of future generations to meet their own needs." The Commission also established that sustainability is a concept that rests on three pillars, or the three-legged stool, namely ecology, economy, and social. Sustainable solutions should be economically viable, socially equitable and ethically responsible, and consistent with the long-term ecological balance of the natural environment, as shown in Figure 1.

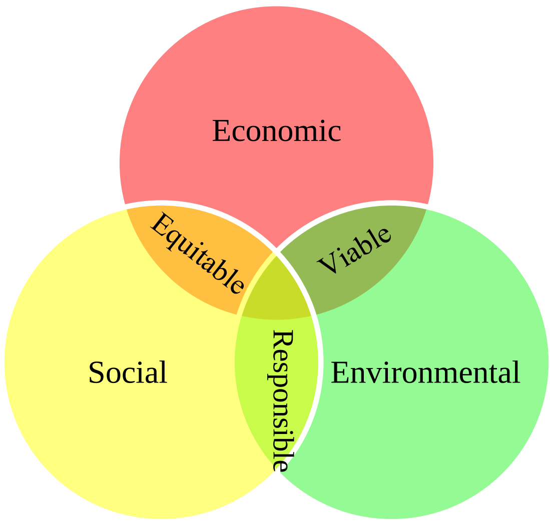

Figure 1. Three pillars of sustainability

According to the American Association of State Highway and Transportation Officials (AASHTO) report: "The overall goals of sustainable development are to meet human needs and improve quality of life; to live within the earth's ecological carrying capacity and maintain or enhance its natural capital; and to protect future generations from reduced quality of life. These goals are achieved by addressing three dimensions of sustainability:

- Economic development: Ensure that the financial and economic needs of current and future generations are met.
- Environmental stewardship: Ensure a clean environment for current and future generations and use resources sparingly.
- Social equity: Improve the quality of life for all people and promote equity between societies, groups, and generations." (AASHTO, 2015)

"Transportation plays a key role in the global economy and in the challenges and opportunities associated with sustainable development. Sustainable transportation can be viewed as *an expression of sustainable development in the transportation sector*. Sustainable transportation addresses local, regional, national, and global issues and therefore requires considerable coordination. It is important to apply sustainable transportation in a holistic and integrated manner across the various sectors (external to transportation) to ensure that key concerns such as depletion of resources, global climate change, disruption of ecosystems, and toxic pollution are effectively addressed." (AASHTO, 2015)

"Numerous authors have developed definitions for sustainable transportation for different contexts. These definitions are based on the broader concept of sustainable development as outlined by the Brundlandt Commission, adapted to meet current and future mobility and accessibility needs without resulting in undue negative externalities. Context specific sustainable transportation definitions generally focus on the three dimensions of sustainable development – *economic development, social equity, and environmental stewardship.*" (AASHTO, 2015)

Transportation planning and the planning field in general have strived to steer development in more sustainable directions in the past few decades. Traffic congestion and environmental issues associated with transportation have been found as serious problems faced by modern cities because of their negative effects on productivity, health and living conditions. The World Bank, (2002) estimates that 0.5 million people in developing countries die each year from transport-related air emissions, with a similar death toll from traffic accidents. In the US, Transportation represents 10 percent of the world's gross domestic product, is responsible for 22 percent of global energy consumption and 25 percent of fossil fuel burning across the world, and produces 30 percent of global air pollution and greenhouse gases (U.S. Dept. of Energy, 2012). In addition, research has indicated that on average, road transportation produces 95% of the carbon monoxide (CO) and 35% of the nitrogen oxides in urban environments (EPA, 2010, FHWA, 2006). These pollutants can have potentially serious effects on both the ecosystem and the human health (Ng and Lo, 2013). As such, the transportation sector will play a key role in addressing global sustainability concerns, including depletion of resources, global climate change, disruption of ecosystems, and toxic pollution.

The pressures to develop sustainable transportation systems are particularly acute in urban areas. The urban population in the developing world is close to 50% and in the developed world is 75% and growing rapidly (Hall, 1998). By rapidly increasing population and growing cities around the world, more people compete for limited urban road infrastructure to travel and designing sustainable transportation systems is considered one of the most pressing issues faced by modern cities. There is debate about what types of urban form, defined by land use and transportation systems are more sustainable.

The integration of different functional zones in urban areas that include housing, commerce, retail, and industrial and service sector needs is an important consideration in land use. An efficient integration of these functionalities requires links among them such as transportation infrastructure elements (i.e., roads, stations, mode change hubs, etc.) and proper land allocation; therefore, an effective solution to this problem is very important to reduce air pollutants in the cities. It is important to know how to redistribute limited city space to multiple transportation modes and infrastructures to understand what level of sustainable mobility can be achieved with different structures.

Land use and transportation systems are closely intertwined, and models used to support transportation planning need to be integrated with land use models as has been discussed numerous times in the literature (Dowling, 2005; Environmental Protection Agency, 2000; Garrett and Wachs, 1996; Miller et al., 1998; Newman and Kenworthy, 1989; Paulley and Webster, 1991; Southworth, 1995; Waddell et al., 2007; Wegener, 2004).

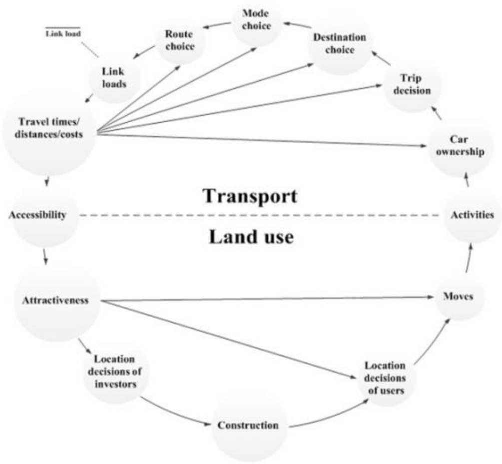

Figure 2. The land-use transport feedback cycle (adopted from Wegener, 1995).

Figure 2 (adopted from (Wegener, 1995)) shows the circular interrelationship between transportation and land-use. In this cycle, land-use and transportation are interdependent through accessibility and activities. Figure 2 provides a comprehensive understanding of the behavior of actors in the urban system while also taking into account the natural processes that take place within this system (Kanaroglou and Scott, 2002).

Newman and Kenworthy (1989) argued that, in modern societies, a city with extremely low land use intensity and degree of concentration has very low traffic restraints and intensive automobile orientation; and further, an extremely poor transit system, very high gasoline use and consequently too much air pollution. In constraint, a city that is organized with very high density and very strong degree of concentration must relate to strong traffic restraints and intensive non-auto modes-public transit, cycling, or walking and less air pollution.

A large number of models have been developed to address the integration of the network design and land use problems such as (Lowty, 1964), DELTA/START

(Simmonds and Still, 1999), IMREL (Anderstig and Mattsson, 1998), IRPUD (Wegener, 1998), ITLUP (BATTY, 1985; Timmermans, 2003), LILT (Mackett, 1983), MEPLAN (Echenique et al., 1969), METROSIM (Anas, 2013), MUSSA (Martinez, 1996, 1992), and TRANUS (Barra et al., 1984). In spite of the fact that there are lots of land use and transportation models in literature, but little attention has been paid to the optimization of land use and transportation (Yim et al., 2011). However these studies focus solely on the economic dimension of sustainability. Decision making for sustainable land use and transportation where alternatives are assessed is still in the early stages of development.

Quantifying the pollutant emissions contributed by the transportation sector is the initial step in developing effective policies for improving environmental sustainability in urban areas. There are two approaches for calculating emissions, micro scale and macro scale (Ryu et al., 2013). Majority of studies implement macro scale models for estimating emissions (Aggarwal and Jain, 2014; Cheng et al., 2015; Hao et al., 2014; D. He et al., 2013; J. Javid et al., 2014; Melo and Ramli, 2014; Sookun et al., 2014; Tongwane et al., 2015). These studies use the bottom-up models to calculate emissions based on energy and fuel consumption. ASIF (Activity Structure Energy Intensity Fuel Mix) (Khanna et al., 2011) and LEAP (Long-range Energy Alternatives Planning System) are two macro scale bottom-up models widely used in emission analysis (Peng et al., 2015).

The macro scale bottom-up approaches have been widely used in emission analysis since the data requirement is generally available and simple. These approaches calculate emissions using energy and fuel consumption based on average speed limit and traveled distances for each vehicle type. However, vehicle speed is different based on traffic congestion on the different roads of a city. Therefore, macro scale approaches do not help decision makers to know about the amount of pollution in different parts of a city and its roads. Recognizing the most polluted roads and areas is very important in finding a solution to improve environmental sustainability in transportation systems.

In micro scale models, the amount of emissions is calculated using passenger travel behavior, vehicle data and road network information. This approach allows the decision maker to analyze the emissions in each road. It means this approach needs the detail information of the transportation network which is not only difficult to collect, but also makes the analysis more difficult.

The average emissions over a trip vary according to the average speed of the trip (Hickman et al., 1999). Additionally, they vary somewhat depending on the type of vehicle and the pollutant. Figure 3 visualizes the relation between the different speeds and their emission values for passenger cars. Generally, high emissions are produced at slow average speeds when the vehicle operation is inefficient - because of stops, starts and delays -, and at high speeds because of the high power demand on the engine. Minimum emissions are produced in the middle speed range (Hickman et al., 1999).

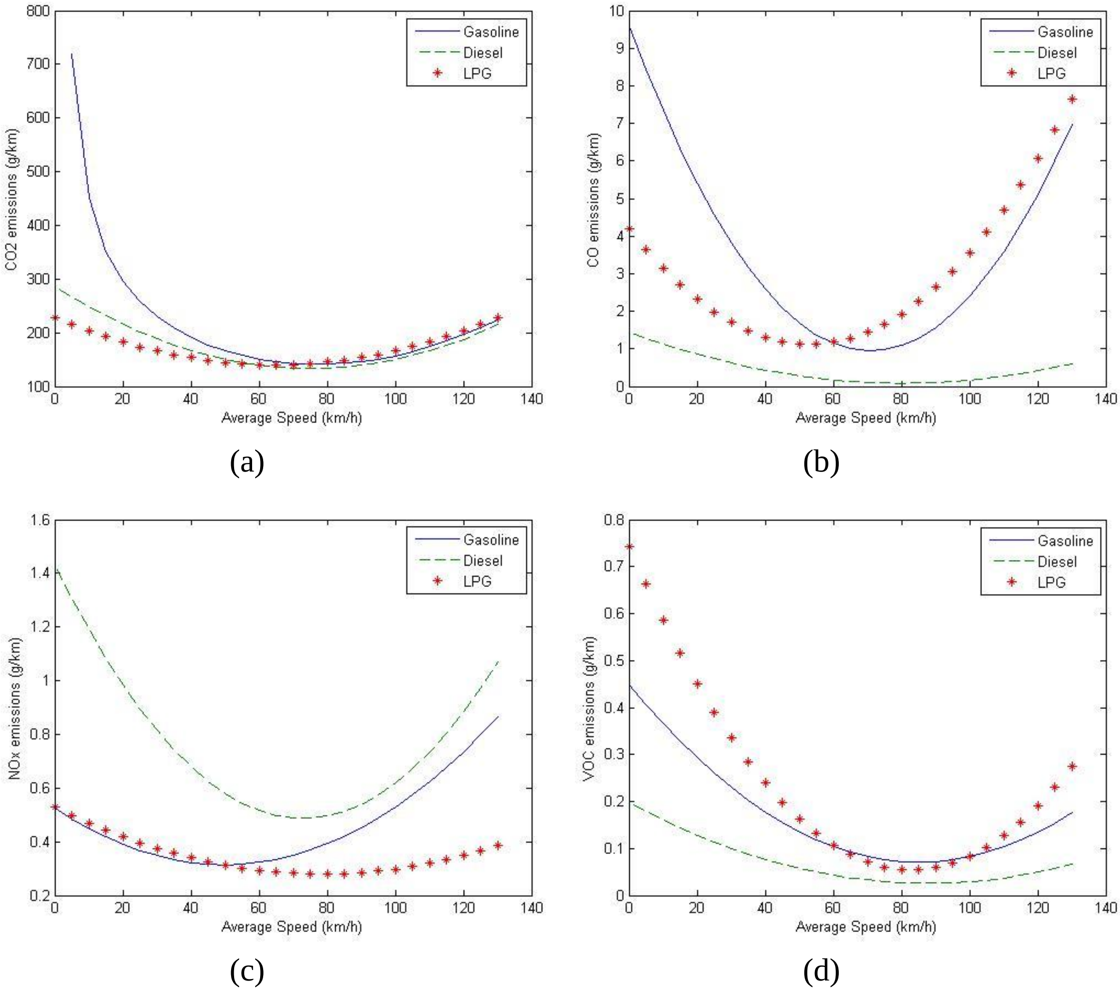

(a) (b) (c) (d)

Figure 3. Relation between average speed and, (a) CO_2 emission, (b) CO emission, (c) NO_X emission and (d) VOC emission

By increasing traffic congestion, fuel consumption and Carbon Dioxide (CO_2) emission increase. There are some studies at the micro scale level, which estimate emissions as a function of traffic volume in each road (Affum et al., 2003; Nejadkoorki et al., 2008; Ryu et al., 2013). Ryu et al., (2013) implement multiple linear regression analysis for developing the relationship between traffic volume in each road and number of vehicles, number of lanes, and time slots. Using this approach, traffic volume is estimated and the emissions are calculated in each road (Ryu et al., 2013). In addition, Affum et al., (2003) and Nejadkoorki et al., (2008) use simulation to estimate the traffic volume and then amount of emission in each road.

A number of optimization models are developed to minimize the environmental aspect represented as the amount of CO emission as a function of traffic volume (Ferguson et al., 2010; Huang, Ke, Jin Zhang, Meiling He, 2010; Li et al., 2012a; Yin and Lu, 1999; Zhou et al., 2008). Zhou et al. (2008), Yin and Lu (1999) and Huang et al. (2010) used total traffic emissions as an indicator. Some studies have developed a multi-objective formulation to incorporate environmental and economic factors (e.g., Yin and Lawphongpanich 2006a; Ferguson et al 2010; Sharma and Mathew 2011; Miandoabchi et al 2011b; Miandoabchi et al 2011c; Zhong et al 2012; Li et al 2012a; Liu et al 2014).

Few studies have developed optimization models to improve environmental sustainability for large scale problems (Sharma and Mathew, 2011). Sharma and Mathew, (2011) have formulated an optimization model based on minimizing CO and NO_X emissions and applied the model for the Indian city of Pune. There are few studies which analyze emissions in macro scale in Turkey (Demirel et al., 2008; Muneer et al., 2011; Soylu, 2007). Soylu, (2007) and Muneer et al., (2011) investigate the effect of different vehicle and fuel types on emission in Turkey. There are few studies to analysis the traffic emissions in Istanbul (IMM, 2014, 2011), but there are no optimization frameworks to analyze the transport emission problem in Istanbul.

Research focused on the network design problem is increasing in urban areas during the last five decades (Farahani et al., 2013). The earliest works modeled road network design problem purely based on the static approach, or their stochastic extensions are for depicting the route choice behavior of travelers or for determining the best system performance (e.g., Ban et al., 2006; Boyce and Janson, 1980; Chen et al., 2010a, 2010b, 2006; Chiou, 2009; Davis, 1994; Farvaresh and Sepehri, 2012; Friesz et al., 1993; Leblanc, 1975; Long et al., 2010; Marcotte, 1986; Meng et al., 2001; Miandoabchi et al., 2013; Qiu Yuzhuo and Chen Senfa, 2007; Szeto et al., 2013; Ukkusuri et al., 2007; Lin and Xie, 2010;Yang et al., 2010). This approach allows analyzing the problem easily but cannot capture the realistic variations in demand. The travel demand highly depends on the pattern of activities in urban areas. The timing and locations of these activities indicate that travel demand is not uniform through a day (Sheffi, 1985). It is also shown that travel demand shows strong variations in a day (Kitamura and Susilo, 2005). In addition a large number of static network design studies focus solely on the economic dimension of sustainability (e.g., Ban et al., 2006; Kim et al., 2007; Lo and Szeto, 2009).

Szeto et al (2010) developed a dynamic land use and transportation optimization model to show the interaction between land use and transportation, Szeto et al (2013b) extended this model to a sustainable model. In this model, environmental, economic and social dimensions of a sustainable system are considered as a multi objective formulation. But in this model travel demand is assumed to be constant.

Urban network design problems are complex since different groups are involved in the decision-making process, which is usually formulated as a bi-level formulation in literature. In addition, considering sustainability also makes the problem even more complex, since we deal with more than one objective function. In literature mostly meta-heuristic algorithms are applied to solve multi-objective bi-level formulation of urban network design problems (Miandoabchi et al., 2013, 2011; Szeto et al., 2013). Unfortunately there have been no studies which have developed exact solution algorithms for the multi objectives and bi-level formulation of urban network design problems with stochastic demand.

There are the following research gaps in the literature of sustainable land use and transportation design problems.

- Incorporating the three dimensions of sustainability to develop optimization models for urban land use and transport design problems
- Incorporating the random nature of the travel demand in mathematical formulations of urban network design problems
- Incorporating the three dimensions of sustainability to develop multi-modal network design problems
- Developing an exact solution algorithm for the multi-objective bi-level formulation of sustainable urban network design problems
- Implementing optimization models to minimize transport emissions for large scale problems, such as those in Istanbul city

In this dissertation, I address these shortcomings by incorporating the three aspects of sustainability and stochastic demand into our model formulation in **chapter 2**. I develop the model presented in **chapter 2** to multi-modal formulation and I develop an exact solution algorithm for bi-level formulation of multi-modal network design problem in **chapter 3** and in **chapter 4** I apply the multi-modal formulation for Istanbul. In addition in **chapter 5**, I focus on the optimal location of electric public charging stations.

Fossil fuel-based road transportation has instigated increasing global demand for oil and air pollution, especially in urban areas (Hoogma et al., 2005). Emerging vehicle technologies that can utilize alternative fuels are considered as potential solutions for these issues, such as electric vehicles (EVs). Although the life cycle environmental implications of EVs depends on the fuel mix of electricity generation (Torchio and Santarelli, 2010), using electricity instead of liquid fossil-based fuels for road transportation can relocate tailpipe emissions from mobile vehicular sources to stack emissions in power plants which are more concentrated and easier to control. Many countries have set goals for EV adoption. For example, the U.S. plans to adopt a total of one million plug-in hybrid electric vehicles (PHEVs); and China hopes to put 500,000 hybrid and electric vehicles on the road by 2015 (Murphy, 2014; U.S. Department of Energy, 2008).

Two research gaps exist in the literature on siting public charging stations. First, methods currently used in estimating charging demand may not reflect the real world situation. Unlike refueling liquid fuels which only takes a few minutes to fill the tank, fully recharging the battery on an EV can take a much longer time, from 30 minutes to several hours depending on the charger power, battery size, and the state of charge of the battery (Dong et al., 2014). Therefore, EV charging is more likely to happen at the end of a trip instead of in the middle of a trip. In addition, EV owners can charge their vehicles at home during the night. As a result, using traffic flow volume or vehicle ownership density to estimate charging demand as predominately used in previous studies may not be valid. Secondly, few studies considered environmental impacts of EV charging as the objective function for global optimal solution. The ultimate goal of EV system deployment is to fulfill more travel needs using electricity instead of fossil-based liquid fuels. I aim to address both gaps in chapter 4, by 1) using large-scale real world vehicle travel data to better model charging demand and 2) maximizing electrified fleet VMT as the objective function to find the global optimal solution.

The main contribution of this dissertation is formulating and developing stochastic and sustainable optimization models for land use and transportation networks in urban areas. Novel optimization models for four land use and transportation problems are developed in four manuscripts in chapter 2, 3, 4 and 5. In the following I explain briefly about each chapter.

In chapter 2, I present two bi-objective stochastic optimization models to analyze the interaction among land use, transportation network and air pollution. The goal is identifying the residential areas and roads in a city that should be expanded. I consider demand as a random variable that affects reliability index, utility function of different income groups and amount of CO emission. In the first model, reliability index and utility function are maximized and the value for CO emission is calculated. By maximizing the reliability function, the probability of traffic congestion is minimized. A closed form expression is formulated to calculate the Cholesky factorization matrix that is implemented as a set of constraints in the optimization model, to estimate the probability of traffic congestion by multivariate normal distribution. In the second model, the utility function is maximized and CO emission is minimized and the value for reliability index is calculated. By developing two separate models, I can find better insights about the relationships of the three objective functions. In addition I propose an effective solution algorithm and illustrate the efficiency of our approach on a large number of instances. In this study, for the first time in literature to our knowledge, an integrated stochastic land use and transportation model is formulated by considering two objective functions.

In chapter 3, I develop a multi-modal transportation model by considering on-road (private cars and buses) and rail vehicles (trams and metros). Travel demand is considered as a random variable which can follow any distribution where its mean and variance are function of origin and destination populations. The presented model incorporates sustainability since I consider minimizing transport emissions and minimizing probability of traffic congestion as the objective functions of upper level problem and minimizing travel cost as objective function of lower level problem. Minimizing transport emissions, minimizing the probability of traffic congestion and minimizing travel cost represent environmental, social and economic aspects of sustainability in our model, respectively.

Urban network design problems are complex since different groups are involved in decision-making process. Therefore, these problems are usually modeled as bi-level problems. There is no general format to develop an exact solution algorithm for these problems with stochastic demand. In this chapter, I present a novel solution algorithm to solve the model formulation exactly. In this research, the closed form expressions of optimality conditions of the lower level problem are formulated using Karush–Kuhn–Tucker (KKT) conditions. These optimality conditions can generate local optimal solutions of the lower stage problem. I incorporate these optimality conditions in the upper level problem as a set of constraints. The integrated model has two objective functions and it is a Mixed Integer Nonlinear Programming (MINLP) problem. I use outer approximation and ϵ-constraint algorithms to develop our algorithm to solve the bi-objective MINLP network problem.

In chapter 4, using micro scale approaches, the amount of emissions in each road of Istanbul transportation network is calculated. The amount of emissions is calculated as a function of the real average speed in each road based on traffic congestion. In this study, the travel production and attraction of 38 districts and detail information of 17,663 Istanbul main roads such as numbers of lanes, length and maximum speed limit in each main road are implemented as the input to the optimization model. I use the developed optimization model in chapter 2 to minimize the pollutant emissions especially CO_2 and overloaded flows. The large data set is successfully handled and the formulated models are solved optimally. The optimal results show the selected roads for capacity expansion and installing additional shared public transports.

In chapter 5, I propose an optimization model based on vehicle travel patterns to capture public charging demand and select the locations of public charging stations to maximize the amount of vehicle miles traveled (VMT) being electrified. Using Beijing, China as a case study, this chapter presents an optimization framework which utilizes large-scale real world vehicle trajectory data for selecting the location of public charging stations to maximize electrified fleet VMT. The demonstrated optimization framework can be applied to other fleets in other cities using similar data. Results from this study can help future decisions on developing public charging stations in Beijing. The proposed optimization model is implemented in GAMS with Cplex solver. In order to accommodate for the large-scale vehicle trajectory data in the model, I identify factors in model formulation, input data format, and settings of Cplex options that need to be adjusted to solve the model efficiently. In summary, major contributions of this study include 1) formulating an optimization model which selects the location of public charging stations to maximize electrified fleet VMT; 2) incorporating vehicle travel patterns by using large-scale individual-based vehicle trajectory data to model public charging demand; 3) studying public charging infrastructure planning in Beijing as a case study; and 4) providing suggestions in model formulation and execution to handle large-scale data.

<u>Contribution of the Dissertation</u>

Manuscript II (Chapter 2)

Narges Shahraki, Metin Türkay, "Analysis of Interaction among Land-Use, Transportation Network and Air Pollution using Stochastic Nonlinear Programming", International Journal of Environmental Science and Technology, 2014, 11(8), 2201-2216.

Brief Summary: Novel optimization models are developed to incorporate the three aspects of sustainability and stochastic demand into the model formulation. Travel demand is considered as a random variable in the formulation which effects on the probability of traffic congestion and the travel cost. I formulate a closed form expression to calculate the Cholesky factorization matrix that is implemented as a set of constraints in the optimization model, to estimate the probability of traffic congestion by multivariate normal distribution.

Manuscript III (Chapter 3)

Narges Shahraki, Metin Türkay, "Multi-Modal Transportation Network Design Problem with Stochastic Demand and Sustainability Considerations", (Submitted to Journal of Network and Spatial Economics).

Brief Summary: A novel stochastic bi-level multi-objective optimization model is developed to design a sustainable transportation network to minimize carbon monoxide emissions, traffic congestion, and travel costs: covering environmental, social, and economic aspects of sustainability. I design a novel solution algorithm to solve the bi-level multi-objective formulation. I formulate the closed form expressions of the lower level problem using Karush–Kuhn–Tucker (KKT) optimality conditions. These optimality conditions are incorporated in the upper level problem as a set of constraints, and a single level model is obtained. The formulated single level model is a Mixed Integer Non-linear Programming (MINLP) problem with two objective functions. I implement outer approximation (OA) and ϵ-constraint methods to establish a base for the custom solution algorithm.

Manuscript IV (Chapter 4)

Narges Shahraki, Metin Türkay, Ulas Akin, "Optimal Transportation Network Structure to Reduce Emissions, a Case Study in Istanbul Metropolitan Area", working paper.

Brief Summary: Optimization models are developed to minimize CO_2 emission produced by transports which has not studied indepth at micro scale in the literture. In this study we use the travel production and attraction of 38 districts and detail information of 17,663 Istanbul main roads such as numbers of lanes, length and maximum speed limit in each road. The result shows specific roads have significant effect on emission production and traffic congestion in Istanbul metropolitan area. This work presents the first optimization framework at micro scale level to analyze traffic emission problem in Istanbul metropolitan area.

Manuscript V (Chapter 5)
Narges Shahraki, Hua Cai, Metin Türkay, and Ming Xu, "Optimal Locations of Electric Public Charging Stations Using Real World Vehicle Travel Patterns", (Submitted to Journal of Transportation Research Part D: Transport and Environment).

Brief Summary: An optimization model is formulated to determine the optimal locations for public charging stations for electric vehicles in Beijing, China, in order to maximize the amount of electrified vehicle miles traveled (VMT) and minimize harmful emissions. Using a large-scale dataset of travel trajectories of taxicabs in Beijing, I characterize the taxi fleet's travel patterns. I develop a discrete optimization framework to identify the optimal number and location of public charging stations to meet our stated objectives.

2 Chapter II

Analysis of Interaction among Land-Use, Transportation Network and Air Pollution Using Stochastic Nonlinear Programming

In this chapter, we present two novel optimization models for land use and transportation to address the development of different functional zones in urban areas by considering the design of an efficient transportation network and reducing air pollution. Objective functions of the first model are maximizing utility function and maximizing reliability index. The utility is formulated as a function of travel cost and zonal attractiveness. Reliability index is defined as the probability that flow in each link of the network is less than the design capacity. Maximizing this probability is equal to minimizing congestion in the network. In addition, maximizing utility and minimizing carbon monoxide emission in the network are considered as objective functions in the second model. The formulated models are non-linear and stochastic. We implement the ϵ-constraint method solving multi-objective optimization problems. We evaluate our presented models through several examples. In addition, we evaluate the relation between central processing unit time and complexity of the model. In this study, for the first time in open literature stochastic bi-objective optimization models are formulated to analyze interaction among land use, transportation structure and amount of air pollution. We also extract and summarize some useful insights on the relationship among land use, transportation network and environmental impact associated with them.

2.1 Introduction

Integrated analysis of land use and transportation is attracting attention of academics and urban designers due to growing interest from public agencies that need to improve their capacity to respond to complex policy questions arising in the context of transportation, land use, and quantifying the environmental impact associated with them. The relationship between transportation and land use is highly complex; spatial interactions between land use and transportation are keys to explaining movements of passengers and freight. Land use is associated with demographic and economic attributes while the transportation system moves passengers and freight by certain modes on the transportation network (Rodrigue, 2004). In addition, interactions among economic, social and environmental impacts of the decisions related to land use and transportation necessitates the development of methodical approaches that would be instrumental in the decision-making process.

An important consideration in the land use and transportation design is the environmental impact assessment. On the average, road transportation contributes 95 % of the carbon monoxide (CO) and 35 % of the nitrogen oxides in urban environments (Federal Highway Administration (FHWA), 2006; US Environmental Protection Agency (EPA), 2010). Most of the air pollution in Tehran metropolitan, the most polluted city among urbanized cities in developing countries, is contributed by transports (Abbaspour and Soltaninejad, 2004). These air pollutants can have potentially serious consequences for both the ecosystem and the human health (Ng and Lo, 2013).

Land use and transportation systems are closely intertwined, and models used to support transportation planning need to be integrated with land use models as has been discussed numerous times in the literature (Dowling, 2005; Environmental Protection Agency, 2000; Garrett and Wachs, 1996; Miller et al., 1998; Newman and Kenworthy, 1989; Paulley and Webster, 1991; Southworth, 1995; Waddell et al., 2007; Wegener, 2004).

A large number of models have been developed to address the integration of the network design and land use problems such as (Lowty, 1964), DELTA/START (Simmonds and Still, 1999), IMREL (Anderstig and Mattsson, 1998), IRPUD (Wegener, 1998), ITLUP (BATTY, 1985; Timmermans, 2003), LILT (Mackett, 1983), MEPLAN (Echenique et al., 1969), METROSIM (Anas, 2013), MUSSA (Martinez, 1996, 1992), and TRANUS (Barra et al., 1984). In spite of the fact that there are lots of land use and transportation models in literature, but little attention has been paid to the optimization of land use and transportation (Yim et al., 2011).

Previously (Lin and Feng, 2003), (Hui and Kefei, 2009), (Ho and Wong, 2007) and (Yim et al., 2011) have presented bi-level models for formulating a land use and network design optimization problem. Lin and Feng (2003b) developed a subprogram as an upper-level to allocate different land uses, links and facilities to different areas of a city, and a lower-level subprogram to design the network. In Hui and Kefei (2009), the location of different communities of a city is considered as an upper-level problem, while the network design is handled at the lower level. Ho and Wong (2007) formulated a bi-level model. In the upper level of the model, a utility function is maximized for the allocation problem and transportation network is designed in the lower level of the problem. Moreover, every parameter is considered as deterministic in these studies. A stochastic land use and transportation optimization model as a bi-level programming problem was presented by Yim et al (2011). Optimal residential allocation, employment allocation, and capacity enhancements are determined by maximizing the reliability index of the network in the upper level. The lower-level subprogram is formulated to determine optimal route choices behavior by minimizing the total travel cost. A genetic algorithm is used as the solution method. Zonal attraction and travel time are also two important factors for residential allocation and employment allocation that are not considered in previous models.

Chang and Mackett (2006) presented a bi-level model to show the relationship between transport and residential location. In this model residents choose their location base on locational attractiveness. Bravo et al (2010) developed a model where households select their resident location base on locational attractiveness and travel cost. Ma and Lo (2012a) formulated a dynamic residents' location and travel choices dynamic model, with considering the housing supply problem. They developed a utility function base on locational attractiveness and travel cost as objective function of residents for selecting their location. In these studies, the travel demand has been considered as static. Meanwhile the travel demand is highly depends on the pattern of activities in urban area. The timing and locations of these activities indicate that travel demand is not uniform throughout the day (Sheffi, 1985). Besides, Kitamura and Susilo (2005) found that that travel demand is not stable over time by doing a statistical analysis.

A large number of static network design studies focus on the economic dimension of sustainability (e.g., Ban et al 2006; Kim et al 2008; Lo and Szeto 2009). Zhou et al (2008), Yin and Lu (1999) and Huang, Ke, Jin Zhang, Meiling He (2010) solely considered environmental sustainability and used total traffic emissions as an indicator. Some studies have developed a multi-objective formulation to incorporate environmental and economic factors (Ferguson et al., 2010; Li et al., 2012a; Miandoabchi and Farahani, 2012; Miandoabchi et al., 2012; Sharma and Mathew, 2011; Yang et al., 2010; Yin and Lawphongpanich, 2006a; Zhong et al., 2012). In these studies land use planning is not incorporated.

Szeto et al (2010a) developed a dynamic land use and transportation optimization model to show the interaction between land use and transportation. Szeto et al (2013b) extended this model to a sustainable model. In this model, environmental, economic and social dimensions of a sustainable system are considered as a multi objective formulation. But in this model demand in each period is constant.

In this chapter, we present two bi-objective stochastic optimization models to analyze the interaction among land use, transportation network and air pollution. We consider demand as a random variable that affects reliability index, utility function of different income groups and amount of CO emission. In the first model, reliability index and utility function are maximized and the value for CO emission is calculated. In the second model, the utility function is maximized and CO emission is minimized and the value for reliability index is calculated. By developing two separate models, we can analyze the relation among reliability index, utility value and CO emission two by two. In this manner, we can find better insights about their relations. In the first model we calculate CO emission value for a city structure with optimal value for utility and congestion. And we analyze the relation between CO emission amount and two objectives. In the second model, we analyze how network structure changes by considering minimizing CO emission as an objective function.

We consider minimization of the probability of congestion by maximizing the reliability in each link, which received little attention in the published literature. Congestion is minimized by changing the distribution of flow in the network and expanding the capacity of the links which are considered as decision variables. And by maximizing the utility function, we minimize travel time and maximize locational attractiveness of residents which are presented as cost in the utility function. Utility value, congestion and CO emission are given in the models respectively as economic, social, and environmental dimensions of a sustainable system.

Developing two models to allocate residential development and designing a transportation network base on four factors, minimizing congestion, maximizing locational attractiveness of residents, minimizing travel cost and minimizing CO emission, by considering stochastic travel demand are the main contribution of this chapter. In addition we propose an effective solution algorithm and illustrate the efficiency of our approach on a large number of instances. In this study, for the first time in literature to our knowledge, an integrated stochastic land use and transportation model is formulated by considering two objective functions. This work is carried out in Koç university, industrial engineering department in 2013 from January to November.

The decision maker in our model is the network planner. Network planner simulates the network and residential behaviors by developing optimization models. The decision maker can find answers for different questions such as, which income group prefers which zones, which zones should be expanded, which roads are more crowded, which roads are more polluted, which roads should be augmented and how much travel cost is in each link, by solving the optimization models.

2.2 Materials and Method

A brief description of the transportation system under investigation is presented in this section. We consider a transportation network $G(N, A)$, where N is the set of nodes and A is the set of links. Some nodes are considered to be origin nodes and some to be destination nodes; the remainders are called intermediate nodes. Origin and destination nodes can represent the same geographical location. P is the set of origin nodes, Q is the set of destination nodes and R is the set of routes between pair p-q.

The decisions by residents include both location (residential location and workplace) and corresponding travel choices. Normally, residents do not control the choice of workplace; this depends on the availability of specific employment types. In addition the decision maker in this process is an individual member. In constraint, residents have more authority in choosing their own housing locations, and residence choice is made jointly by a household that may have multiple members (Ma and Lo, 2012). In this study, the workplace choices by residents are not considered.

The choice of residential location is the result of a trade-off between attraction and travel time. A more plausible assumption would be that the residents try to accomplish two goals: travel to the destination with the highest attraction measure while spending the minimum time in transit (Sheffi, 1985). Ibeas et al (2013) found that home-work journey times are a statistically significant factor in household location choice, by implementing their model in a real case. In this research, we consider home-work journey flows in our model.

In this problem, we divide the residential development with workplace at q, into k different groups based on their income. They try to choose their residential locations in one of the origin nodes that maximize their utility. This utility is function of zonal attractiveness and travel time. In addition, we consider that the network planner also has resources to improve the network by augmenting the capacity of the existing links in the network. Network planner tries to maximize the reliability of the network by expanding the capacity of the links. We assume the decision maker in both problems is network planner and we develop a single model. The decision maker tries to simulate residential behavior to make decision for expanding capacity of zones and links of the network. In this problem we formulate an environmental objective to minimize transport CO emission. We consider CO emission because of three reasons, (1) almost all CO emissions in the air are produced by vehicles, (2) CO is the most important pollutant among the different types of vehicular emissions, which include nitrogen oxide, CO, nitrogen dioxide, sulfur dioxide, ozone, and particulates, and (3) the emission rates of other pollutants are similar to that of CO (Li et al., 2012c).

2.3 Mathematical Model for Land Use and Transportation

In this chapter, we assume that the demand from origin to destination nodes, d_{pq}, is a random variable that follows a certain probability distribution with mean and variance as follows:

$$E(d_{pq}) = \bar{d}_{pq} \tag{2-1}$$

$$var(d_{pq}) = \sigma_{pq}^2 \tag{2-2}$$

Considering demand as a random variable is more realistic than considering it as a constant value.

Also, we assume that the demands from origin to destination nodes are mutually independent. The flow in each link is defined as in Eq. (2-3).

$$x_a = \sum_{p\in P} \sum_{q\in Q} \sum_{r\in R_{pq}} d_{pq}\, \gamma_{pqr} \delta_{pqra} \tag{2-3}$$

In Eq. (2-3), γ_{pqr} is the vector of route choice proportions and δ_{pqra} is the link-path incidence matrix that is equal to 1 if the route r passes through link a otherwise it is equal to 0. x_a is a random variable that is function of transportation demand as shown in Eq. (2-3). The demand (d_{pq}) is function of residential development amount, so flow in each link (x_a) is indirectly a function of amount of developments. The average of flow in each link formulates as follows,

$$\bar{x}_a = \sum_{p\in P}\sum_{q\in Q}\sum_{r\in R_{pq}} \bar{d}_{pq}\,\gamma_{pqr}\delta_{pqra} \tag{2-4}$$

Considering d_{pq} as a random variable makes the problem non-linear since γ_{pqr} is also decision variable in our model. In Previous studies except in Yim et al (2011), a variable introduces instead of $d_{pq}\gamma_{pqr}$, since d_{pq} is not considered as a random variable. So, those models do not suffer from this non-linear term.

We consider reliability index as the first objective in our problem. The reliability index as shown in Eq. (2-5) is the probability that flow in each link be less the practical capacity (Ca_a) of the link plus the amount of capacity expansion (y_a) that is a decision variable in our problem.

$$\pi = P\{x_a \leq Ca_a + y_a\} \tag{2-5}$$

This probability can be obtained from the approximated multivariate normal distribution presented by Genz (1992). The algorithm is composed of five steps, in step two, the lower triangle of Cholesky factorization matrix must be calculated. The reader can refer to Genz (1992) for the details of this five-step algorithm.

The elements of the Cholesky matrix can be derived from the covariance of flow between links, and the covariance is function of mean demand and route choice proportion that are decision variables of the problem, as shown in Eq. (2-6).

$$cov(x_a, x_{\hat{a}}) = E\big((x_a - \bar{x}_a)(x_{\hat{a}} - \bar{x}_{\hat{a}})\big) = \sum_{p\in P}\sum_{q\in Q}\sum_{r\in R_{pq}}\sum_{\hat{r}\in R_{\hat{p}\hat{q}}} E\big(d_{pq} - \bar{d}_{pq}\big)^2 \gamma_{pqr}\gamma_{\hat{p}\hat{q}\hat{r}}\,\delta_{pqra}\,\delta_{\hat{p}\hat{q}\hat{r}\hat{a}} = \sum_{p\in P}\sum_{q\in Q}\sum_{r\in R_{pq}}\sum_{\hat{r}\in R_{\hat{p}\hat{q}}} \sigma_{pq}^2\gamma_{pqr}\gamma_{\hat{p}\hat{q}\hat{r}}\,\delta_{pqra}\,\delta_{\hat{p}\hat{q}\hat{r}\hat{a}} \tag{2-6}$$

We present a closed form expression for calculating lower triangle of the Cholesky factorization matrix as shown in Figure 4 and implement this expression in our model as a set of constraints. In Figure 4, c_{ij} are the elements of the Cholesky matrix and a_{ij} are the elements of the matrix of the covariance of flow between the links.

$$
\begin{array}{l}
\text{for } j = 1,...,N; \\
\quad \text{if } j = 1,\ c_{jj} = \sqrt{a_{jj}} \\
\quad \text{otherwise, } c_{jj} = \sqrt{a_{jj} - \sum_{n=1}^{j-1} c_{jn} c_{jn}} \\
\quad\quad \text{for } i = 1,...,j-1; \& j \geq 2; \\
\quad\quad\quad c_{ij} = 0 \\
\quad\quad \text{end} \\
\quad\quad\quad \text{for } i = j+1,...,N; \\
\quad\quad\quad\quad \text{if } j = 1,\ c_{ji} = \dfrac{1}{c_{jj}} a_{ji} \\
\quad\quad\quad\quad \text{otherwise, } c_{ji} = \dfrac{1}{c_{jj}} \left(a_{ji} - \sum_{n=1}^{j-1} c_{jn} c_{in} \right) \\
\quad\quad\quad \text{end} \\
\text{end}
\end{array}
$$

Figure 4. algorithm for calculating the lower triangle of Cholesky factorization matrix

The problem assumes that each residential location is associated with an attraction measure. Travelers are assumed to choose destinations that are attractive, on the one hand, and close by low travel cost value, on the other. In this model destinations are chosen so that the utility function that is the difference between travel cost value and attractiveness value is maximized. We consider the utility function as shown in Eq. (2-7) (Ma and Lo, 2012) as the second objective in our model. In this function, I^k is the income of group *k*, and $g(\varphi^{qk})$ is the expenses set aside to achieve the resident's desired level of utility φ_{qk} in aspects other than transport and location choices. In addition, μ^{pqk} is travel cost between zone *p* and *q* for income group *k* and l^{pk} is the attractiveness of zone *p* as valuated by income group *k*.

$$\varphi = I^k - g(\varphi^{qk}) - \mu^{pqk} + l^{pk} \tag{2-7}$$

where,

$$l^{pk} = l_0^{pk} - \theta_1^{pk} \left(\frac{h_p + H_p}{K_p} \right)^{\theta_2^{pk}} \tag{2-8}$$

$$\mu^{pqk} = \delta_{pqra} (vot^k \ t_a + \rho_a) \tag{2-9}$$

The utility function defined in Eq. (2-7) represents the value that a household of income group *k* with workplace at *q* is willing to pay for residential location *p*. The fourth term in this function l^{pk} shows the impact of population allocation on zonal attractiveness. As shown in Eq. (2-8) this term includes two types of zonal attractiveness. The l_0^{pk} is called intrinsic attractiveness which is an exogenous constant, and second term in Eq (8) is a measure of the effect of land use intensity or congestion on zonal attractiveness. H_p and h_p are total existing population in zone *p*, and total amount of residential development in zone *p*, respectively. K_p shows the holding capacity within zone *p*. In addition, θ_1^{pk} and θ_2^{pk} are constant coefficients.

Ma and Lo (2012b) stated that to better model the impact of zonal attractive measures, other aspects of a zone such as hedonic housing attributes, like lot size, building age, floor level, and living amenities can be considered. Also, environmental condition of a zone can be an important aspect to attract residents.

In Eq. (2-9), t_a is the travel time in each link that is multiplied by the value of time (vot^k) of residents in income group k, and this expression is added to toll charges (ρ_a) to show the travel cost in link a. We use the Bureau of Public Roads (BPR) link impedance function in Eq. (2-10) in order to formulate the total travel time function.

$$t_a = t_0^a\left(1+\beta\left(\frac{x_a}{Ca_a}\right)^{\alpha}\right) \tag{2-10}$$

In Eq. (2-10), t_a^0 is the free-flow travel time of link a, and β and α are the model parameters. The values for β and α are typically considered equal to 0.15 and 4.0 respectively. In this problem the practical capacity of a link is summation of initial capacity of the link plus amount of expansion which is decision variable in our problem. So, the long-run perceived travel time can be presented as follows:

$$E(t_a) = t_0^a\left(1+\frac{0.15}{(Ca_a+y_a)^4}E(x_a^4)\right) \tag{2-11}$$

We assume that x_a follows normal distribution with mean $\bar{x}_a$ and standard deviation σ_a. The fourth uncentered moment of the distribution can be expressed from the central limit theorem as follows.

$$E(x_a^4) = \bar{x}_a^4 + 6\sigma_a^2\bar{x}_a^2 + 3\sigma_a^4 \tag{2-12}$$

Therefore, we can rewrite the long-run perceived travel time as in Eq. (2-13).

$$\bar{C}_a(\bar{x}_a;\bar{d},\gamma,\delta) = t_a^0\left(1+\frac{0.15}{(Ca_a+y_a)^4}(\bar{x}_a^4 + 6\sigma_a^2\bar{x}_a^2 + 3\sigma_a^4)\right) \tag{2-13}$$

The variance of the link flow can be expressed as a function of the mean origin-destination demands, route choice proportions, and link-path incident matrix as shown in Eq. (2-14).

$$\begin{aligned}\sigma_a^2 &= \mathrm{var}(x_a) = E\left((x_a-\bar{x}_a)^2\right)\\ &= E\left(\left(\sum_{p\in P}\sum_{q\in Q}\sum_{r\in R_{pq}}(d_{pq}-\bar{d}_{pq})\gamma_{pqr}\delta_{pqra}\right)^2\right)\\ &= \sum_{p\in P}\sum_{q\in Q}\sum_{r\in R_{pq}}\sum_{\hat{r}\in R_{pq}}\sigma_{pq}^2\gamma_{pqr}\gamma_{pq\hat{r}}\delta_{pqra}\delta_{pq\hat{r}a}\end{aligned} \tag{2-14}$$

CO emission in each link is calculated by Eq. (2-15). The amount of CO emission is function of the length of each link (l_a), the travel time in each link (t_a) and the travel speed in each link (l_a/t_a). This formula has been discussed in detail in (Yin and Lawphongpanich, 2006a), (Szeto et al., 2012) and (Ng and Lo, 2013).

$$e_a = 0.2038 t_a \exp^{0.7962(l_a/t_a)} \tag{2-15}$$

2.3.1 Model I: Reliability Probability and Utility

The objective functions of model I are presented in Eqs (2-16) and (2-17) that are reliability probability and utility respectively. The model contains 16 different set of constraints (Eqs. (2-18)-(2-19)). Eq. (2-18) expresses the amount of residential developments of each income group that is allocated to origin nodes and Eq. (2-19) shows the total amount of residential development. In Eq. (2-20), the budget limit for allocating and enhancing the capacity of each link is given. Eq. (2-21) shows there is limitation in income of each group. So, the average price of a house in zone p plus average travel cost of group k to travel to zone p should be less than the income of group k. Eq. (2-22) shows the minimum and maximum capacity expansion limits on link a. Eq. (2-23) expresses that the summation of the vector of route choice proportions between origin–destination pair p–q should be equal to 1. To illustrate the amount of production/attraction in origin and destination zones, Eqs (2-24) and (2-25) are presented. The amount of household development of income group k at the workplace q is represented with z_q^k and E_q is total existing population in zone q. Eq. (2-26) expresses the capacity limit in each zone. Also, Eq. (2-27) shows the average flow in each link. Besides, amount of CO emission in the network is formulated in Eq. (2-28). The decision variables are h_p^k, $\bar{x}_a$, γ_{pq}, y_a and $\bar{d}_{pq}$ that are respectively, the amount of household of each income group that is allocated to origin zones, the average flow in each link, the vector of route choice proportions, the capacity expansion of each link and the average demand between origin and destination nodes.

$$\max \quad \pi = P\left(x_a \le Ca_a + y_a\right) \tag{2-16}$$

$$\max \quad \varphi = I^k - g\left(U^{qk}\right) - \mu^{pqk} + I^{pk} \tag{2-17}$$

subject to

$$\sum_{p\in P} h_q{}^k = z_q{}^k \quad \forall q \in Q, \forall k \in K \tag{2-18}$$

$$\sum_{k\in K} h_p^k = h_p \quad \forall p \in P \tag{2-19}$$

$$B_o\left(O\right) + B_y\left(y\right) \le B_g \tag{2-20}$$

$$\bar{\rho}_p + \sum_{k\in k}\sum_{q\in Q} \mu^{pqk} \le I^k \quad \forall p \in P, \forall k \in K \tag{2-21}$$

$$0 \le y_a^{\min} \le y_a \le y_a^{\max} \quad \forall a \in A \tag{2-22}$$

$$\sum_{r\in R_{pq}} \gamma_{pqr} = 1 \tag{2-23}$$

$$\sum_{p\in P} \bar{d}_{pq} = E_q + \sum_{k\in K} z_q^k \quad \forall q \in Q \tag{2-24}$$

$$\sum_{q\in Q} \bar{d}_{pq} = H_p + \sum_{k\in K} h_p^k \quad \forall p \in P \tag{2-25}$$

$$h_p + H_p \le K_p \quad \forall p \in P \tag{2-26}$$

$$\sum_{p\in P}\sum_{q\in Q}\sum_{r\in R_{pq}} \bar{d}_{pq}\gamma_{pqr}\delta_{pqra} = \bar{x}_a \quad \forall a \in A, \forall k \in K \tag{2-27}$$

$$e = \sum_{a\in A} 0.2038 t_a \exp^{0.7962(l_a/t_a)} \tag{2-28}$$

$$\bar{x}_a \geq 0 \quad \forall a \in A \tag{2-29}$$

$$y_a \geq 0 \quad \forall a \in A \tag{2-30}$$

$$\gamma_{pqr} \geq 0 \quad \forall p \in P, \forall q \in Q, \forall r \in R \tag{2-31}$$

$$\bar{d}_{pq} \geq 0 \quad \forall p \in P, \forall q \in Q \tag{2-32}$$

$$h_p^k \geq 0 \quad \forall p \in P \tag{2-33}$$

The presented mathematical model is a bi-objective non-linear problem (NLP). The bi-linear term $\bar{d}_{pq}\gamma_{pqr}$ in Eqs (2-16), (2-17) and (2-27) introduces non-convexities. In Eq. (2-17), Cholesky matrix elements should be used which include bilinear terms are and also the travel cost in Eq. (2-16) has this bilinear term.

2.3.2 Model II: CO Emission and Utility

In previous section we developed a model to design land use and transportation network base on maximizing utility and reliability index, and CO emission is calculated as a constraint. The goal for developing previous model is to analyze the relationship between different land use and transport system structure and amount of CO emission. In this part, we introduce another model whose is minimizing CO emission and maximizing utility value. Examining how the decisions by travelers and network structure change based on minimizing emission is the aim of this model. In addition, we can find if there are significant differences between results of two models or not.

The difference between this model and previous model (Eq. (2-16)-(2-33)), is in the objective functions. We consider minimizing total CO emission in the network as the first objective Eq. (2-34) and maximizing utility as the second objective function Eq. (2-17). The reliability index is given as a constraint in our model ($\pi = P\ (x_a \leq Ca_a + y_a)$). The rest of the constraints are same as in the previous model (Eq. (2-16)-(2-33)).

$$\min \quad e = \sum_{a \in A} 0.2038 t_a \exp^{0.7962(l_a/t_a)} \tag{2-34}$$

2.4 Solution Algorithm

There are a number of methods to solve multi-objective problems. One of these methods is ϵ-constraint method. This method is applicable for both linear and non-linear problems. In this approach, the multi-objective problem is reformulated by keeping one of the objectives and restricting the rest of the objectives within user-specified values. The modified problem in its generic form is as follows:

$$
\begin{aligned}
&\min \quad f_\mu(x) \\
&\text{subject to} \\
&f_m(x) \le \epsilon_m \quad m = 1, 2, ..., M \text{ and } m \ne \mu \\
&g_j(x) \le 0 \quad j = 1, 2, ..., J \\
&h_k(x) = 0 \quad k = 1, 2, ..., K \\
&x_i^{(L)} \le x_i \le x_i^{(U)} \quad j = 1, 2, ..., I
\end{aligned}
\tag{2-35}
$$

where the parameters ϵ_m represents an upper bound of the value of the m^{th} objective function, f_m (Deb, 2001).

The optimization models presented in the previous sections (Eq. (2-16)-(2-34)) are bi-objective optimization problems: the first objective of model I is maximizing the reliability index and the first objective of model II is minimizing CO emission. The second objective of both problems is maximizing the utility. In our implementation of the solution algorithm, we keep the first objective (reliability index in model I and CO emission in model II) as the objective function of the problem and we consider the second objective as a constraint that should be greater than a ϵ. where ϵ is a lower bound of the utility value. ϵ should change from the worst to the best value of the utility to generate the family of solutions representing the Pareto set. We define a variable named "counter" to generate different Pareto points, and we substitute the constraint $\varphi \ge \epsilon$ with the following constraint,

$$\varphi \ge \varphi_{upper} - \tau(counter) \tag{2-36}$$

With

$$\tau(counter) = ord(counter) * \omega \tag{2-37}$$

$$w = (\varphi_{upper} - \varphi_{lower}) / card(counter) \tag{2-38}$$

where φ_{lower} and φ_{upper} are lower and upper bounds for the utility function respectively.

Our modified problems are as follow:

$$
\begin{aligned}
&max \quad \pi \\
&\text{subject to} \\
&\varphi \ge \varphi_{upper} - \tau(counter) \\
&e = \sum_{a \in A} 0.2038 t_a exp^{0.7962(l_a / t_a)} \\
&Eqs.(18) - (33)
\end{aligned}
\tag{2-39}
$$

$$
\begin{aligned}
&\min \quad e \\
&\text{subject to} \\
&\varphi \ge \varphi_{upper} - \tau(counter) \\
&\pi = P\left(x_a \le Ca_a + y_a\right) \\
&\text{Eqs.(18)-(33)}
\end{aligned}
\tag{2-40}
$$

We define two problems to calculate the upper and lower values for the utility. By solving Eqs. (2-39) - (2-40) without considering $\varphi \ge \varphi_{upper} - \tau(counter)$, we obtain the best value for the first objectives. By inserting the results of this problem in utility function, we obtain lower bound for utility value. In the same manner, by optimizing the problem in Eq. (2-41), we obtain the upper value for the utility function. We obtain the worst value for the first objective functions by putting the results of this problem in the first functions.

$$\begin{aligned} &\max \quad \varphi \\ &\text{subject to} \\ &\text{Eqs.(18)-(33)} \end{aligned} \tag{2-41}$$

We generate Pareto optimal solutions for model I and model II by optimizing Eqs. (2-39) and (2-40) respectively, for "counter" between 1, to N.

2.5 Results and Discussion

In this section, first an illustrative example is presented. Then, a sensitivity analysis of key parameters is provided for this illustrative example. Last, we provide results for a large set of problems.

2.5.1 Illustrative Example

We use the data presented in (Yim et al., 2011), (Ma and Lo, 2012) and (Ng and Lo, 2013) for the illustration of our models and the results. Figure 5 shows the layout of the example network consisting of six nodes, seven links, two origins, and two destinations. The characteristics of links, zones and income groups are listed in Table 1. We assume that demand follows Poisson distribution with equal mean and variance. The capacity of network links is allowed to expand up to 20% of the existing link capacity. Hence, we have $0 \le y_a \le 0.2C_a$. The budget for network expansion and residential developments is given by,

$$B_y = \sum_{a \in A} 0.3 y_a^2,\ B_h = \sum_{p \in P} h_p^2 \tag{2-42}$$

The maximum budget for the land use development and network enhancement is assumed as 450 million dollar. In addition, we consider that there is population growth of 20 thousand, which requires the land development equal to 20 house units in the city. The values of parameters θ_1^{pk} and θ_2^{pk} are considered 5 and 2 respectively.

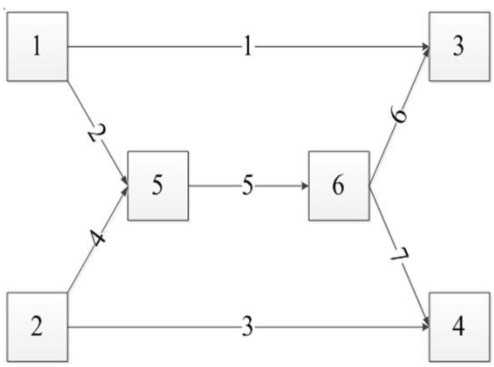

Figure 5. The schematic drawing of the numerical example

Table 1. The characteristics of the illustrative example presented in Chapter II

Link number	t_a^0	Ca_a	ρ_a	d_a
1	10	78	78	8
2	4	23	23	2
3	12	23	23	9
4	4	43	43	3
5	4	93	93	6
6	5	43	43	3
7	4	43	43	4

Zone	H_p/E_q	K_p	l_0^p
Origin node 1	50	100	15
Origin node 2	60	100	30
Destination node 3	50		
Destination node 4	60		

Income group	z_q^k	vot^k	I^k
High	6	5	1000
Low	14	4	900

The results of solving the problem by implementing model I and model II are reported in section 2.5.2 and 2.5.3 respectively and the efficient frontiers of optimal solutions are plotted in Figure 6. All runs were performed on a PC Intel(R), Xeon(R), central processing unit (CPU) 3.33GHz dual-core, 32 GB RAM running Windows 7 using CONOPT (Drud, 1994) in GAMS (Rosenthal, 2012). GAMS is Generalized Algebraic Modeling System. It offers many advantages compare to other computer optimization systems (Rosenthal, 2012). In this research, GAMS software is implemented mainly because it has advance features to handle large-scale models. GAMS includes a number of solvers to solve a NLP algorithm, CONOPT is one of these solvers. CONOPT is designed for large and spares models, and also it is suitable for models with very non-linear constraints. CONOPT may not find a global solution for non-convex models. However solvers designed for finding a global solution can not usually solve large and complex models (Drud, 1994).

2.5.2 Results for Model I

There are 19 efficient solutions out of 20 runs as shown in Figure 6(a). According to Eq. (2-36), when the value for $\tau(.)$ increases, the right hand side of this constraint decreases. By decreasing the right hand side, feasible region of the problem increases, and the objective value improves. As it is clear from Figure 6 (a), by increasing the $\tau(.)$ from left to right, reliability index improves. Both objectives have maximum values in *NADIR* point and in *UTOPIA* point both objectives have their minimum values as shown in Figure 6. It is possible to draw more accurate efficient frontiers by adjusting a greater grid point number instead of 20, but CPU time increases. So, implementing ϵ-constraint method is efficient by defining a small grid point number however we have to approximate efficient frontiers with these limited points.

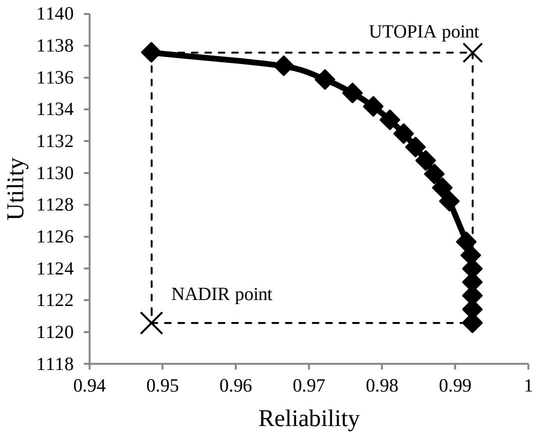

(a)

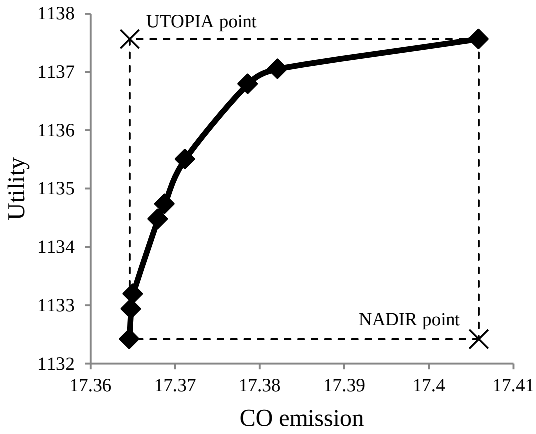

(b)

Figure 6. Efficient frontier of the optimal solutions for (a) model I and (b) model II

The result of running the model for 5 solutions, first, last and three intermediate solutions are shown in Table 2. In solution 19, utility has the minimum possible value and reliability index has its maximum value. While, the utility has its maximum value and the reliability has the minimum possible value in solution 1. The decision maker should select one of the optimal solutions in the efficient frontier based on his/her strategy.

As it is obvious from Table 2 from solution 19 to 1, utility value increases and travel cost decreases because the fraction of flow to capacity decreases and travel time decreases according to Eq. (2-13). In addition, because node 1 has less congested than node 2 as shown in Table 1, according to Eq. (2-8) most of the household development is allocated to node 1.

Table 2. Solutions of the illustrate example model I

		1	6	12	15	19
Emission index		17.406	17.43	17.47	17.53	17.550
Reliability index		0.9484843	0.981104	0.989215	0.99239362	0.99239362
Utility value		1137.565	1133.316	1128.219	1123.971	1120.572
Total travel cost		843.985	848.234	853.331	857.579	860.978
Total budget used		450.000	450.000	450.000	450.000	387.069
Budget used for network enhancement		200.000	200.000	200.000	200.000	137.069
Budget used for land development		250.000	250.000	250.000	250.000	250.000
Capacity expansion	1	15.600	15.600	15.600	15.600	15.600
	2	4.600	4.600	4.600	4.600	4.600
	3	4.600	4.600	4.600	4.600	4.600
	4	8.600	8.600	8.600	8.600	8.600
	5	15.267	15.007	14.593	14.341	0
	6	0.022	2.805	4.484	5.235	4.827
	7	8.600	8.600	8.600	8.600	8.600
Residential development for high income group	1	6.000	1.000	1.000	1.000	1.000
	2	0	5.000	5.000	5.000	5.000
Residential development for low income group	1	9.000	14.000	14.000	14.000	14.000
	2	5.000	0	0	0	0
Link flow	1	57.411	45.062	40.733	38.435	38.435

	2	7.589	19.938	24.267	26.565	26.565
	3	21.724	22.025	22.169	23.685	24.796
	4	43.276	42.975	42.831	41.315	40.204
	5	50.865	62.913	67.098	67.880	66.769
	6	2.589	14.938	19.267	21.565	21.565
	7	48.276	47.975	47.831	46.315	45.204
O-D mean demand	Zone 1- Zone 3	57.411	58.562	58.562	60.000	58.562
	Zone 1- Zone 4	7.589	6.438	6.438	5.000	6.438
	Zone 2- Zone 3	2.589	1.438	1.438	0	1.438
	Zone 2- Zone 4	62.411	63.562	63.562	65.000	63.562
Optimal route choice	Zone 1- Zone 3	100% from route1	76.9% from route1 23.1% from route2	69.6% from route1 30.4% from route2	64.1% from route1 35.9% from route2	65.6% from route1 34.4% from route2
	Zone 1- Zone 4	100% from route 1	100% from route 1	100% from route 1	100% from route 1	100% from route 1
	Zone 2- Zone 3	100% from route 1	100% from route 1	100% from route 1	100% from route 1	100% from route 1
	Zone 2- Zone 4	65.2% from route1 34.8% from route2	65.3% from route1 34.7% from route2	65.1% from route1 34.9% from route2	63.6% from route1 36.4% from route2	61% from route1 39% from route2

The amount of CO emission is calculated for each efficient solution. The relation between CO emission and utility is plotted in Fig. A.1 of Appendix I. By increasing utility because travel time decreases CO emission reduces. CO emission does not change significantly by increasing utility after a threshold and it stabilizes to an asymptotic value.

2.5.3 Result for Model II

The Pareto optimal solutions of model II are shown in Figure 6 (b). By increasing the emission, utility value increases. In addition, the result of running the model for 4 solutions, first, last and two intermediate solutions are summarized in Table 3. The result shows that the behavior of residents for selecting residential location is almost the same in model II and model I. The difference between the results of two models is flow distribution in the network. Compared with model I, more flow is allocated to route 1, to satisfy demand between nodes 1 and 3 in model II. It is because of in this model, we also consider the length of the links. In addition, utility improves in this model. By understanding the optimum network and also current situation, network planner can define policies to attract people to use some links and routes more than others to reduce CO emission.

Table 3. Solutions of the illustrate example for model II

	1	6	15	20
Emission index	17.406	17.371	17.368	17.365
Reliability index	0.948	0.960	0.960	0.965
Utility value	1137.565	1135.507	1134.479	1132.421
Total travel cost	843.985	846.043	847.071	849.129
Total budget used	450.000	444.027	404.422	402.268

Budget used for network enhancement		200.000	194.027	154.422	152.268
Budget used for land development		250.000	250.000	250.000	250.000
Capacity expansion	1	15.600	15.600	15.600	15.600
	2	4.600	4.600	4.600	4.600
	3	4.600	4.600	4.600	4.600
	4	8.600	8.600	8.600	8.600
	5	15.267	11.798	2.679	0
	6	0.022	8.600	8.600	8.600
	7	8.600	8.600	8.600	8.600
Residential development for high income group	1	6.000	1.542	1.000	1.000
	2	0	4.458	5.000	5.000
Residential development for low income group	1	9.000	13.458	14.000	14.000
	2	5.000	0.542	0	0
Link flow	1	57.411	53.413	53.400	51.688
	2	7.589	11.587	11.600	13.312
	3	21.724	18.400	18.368	17.405
	4	43.276	46.600	46.632	47.595
	5	50.865	58.187	58.232	60.907
	6	2.589	6.587	6.600	8.312
	7	48.276	51.600	51.632	52.595
O-D mean demand	Zone 1- Zone 3	57.411	59.997	58.599	58.562
	Zone 1- Zone 4	7.589	5.003	6.401	6.438
	Zone 2- Zone 3	2.589	0.003	1.401	1.438
	Zone 2- Zone 4	62.411	64.997	63.599	63.562
Optimal route choice	Zone 1- Zone 3	100% from route1	89% from route1 11% from route2	91.1% from route1 8.9% from route2	88.3% from route1 11.7% from route2
	Zone 1- Zone 4	100% from route 1	100% from route 1	100% from route 1	100% from route 1
	Zone 2- Zone 3	100% from route 1	100% from route 1	100% from route 1	100% from route 1
	Zone 2- Zone 4	65.2% from route1 34.8% from route2	71.7% from route1 28.3% from route2	71.1% from route1 28.9% from route2	72.6% from route1 27.4% from route2

2.5.4 Sensitivity Analysis

In any design and quantitative assessment study, it is necessary to understand the sensitivity of optimal solutions with respect to important parameters of the problem. In this section, by considering the data of the illustrative example, we change the value of the budget for network expansion and residential developments and the existing population in the origin zones to analyze the behavior of the model I and model II.

We set “counter” (Eq.(2-36)) equal to 20 in our solution algorithm, so we have a number of efficient solutions for each scenario. In order to compare the results, we summarize the results for the first and last runs of each scenario that show the worst and the best value for each objective. We change the value of the allocated budget between 300 and 500. By increasing the budget the value of reliability index and utility increase and CO emission reduces, as it is shown in Figure 7(a) and (b). By increasing the budget we can expand the capacities of link more, so congestion decreases in the links and reliability index increases. Also by increasing the capacity of the links, according to Eq. (2-13) the fraction of flow to link capacities decreases and travel time decreases, utility index increases and CO emission reduces. As it is shown in Figure 7(a), by more augmenting the link capacities, we can improve the reliability and utility of the network. Also, CO emission reduces as it is shown in Figure 7(b). The detail results for models I and II are summarized in Table A. 1 and Table A. 2 of supplementary material, respectively.

We change the existing population in origin nodes from 60-50 in node 1 and node 2 respectively to (50-60), (55-55) and (45-65). In each scenario, most amount of the population growth is allocated to the origin nodes with less existing population because of less crowded zones are more attractive according to Eq. (2-7). The detail results are provided in Table A. 3 and Table A. 4 of supplementary material. In addition, efficient frontiers of optimal solutions are shown in Figure 7(c) and (d). We can conclude from Figure 7(c) and (d) that by distributing the population more symmetric in the origin and destination nodes, the reliability and utility in the network improve, and CO emission reduces.

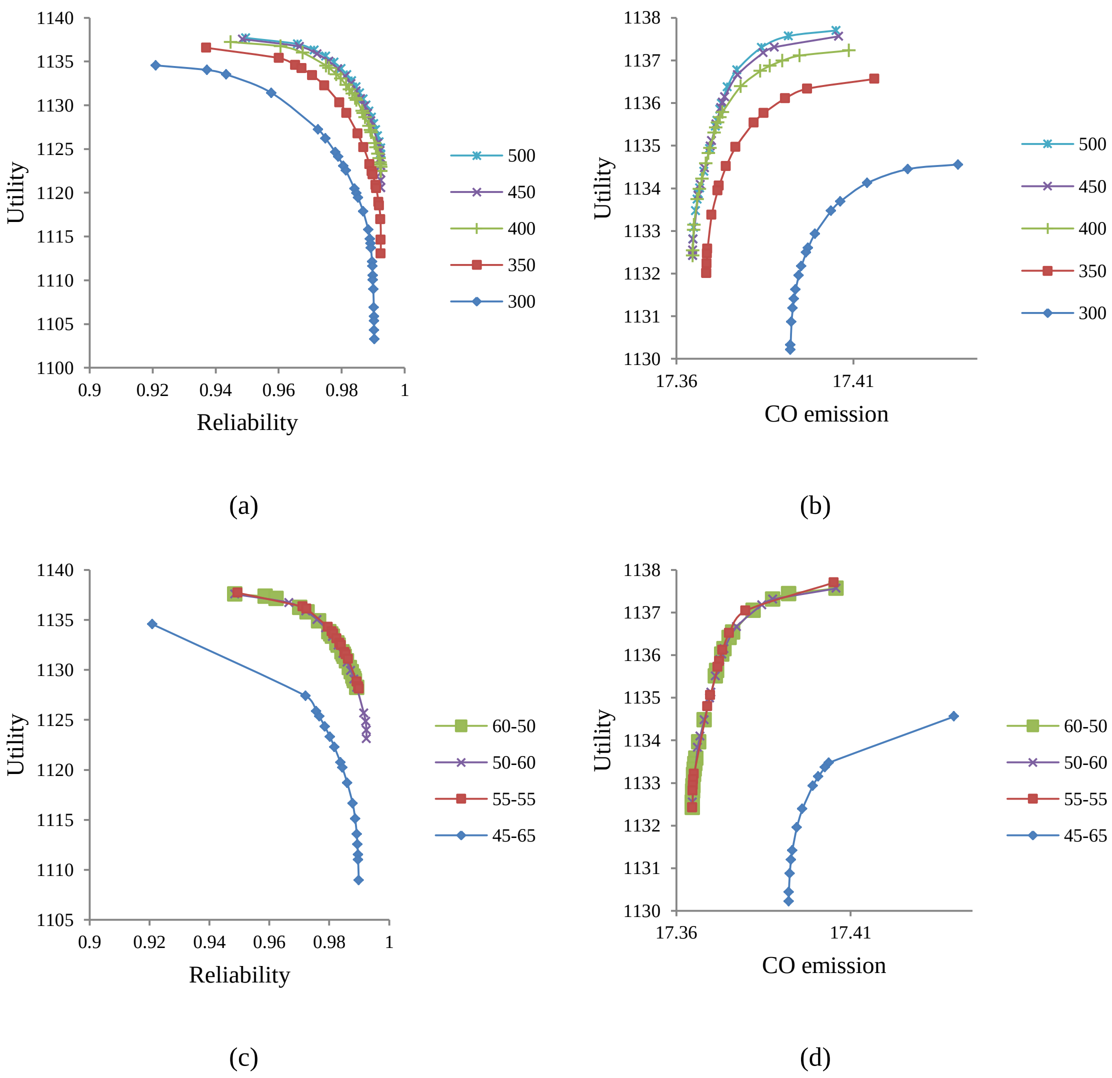

Figure 7. Efficient frontiers by changing the budget for (a) model I and (b) II and changing zonal existing population for (c) model I and (d) II

2.5.5 Results for a Large Set of Problems

To evaluate the performance of our integrated model, we generate different layouts for the city network using JAVA programming language and by implementing the generated layout we develop models I and II and solve them in GAMS environment. We change 4 parameters, *p*, *q*, *s* and *n*, which show, respectively, the number of origin nodes, the number of destination nodes, the number of echelons and the number of nodes in the intermediate echelons to generate different feasible layouts. After determining the values for *p*, *q*, *s* and *n*, links will connect all nodes in each echelon to all nodes in the previous and subsequent echelons. The number of routes that connect each origin node to each destination node will be counted and it will consider in the models. By changing the values of *p* and *q* between 2 and 5, the value of s between 3 and 4 and the value of n between 1 and 5, we create 10 scenarios of which are labeled by vector (*p*,*q*,*s*,*n*). These ten scenarios are selected because they have different number of nodes and links and we can survey the relation between number of nodes and links of a network with CPU time.

For these examples, we consider 60 existing population for each node in origin and destination nodes and we consider 20 population developments. The data related to links is considered the average values of each parameter in Table 1, and the data related to income group is considered the same as the data in Table 1. The networks structures of these ten problems are given in the supplementary material.

Table 4. Complexity of the problem presented in Chapter II

No	Scenario name	# of nodes	# of links	# of variables	# of equations	# of efficient solutions		CPU time (s)	
						model I	model II	model I	model II
1	(2,2,3,1)	5	4	195	195	10	10	0.078	1.25
2	(2,2,3,2)	6	8	421	482	10	10	23.026	17.862
3	(2,2,3,3)	7	12	695	827	10	10	27.937	22.557
4	(2,2,3,4)	8	16	1,017	1,253	10	8	246.433	30.046
5	(3,3,3,3)	9	18	1,233	1,527	7	8	33.18	321.987
6	(3,3,3,4)	10	24	1,851	2,381	10	10	163.834	79.766
7	(4,4,3,3)	11	24	1,899	2,420	10	9	235.968	391.654
8	(3,3,4,3)	12	27	2,322	2,958	10	7	519.67	452.387
9	(5,5,3,3)	13	30	2,693	3,507	10	9	316.197	420.111
10	(4,4,4,3)	14	33	3,276	4,204	10	9	1684.622	1665.605

The results presented in Table 4 show the problem complexity, model statistics and the CPU time required to obtain optimal solutions to each problem. The set of 10 scenarios are successfully optimized in reasonable CPU times for all values considered. So, we expect to implement this model for real problems.

The first four problems listed in Table 4 have the same number of origin and destination nodes, but from first to fourth one the numbers of links in the network increase. As shown in the efficient frontiers of these four problems for model I in Figure 8(a), (b), (c) and (d), by increasing the number of links, the minimum and maximum values of the reliability index increases and the maximum value approaches to 1. Because by increasing the number of links in the network and having the same population, flow in links decreases and congestion decreases and reliability increases. But the utility value decreases because travel time increases and travel cost increases. We have the same condition for problems (3,3,3,3), (3,3,3,4) and (3,3,4,3), also for problems (4,4,3,3) and (4,4,4,3) as shown in Fig. A. 6 and Fig. A. 8 of the supplementary material. In addition the efficient frontiers of optimal solutions of the first four problems are plotted for model II in Figure 8(e), (f), (g) and (h). As it is shown in Figure 8(e), (f), (g) and (h) by increasing the number of links the minimum and maximum values for utility index decrease and minimum and maximum values for CO emission increase, because travel time increases in the larger networks. We conclude same results for problems (3,3,3,3), (3,3,3,4) and (3,3,4,3), also for problems (4,4,3,3) and (4,4,4,3) as shown in Fig. A. 7 and Fig. A. 9 of the supplementary material. So, the best city structure can be a structure that considers trade off between two situations, very low land use intensity and degree of concentration structure, and very high-density land use structure. By considering the result of sensitivity analysis part; we can conclude that expanding the capacity of the existing links is a better policy than constructing new links for expanding a city network. Because by augmenting the capacity of the links, we can improve the reliability, utility and CO emission in urban areas.

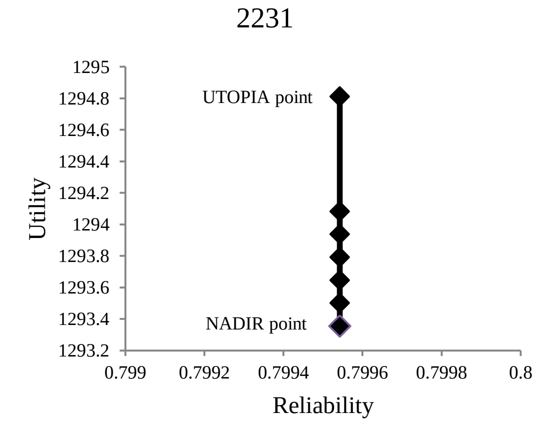

(a)

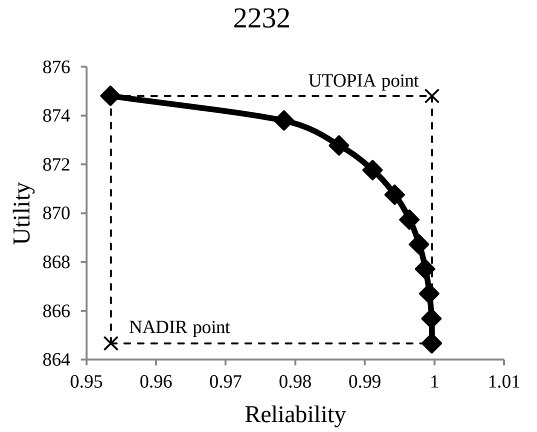

(b)

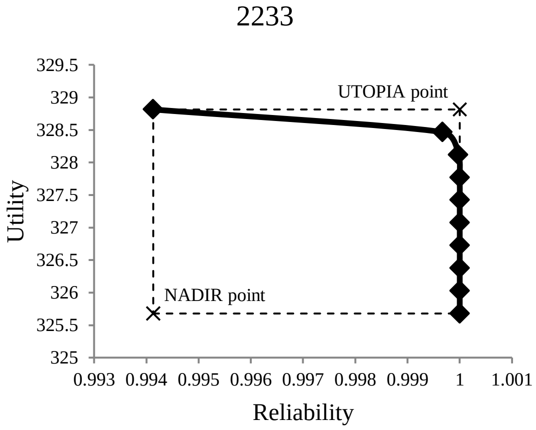

(c)

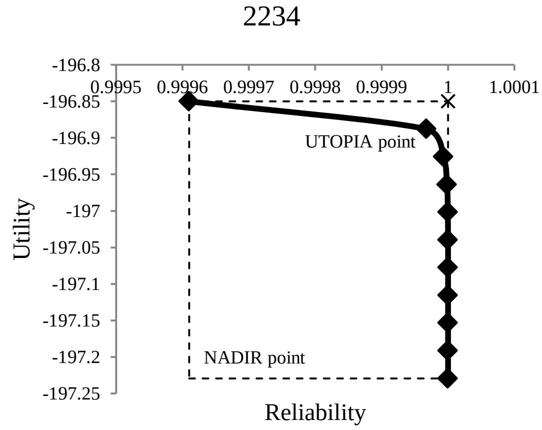

(d)

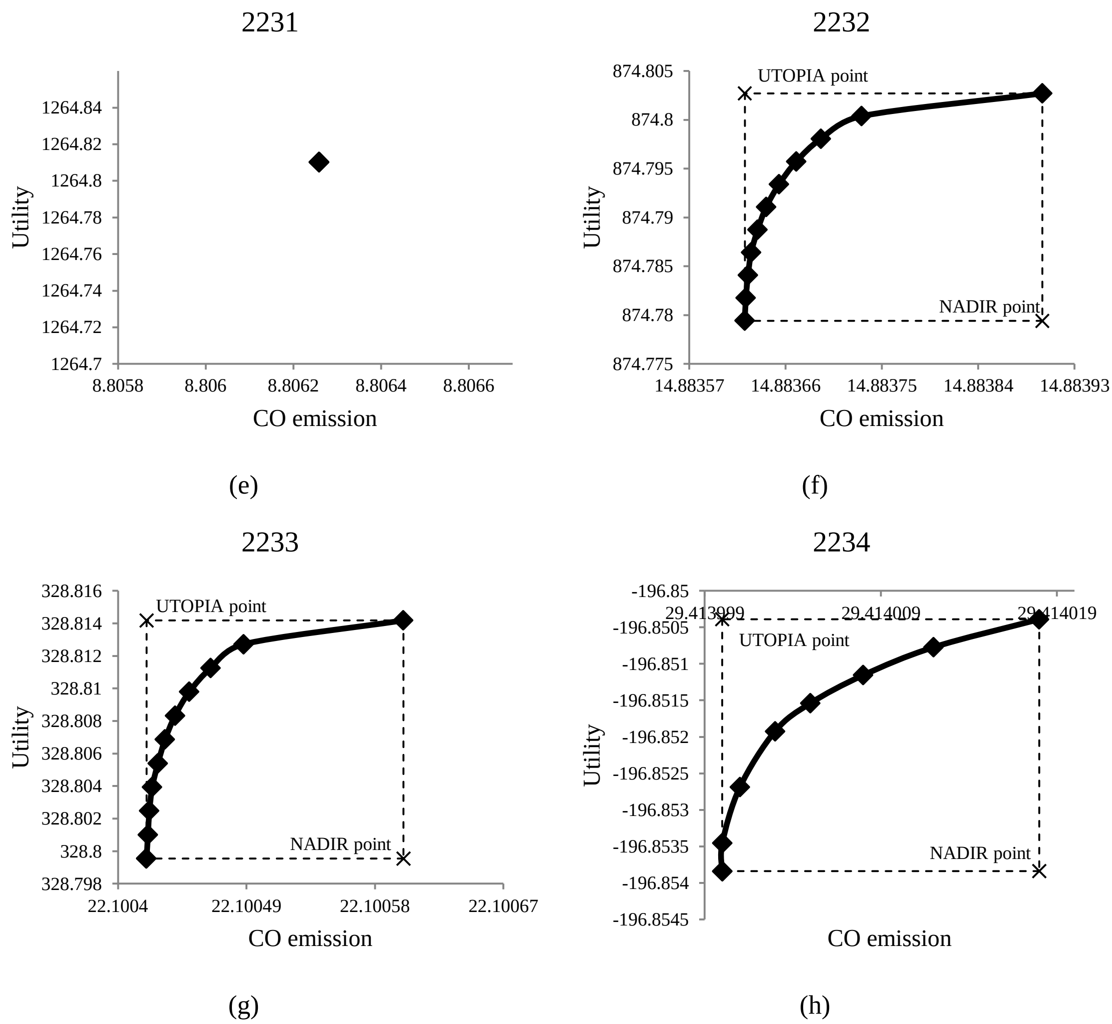

Figure 8. The efficient frontiers of problem (a) “2,2,3,1”,(b) “2,2,3,2”,(c) “2,2,3,3”and (d) “2,2,3,4” for model I and the efficient frontiers of problem (e) “2,2,3,1”,(f) “2,2,3,2”,(g) “2,2,3,3”and (h) “2,2,3,4” for model II

2.6 Conclusions

In this chapter, we present two bi-objective optimization models for land use and transportation problem. Objective functions of the first model are utility value and reliability index, and objective functions of second model are utility value and amount of CO emission. Relation between different land use and transport structure and amount of CO emission is analyzed.

By defining reliability probability, we minimize congestion. We formulate a closed form expression to calculate the Cholesky factorization matrix that is implemented as a set of constraints in the optimization model, to estimate the reliability index by multivariate normal distribution. Utility value captures travel time and attractiveness of each zone as a cost function. We use BPR link impedance function to estimate average travel time. In addition we consider zonal attractiveness as a function of intensity or congestion of each zone. And, CO emission is calculated by an equation which is function of travel time and speed in each link.

We proposed ϵ-constraint method as a solution algorithm, and we analyzed model behavior through several experiments. We tested our approach on ten different problems with different sizes as summarized in Table 4. We found that CPU time does not suffer from the size of the problems. By analyzing the model behavior, we found that expanding the capacity of existing links instead of constructing the new links can be a better policy. By augmenting the link capacities, both reliability and utility improve, while by constructing the new links just reliability improve. In addition amount of CO emission reduces by augmenting the link capacities. Besides, distributing the population more symmetrically in the origin and destination zones can help to improve the reliability and the utility of the network and reducing CO emission. Considering CO emission as objective function instead of reliability index effects on the distribution of flow in the network and improves the utility value.

Appendix is given in Annex I

3 Chapter III

Multi-Modal Transportation Network Design Problem with Stochastic Demand and Sustainability Considerations

In this paper, we present a bi-level optimization model that considers the use of multiple transportation modes, stochastic travel demand and sustainability in transportation network design simultaneously. Travel demand is allowed to follow a general probability distribution where its mean and variance are functions of the population in the origin and destination areas. The problem is formulated as a bi-level optimization problem. In the lower level, a transportation design problem is formulated to minimize total travel costs and in the upper level we consider minimizing carbon monoxide emission productions and minimizing probability of traffic congestion. The two-stage model is formulated as a single stage model by considering optimality conditions of lower level problem as a set of constraints in the upper level model. The formulated single stage model is a Mixed Integer Non-linear Programming (MINLP) problem with two objective functions. An exact solution algorithm based on outer approximation and ϵ-constraint method is implemented to generate the set of Pareto solutions of the bi-objective MINLP problem. In this study, for the first time in the open literature, a stochastic multi-modal, bi-level optimization model is formulated for the transportation network design problem in urban regions and an efficient solution algorithm is presented to solve the model. We also illustrate effectiveness of our approach on an illustrative example and a set of benchmark problems.

3.1 Introduction

Traffic congestion and environmental issues associated with transportation have been considered as an important problems faced by modern cities because of their negative effects on productivity, health, and living conditions. Research has indicated that on the average, road transportation contributes 95 % of the carbon monoxide (CO) and 35 % of the nitrogen oxides in urban environments (EPA, 2010, FHWA, 2006). These pollutants can have potentially serious effects on both the ecosystem and the human health (Ng and Lo 2013). Nowadays, governments attempts to control the traffic volume in urban areas to improve or maintain the air quality of the cities and achieve a more sustainable mobility (Zhong et al 2012).

By rapidly increasing population and growing cities around the world, more people compete for limited urban road infrastructure to travel. Therefore, it is important to understand how the space in cities should be managed to improve accessibility for travelers as well as improve sustainability in cities. Recently, many researchers proposed modeling and optimization tools, which will contribute on how to redistribute limited city space to multiple transportation modes and to understand what level of sustainable mobility can be achieved with different structures.

Due to increasing urbanization, research focused on the network design problem in urban areas during the last five decades (Farahani et al 2013). The earliest works modeled road network design problem purely based on a static approach, or their stochastic extensions are for depicting the route choice behavior of travelers or for determining the best system performance (e.g., Ban et al., 2006; Boyce and Janson, 1980; Chen et al., 2010a, 2010b, 2006; Chiou, 2009; Davis, 1994; Farvaresh and Sepehri, 2012; Friesz et al., 1993; Leblanc, 1975; Long et al., 2010; Marcotte, 1986; Meng et al., 2001; Miandoabchi et al., 2013; Qiu Yuzhuo and Chen Senfa, 2007; Szeto et al., 2013; Ukkusuri et al., 2007; Lin and Xie, 2010;Yang et al., 2010). This approach allows analyzing the problem easily but cannot capture the realistic variations in demand. The travel demand highly depends on the pattern of activities in urban areas. The timing and locations of these activities indicate that travel demand is not uniform through a day (Sheffi 1985). It is also shown that travel demand shows strong variations throughout a day (Kitamura and Susilo 2005). In addition, a large number of static network design studies focus solely on the economic dimension of sustainability (e.g., Ban et al., 2006; Kim et al., 2007; Lo and Szeto, 2009). Some research considered environmental index as the objective to capture the environmental effects of transportation related activities (Yin and Lu 1999; Zhou et al 2008; Huang, Ke, Jin Zhang, Meiling He 2010).

Miandoabchi et al., (2011a, 2011b) developed bi-modal formulations by considering static demand in each period. Szeto et al., (2013) developed a model for the urban network design considering sustainability. In this model, environmental, economic and social dimensions of a sustainable system are considered in a multi-objective formulation. But in this model demand in each period is constant and only bi-modal transportation is considered. Meta heuristic solution algorithms are implemented to solve these problems.

Only a few studies have incorporated the three aspects of sustainability, namely environmental, economic and social features, to formulate the transportation network design problem. In addition, these formulations solely consider on-road modes and travel demand is assumed to be static. We address these shortcomings by incorporating the three dimensions of sustainability, rail transportation in addition to on-road, and stochastic demand in our problem formulation.

Urban network design problems are complex since different groups are involved in the decision-making process. Therefore, these problems are usually modeled as bi-level problems. There is no general format to develop an exact solution algorithm for these problems with stochastic demand. In this paper, we present a novel solution algorithm to solve the model formulation exactly.

This paper contributes to urban transportation research by including innovations in the model formulation and the design of a novel solution algorithm for multi-modal transportation network design problem with stochastic demand and considering sustainability.

In this paper, we develop a multi-modal transportation model by considering on-road (private cars and buses) and rail vehicles (trams and metros). Travel demand is considered as a random variable that can follow any distribution where its mean and variance are functions of origin and destination populations. We define a reliability index to measure the probability of traffic congestion in the network. The presented model incorporates sustainability by considering minimization of transport emissions and minimization of the probability of traffic congestion as objective functions of the upper level problem and minimization of the travel cost as the objective function of the lower level problem. Minimizing transport emissions, minimizing the probability of traffic congestion and minimizing travel cost are environmental, social and economic aspects of our model. In addition, in this study we present a novel solution algorithm for this problem. In this research, the closed form expressions of optimality conditions of the lower level problem are formulated. We incorporate these optimality conditions in the upper level problem as a set of constraints. The integrated model has two objective functions and it is a Mixed Integer Nonlinear Programming (MINLP) problem. MINLPs are categorized as the most difficult problems as they include both discrete and continuous variables and involve nonlinearity in the objective function and constraints. Several methods proposed to solve MINLPs, including NLP-based branch and bound (Nabar, S., Schrage 1991), Generalized Benders Decomposition (Geoffrion 1972), and outer approximation (OA) (Duran and Grossmann 1986). In this study, OA algorithm is used to establish the core of the custom solution algorithm. This method involves repeatedly solving the NLP sub problems, generated by fixing the values of discrete variables, and the Master problem, constructed by replacing the nonlinear functions by their linear approximations, until the bounds from these two problems converge. In this paper, we use OA and ϵ-constraint algorithms to develop our algorithm to solve the bi-objective MINLP network problem.

3.2 Problem Description

Let $G(N, A)$ be a multi-modal network with nodes set N, arcs set A. Some nodes are considered to be origin nodes and some to be destination nodes; the remaining nodes are called intermediate nodes or transit nodes, as shown in Figure 9. M is the set of transport modes. Each link can be a candidate to be used by different transport types. Origin and destination nodes can represent the same geographical location. P is the set of origin nodes, Q is the set of destination nodes, R_{pq} is the set of routes between pair of origin p and destination q. Multi-modal network design problems have intrinsically more than one objective, since the design alternatives must be assessed based on various criteria of network users and the network authority (Miandoabchi et al., 2011).

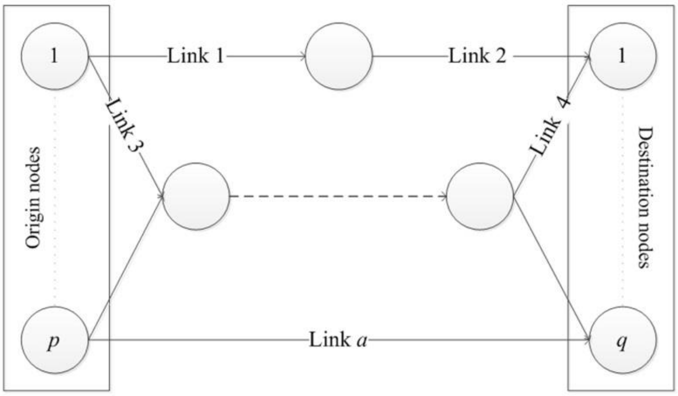

Figure 9. The schematic representation of the network

In this problem, we consider three distinct transportation types, passenger cars, buses, and railway vehicles. We consider the residents in k different groups based on their income levels. We assume the travelers are strategic and the network planner is developing solutions to address the needs of the strategic travelers. The travelers try to choose their route and transportation types to reach their workplaces in destination nodes (q) with the objective of minimizing the total travel cost of the transportation network. While, the network planner goals are minimizing emissions and traffic congestion by augmenting the capacity of the existing links and constructing new buses and railway facilities in the network. Naturally, the problem is a bi-level decision problem; the travelers determine their route and transportation types to minimize the total travel cost in the lower level problem and the network planner tries to minimize carbon monoxide (CO) emission and minimize the probability of traffic congestion in the network by allocating new transport facilities and extending the link capacities in the upper level problem. We consider CO emission for environmental impact because of three reasons: (1) almost all CO emissions in the air are produced by vehicles, (2) CO is the most important pollutant among the different types of vehicular emissions, which include nitrogen oxide, CO, nitrogen dioxide, sulfur dioxide, ozone, and particulates, and (3) the emission rates of other pollutants are similar to that of CO (Li et al., 2012c). We assume buses and cars are non-electric vehicles while railway vehicles are electric which are either underground or on-road with separate lines. Electric vehicles have zero tailpipe CO emissions, but emissions may be produced at the source of electrical power, such as a power plant which is not considered in this study.

In this study, we assume a basic network with two-way links where all bus routes share the street lanes with passenger cars. Passenger car and buses travel demands on shared lanes influence each other, and thus the travel time/cost function for these two modes is asymmetric. We focus on network planning and not the actual operation, so we should propose a formulation that can handle large networks. The existing bus and railway lines are given. Attributes of network links such as capacities, length, and free travel times are known. Besides, we know candidate links for constructing bus and railway facilities, and the total budget for constructing new bus and railway facilities and expanding capacity of links. In this study, we assume the same link structure for both railway vehicles and on-road transports. In addition, the value of walking, waiting and free travel demand travel times, car toll, bus and railway vehicle fares are given. The outputs of model are the amount of expansions of links, and the roads selected for installing new bus and railway facilities.

3.3 Mathematical formulation for Multi-Modal Transportation Network Design with Uncertain Demand

We assume that the travel demand between origin p and destination q, d_{pq}, is a random variable that follows a general distribution with a mean and variance as shown in Eq. (3-1) and (3-2).

$$E(d_{pq}) = \bar{d}_{pq} \quad \forall p \in P, \forall q \in Q \tag{3-1}$$

$$var(d_{pq}) = \sigma_{pq} \quad \forall p \in P, \forall q \in Q \tag{3-2}$$

Demand between pair p and q follows a general distribution which its mean and variance are equal to a value between zero and the total population in zone p and q. Therefore, we can define a general formula for mean and variance of demand as shown in Eq. (3-3) and (3-4), respectively.

$$\bar{d}_{pq} = \tau(H_p + E_q) \quad 0 \le \tau \le 1, \forall p \in P, \forall q \in Q \tag{3-3}$$

$$\sigma_{pq} = \Omega(\bar{d}_{pq}) \qquad 0 \le \Omega \le 1, \forall p \in P, \forall q \in Q \tag{3-4}$$

where H_p and E_q are the population amount in origin p and destination q, respectively. And τ and Ω are deterministic scalars set by the network planner.

The travel demand in each link (passenger per hour) is defined as a function of total travel demand between pair p and q according to Eq. (3-5).

$$\acute{x}_a = \sum_{p\in P} \sum_{q\in Q} \sum_{r\in R_{pq}} d_{pq}\gamma_{pqr}\delta_{pqra} \quad \forall a \in A \tag{3-5}$$

In Eq. (3-5), γ_{pqr} is the vector of route choice proportions and δ_{pqra} is the link-path incidence matrix that is equal to 1 if the route r passes through link a otherwise it is equal to 0. We assume that the travel demands between origin and destination nodes are mutually independent and identically distributed random variables. Therefore, using the central limit theorem, we can assume $\acute{x}_a$ follows normal distribution with mean $\overline{\acute{x}_a}$ and variance $\acute{\sigma}_a$. The mean and the variance of the travel demand in each link can be expressed as functions of the mean and variance origin-destination demands, route choice proportions, and link-path incident matrix as shown in Eq. (3-6) and (3-7).

$$\overline{\acute{x}_a} = \sum_{p\in P}\sum_{q\in Q}\sum_{r\in R_{pq}} \bar{d}_{pq}\gamma_{pqr}\delta_{pqra} \quad \forall a \in A \tag{3-6}$$

$$\acute{\sigma}_a = \sum_{p\in P}\sum_{q\in Q}\sum_{\acute{r}\in \acute{R}_{pq}}\sum_{r\in R_{pq}} \sigma_{pq}\gamma_{pqr}\gamma_{pq\acute{r}}\delta_{pqra}\delta_{pq\acute{r}a} \quad \forall a \in A \tag{3-7}$$

Travel demand on link a ($\acute{x}_a$) is the summation of the travel demand for transport m on link a (x_a^m) as shown in Eq. (3-8).

$$\acute{x}_a = \sum_{m\in M} x_a^m \quad \forall a \in A \tag{3-8}$$

We assume that the travel demand for passenger cars (x_a^{car}), buses (x_a^{bus}) and railway vehicles (x_a^{rail}) are independent and follow normal distribution with means $\bar{x}_a^{auto}$, $\bar{x}_a^{bus}$ and $\bar{x}_a^{metro}$ and variances σ_a^{auto}, σ_a^{bus} and $\sigma_a^{railway}$, respectively. Therefore, the mean and the variance of the travel demand in each link are equal to the summation of the mean and variance of the mode-specific travel demand as shown in Eq. (3-9) and Eq. (3-10), respectively. If we substitute Eq. (3-9) and Eq. (3-10) in Eq. (3-6) and Eq. (3-7) respectively, then we will have Eq. (3-11) and Eq. (3-12). In the optimization model the total average travel demand in each link ($\acute{x}_a$) is distributed for different transport types to minimize the travel cost, the amount of emission productions and traffic congestion. In the constraints of the optimization model, we define the feasibility of having different transport types in each link. According to Eq. (3-11) and Eq. (3-12), the mean and variance of the mode-specific travel demand in each road are the functions of total demand between pair p and q and the route choice proportions.

$$\overline{\acute{x}_a} = \sum_{m\in M} \bar{x}_a^m \quad \forall a \in A \tag{3-9}$$

$$\acute{\sigma}_a = \sum_{m\in M} \sigma_a^m \quad \forall a \in A \tag{3-10}$$

$$\sum_{m\in M} \bar{x}_a^m = \sum_{p\in P}\sum_{q\in Q}\sum_{r\in R_{pq}} \bar{d}_{pq}\gamma_{pqr}\delta_{pqra} \quad \forall a \in A \tag{3-11}$$

$$\sum_{m\in M} \sigma_a^m = \sum_{p\in P}\sum_{q\in Q}\sum_{\acute{r}\in \acute{R}_{pq}}\sum_{r\in R_{pq}} \sigma_{pq}\gamma_{pqr}\gamma_{pq\acute{r}}\delta_{pqra}\delta_{pq\acute{r}a} \quad \forall a \in A \tag{3-12}$$

The on-road travel demand on link a is calculated as shown in Eq. (3-13): x_a^{car} and x_a^{bus} are based on passenger per hour, while on road travel demand is based on the number of passenger cars.

$$x_a = \frac{x_a^{car}}{\pi} + \omega \frac{x_a^{bus}}{\theta} \quad \forall a \in A \tag{3-13}$$

In Eq. (13), π and θ are the average number of passengers in one passenger car and in one bus respectively and, ω is a parameter to convert the bus travel demand to the equivalent passenger car travel demand. The variable x_a has normal distribution with the mean and variance formulated in Eq. (3-14) and Eq. (3-15), respectively. Using Eq. (3-11) and Eq. (3-12), the mean and variance of the mode-specific travel demand in each road will be calculated through the optimization and based on the results, the mean and variance of the on-road travel demand in each road are calculated using Eq. (3-14) and (3-15).

$$\bar{x}_a = E\left(\frac{x_a^{car}}{\pi} + \omega \frac{x_a^{bus}}{\theta}\right) = \frac{\bar{x}_a^{car}}{\pi} + \omega \frac{\bar{x}_a^{bus}}{\theta} \quad \forall a \in A \tag{3-14}$$

$$\sigma_a = var\left(\frac{x_a^{car}}{\pi} + \omega \frac{x_a^{bus}}{\theta}\right) = \frac{\sigma_a^{car}}{\pi^2} + \omega^2 \frac{\sigma_a^{bus}}{\theta^2} \quad \forall a \in A \tag{3-15}$$

Eq. (3-16) gives the travel cost function between zone p and q for income group k. The travel cost is a function of the travel time on link a using transport m (t_a^m). The travel time as shown in Eq. (3-18) and Eq. (3-19) is a function of the travel demand on link a for transport m (x_a^m). The travel demand on link a for transport m is a function of the total travel demand and the route choice proportion as shown in Eq. (3-5) and (3-8). Therefore, the travel cost is a function of total travel demand between pair p and q and the proportion of passengers choosing the particular route r.

$$TC^{pqk} = \sum_{r \in R_{pq}} \sum_{m \in M} \sum_{a \in A} y_a^m \, \delta_{pqra}\left(vot^k(t_a^m) + p_a^m\right) \tag{3-16}$$

Above, t_a^m is multiplied by the time value of residents of income group k (vot^k), and this expression is added to toll charges (p_a^m) which are per transport type, to show the travel cost on link a. The parameter y_m^a is equal to 1 if there are facilities for transport type m on link a otherwise it is equal to 0. The travel time function for passenger cars and buses on a bimodal link is defined by the well-known BPR function as shown in Eq. (3-17).

$$t_a = t_0^a\left(1 + \beta\left(\frac{x_a}{Ca_a + e_a}\right)^{\alpha}\right) \tag{3-17}$$

In Eq. (3-17), t_0^a is the free-flow travel time of link a, and β and α are the model parameters. The values for β and α are typically considered equal to 0.15 and 4.0 respectively. In this problem, the practical capacity of a link is the summation of the initial capacity of link a (Ca_a) plus the amount of expansion of link a (e_a) which is a decision variable in our problem.

The travel cost function of passenger cars on a bimodal link is defined by Eq. (3-18) (Uchida et al., 2006).

$$t_a^{car} = \check{t}_0^a \left(1 + 0.15 \left(\frac{\frac{x_a^{car}}{\pi} + \omega \frac{x_a^{bus}}{\theta}}{Ca_a + e_a} \right)^4 \right) \tag{3-18}$$

where $\check{t}_0^a$ is the free flow travel time of passenger cars on link *a*.

The travel cost function of passenger buses on bimodal link is defined by Eq. (3-19).

$$t_a^{bus} = \hat{t}_0^a \left(1 + 0.15 \left(\frac{\frac{x_a^{car}}{\pi} + \omega \frac{x_a^{bus}}{\theta}}{Ca_a + e_a} \right)^4 \right) \tag{3-19}$$

where $\hat{t}_0^a$ is the free flow travel time of buses on link *a*.

Therefore, the long-run perceived travel time for passenger cars and buses can be presented respectively in Eq. (3-20) and (3-21).

$$E(t_a^{car}) = \check{t}_0^a \left(1 + \frac{0.15}{(Ca_a + e_a)^4} E(x_a^4) \right) \tag{3-20}$$

$$E(t_a^{bus}) = \hat{t}_0^a \left(1 + \frac{0.15}{(Ca_a + e_a)^4} E(x_a^4) \right) \tag{3-21}$$

The fourth uncentered moment of the distribution can be expressed from the central limit theorem as follows.

$$E(x_a^4) = \bar{x}_a^4 + 6\sigma_a \bar{x}_a^2 + 3\sigma_a^2 \tag{3-22}$$

Therefore, we can rewrite the long-run perceived travel time as shown in Eq. (3-23).

$$E(t_a^m) = t_a^0 \left(1 + \frac{0.15}{(Ca_a + e_a)^4} (\bar{x}_a^4 + 6\sigma_a \bar{x}_a^2 + 3\sigma_a^2) \right) \tag{3-23}$$

where $\bar{x}_a$ and σ_a are calculated according to Eq. (3-14) and (3-15).

Eq. (3-24) shows the long-run perceived travel cost between nodes *p* and *q* for income group *k*. The long-run perceived travel cost is a function of the mean travel time on link *a* using transport *m* ($E(t_a^m)$). As shown in Eq.(3-20), (3-21) and (3-22), the mean travel time is a function of the mean and variance of on-road travel demand. The mean and variance of the on-road travel demand are functions of the mean and variance of the travel demand on link *a* for transport *m* as shown in Eq. (3-14) and (3-15). The mean and variance of the travel demand on link *a* for transport *m* are functions of total travel demand and the route choice proportion as shown in Eq. (3-11) and (3-12). Finally, the long-run perceived travel cost is a function of total travel demand between pair *p* and *q* and the proportion of passengers choosing the particular route *r*.

$$\vartheta^{pqk} = \sum_{r \in R_{pq}} \sum_{a \in A} \sum_{m \in M} \delta_{pqra}\, y_a^m (vot^k (E(t_a^m) + \bar{t}_{wk}^m + \bar{t}_{wt}^m) + p_a^m) \tag{3-24}$$

where,

$$E(t_a^{car}) = \check{t}_0^a \left(1 + \frac{0.15}{(Ca_a+e_a)^4} E\left((\bar{x}_a^4 + 6\sigma_a \bar{x}_a^2 + 3\sigma_a^2)\right)\right) \tag{3-25}$$

$$E(t_a^{bus}) = \hat{t}_0^a \left(1 + \frac{0.15}{(Ca_a+e_a)^4} E\left((\bar{x}_a^4 + 6\sigma_a \bar{x}_a^2 + 3\sigma_a^2)\right)\right) \tag{3-26}$$

$$E\left(t_a^{rail}\right) = \acute{t}_0^a \tag{3-27}$$

where $\acute{t}_0^a$ is the free flow travel time of railway vehicles on link a.

As shown in Eq. (3-24), the average values for waiting times for buses and railway vehicles are considered equal to $\bar{t}_{wt}^{bus}$ and $\bar{t}_{wt}^{rail}$, respectively. Furthermore, The average time required to access the bus and railway vehicle stations by walking are considered equal to $\bar{t}_{wk}^{bus}$ and $\bar{t}_{wk}^{rail}$, respectively. Based on the optimization results, some links are selected to install bus and railway facilities. According to the optimization results, some passengers may able to travel from their origin place to their destination just using one transport type or they may have to change their transport types in the intermediate nodes.

CO emission in each link is calculated by Eq. (3-28). The amount of CO emission for non-electric mode m on link a ($ec^m{}_a$) is function of the length of link a (l_a), the mean travel time in each link ($E(t^m{}_a)$), the average travel speed in each link ($l_a/ E(t^m{}_a)$) and the number of passenger cars which are equivalent to the number of vehicle type m on link a ($v^m{}_a$) (Ng and Lo, 2013; Szeto et al., 2013; Yin and Lawphongpanich, 2006b). In this study, we assume that the buses and cars are non-electric and Eq. (3-28) is used to calculate the emission production for them.

$$ec_a^m = 0.2038E(t_a^m)\exp\left(0.7962(l_a/E(t_a^m))\right)v_a^m \quad \text{if } m \text{ is a non-electric mode} \tag{3-28}$$

where

$$v_a^{auto} = \frac{\bar{x}_a^{car}}{\pi} \tag{3-29}$$

$$v_a^{bus} = \frac{\omega\,\bar{x}_a^{bus}}{\theta} \tag{3-30}$$

Minimizing CO emission, Eq. (3-28), and maximizing reliability index in Eq. (3-31) are considered as the first and second objective of upper level problem, respectively. The reliability index is the probability that travel demand in each link be less the initial capacity (Ca_a) of the link plus the amount of capacity expansion (e_a) that is a decision variable in our problem. Maximizing the reliability probability is equal to minimizing probability of traffic congestion in the network.

$$\pi = P(x_a \leq Ca_a + e_a) \tag{3-31}$$

This probability can be obtained from the multivariate normal distribution shown in Eq. (3-32).

$$F(0, Ca+e) = \frac{1}{\sqrt{|\Sigma|(2\pi)^a}} \int_0^{Ca_1+e_1} \int_0^{Ca_2+e_2} \dots \int_0^{Ca_a+e_a} e^{-\frac{1}{2}x^t\Sigma^{-1}x}\, dx \qquad (3\text{-}32)$$

where $x = (x_1, x_2, \dots, x_a)^t$ and Σ is an $n \times n$ symmetric covariance matrix.

In this study, the algorithm developed by Genz (1992) is applied to calculate the multivariate normal probability. The steps of this algorithm are considered as a set of constraints in the optimization model. Therefore through the optimization this probability is calculated using multivariate normal probabilities algorithm. The readers may refer to Shahraki and Turkay (2014) for further details on implementing the probabilities. The covariance matrix is calculated according to Eq. (3-33).

$$\Sigma_{x_a x_{\acute{a}}} = \rho_{a\acute{a}} \sqrt{\sigma_a \sigma_{\acute{a}}} \qquad (3\text{-}33)$$

ρ is correlation coefficient matrix. Here it is used to show the correlation between two roads. The elements of this matrix can have any value between -1 and 1. For example, if ρ is equal to 1, it shows the traffic congestion in a road has a strong effect on the traffic congestion in the other road, and -1 shows they do not affect each other at all.

3.4 Optimization Model

In this paper, we assume the travelers are strategic and the network planner is trying to develop solutions for strategic travelers. The problem is formulated as a bi-level problem. The lower level problem is related to the travelers. They determine their route and their transport to minimize the total travel cost of the transportation system. The upper level problem is related to the network planner. The goals of the network planner are minimizing air pollution and maximizing network reliability by installing new transport facilities and augmenting the capacity of the links.

Upper level model is formulated by Eq. (3-34)-(3-44). The network planner objectives are shown in Eq. (3-34) and (3-35) which are minimizing air pollution and maximizing network reliability, respectively. Eq. (3-36) show there is limited budget for constructing specific numbers of bus and railway lines (B_m). There are maximum and minimum values for capacity expansions in Eq. (3-37). Binary variables are defined in Eq. (3-38) show whether facilities for the transport type m are installed in the links in set A_2 or not. A_2 is the set of candidate links for constructing bus and railway facilities. If it is not possible to install specific transport types on specific links, their corresponding binary variables are fixed to zero. Eq. (3-39) and (3-41) present the minimum travel demand in each link in order to have bus or railway facilities in each link. Eq. (3-40) and (3-42) show the maximum travel demand can be satisfied by bus and railway facilities in one hour. These constraints do not force the passengers to use particular services. The passengers make their choices based on the existing bus and railway facilities. That is why the binary variables which are decision variables in the upper level for the network planner are parameters for the lower level problem. The network planner decides to select the optimal links for installing bus and railway facilities to minimize emissions and traffic congestion. The travelers consider the existing network structure and decide which routes and transports should be selected to travel from their origin to their destinations to minimize the total travel cost that is modeled in the lower level problem.

Upper level model

$$z_1 = min\ \sum_{a \in A} \sum_{m \in M} 0.2038 y_a^m E(t_a^m) \exp\left(0.7962(l_a/E(t_a^m))\right)\ v_a^m \quad \text{if } m \text{ is a non-electric mode} \tag{3-34}$$

$$z_2 = max\ \ P(x_a \leq Ca_a + e_a) \tag{3-35}$$

subject to

$$y_a^m \leq B_m\ \forall a \in A_2\ \forall m \in bus, rail \tag{3-36}$$

$$0 \leq e_a^{min} \leq e_a \leq e_a^{max} \quad \forall a \in A \tag{3-37}$$

$$y_a^m = 0\ or\ 1\ \ \forall a \in A_2\ \ \forall m \in bus, rail \tag{3-38}$$

$$\bar{x}_a^{rail} \geq f_{min}^{rail}\ y_a^{rail} \quad \forall a \in A_2 \tag{3-39}$$

$$\bar{x}_a^{rail} \leq f_{max}^{rail}\ y_a^{rail} \quad \forall a \in A_2 \tag{3-40}$$

$$\bar{x}_a^{bus} \geq f_{min}^{bus}\ y_a^{bus} \quad \forall a \in A_2 \tag{3-41}$$

$$\bar{x}_a^{bus} \leq f_{max}^{bus}\ y_a^{bus} \quad \forall a \in A_2 \tag{3-42}$$

$$\bar{x}_a^{bus} \leq M\ y_a^{car} \quad \forall a \in A \tag{3-43}$$

$$\bar{x}_a^{car} \geq 0\ \ \forall a \in A \tag{3-44}$$

We use the system optimum (SO) concept to formulate the lower level problem instead of user equilibrium formulation (UE). SO formulation is more normative in nature than UE (Sheffi, 1985). The lower level problem is formulated in Eq. (3-45)-(3-60). In this model, travelers select their route and their modes to move from origin to destination nodes to minimize the total travel cost of the transportation network considered as the objective function in Eq. (3-45). The travel cost in Eq. (3-45) is a function of mean travel time in each link as shown in Eq. (3-24). The mean travel time for each transport in each link ($E(t_a^m)$) is a function of the mean and variance of the on road travel demand in each link as shown in Eq. (3-23). The mean and variance of the on-road travel demand are functions of the specific-mode travel demand in each road as shown in Eq. (3-14) and Eq. (3-15). Finally, according to Eq. (3-11) and Eq. (3-12), the mean and variance of the specific-mode travel demand are functions of the mean and variance of total demand between pair *p*-*q* and the route choice proportion as shown in Eq. (3-11) and Eq. (3-12). Therefore the total travel cost is a function of the total demand and route choice proportions. Eq. (3-46)-(3-59) are model constraints. Eq. (3-46) shows the summation of route choice proportion between origin and destination nodes should be equal to 1. The mean and variance of demand for each mode between origin *p* and destination *q* are formulated in Eq. (3-47) and Eq. (3-48), which are known. Besides, the mean and variance of travel demand for mode *m* on link *a* are formulated in Eq. (3-49), (3-50) and (3-51). Eq. (3-52)-(3-55) show if there are railway and bus facilities on link *a* or not. In addition the mean and variance of on road travel demand are formulated in Eq. (3-56) and (3-57) respectively. Eq. (3-58), (3-59) and

(3-60) shows the mean and variance of the specific-mode travel demand on link *a* and route choice proportions should be positive, respectively. The formulation is based on SO concept because each traveler behaves cooperatively in choosing his/her own route and transportation types to minimize the total travel cost of the system.

Lower level model

$$z_3 = \min \sum_{p \in P} \sum_{q \in Q} \sum_{k \in K} \vartheta^{pqk} \tag{3-45}$$

subject to

$$\sum_{r \in R_{pq}} \gamma_{pqr} = 1 \tag{3-46}$$

$$\bar{d}_{pq} = \tau\left(H_p + E_q\right) \quad 0 \le \tau \le 1, \forall p \in P, \forall q \in Q \tag{3-47}$$

$$\sigma_{pq} = \Omega\left(\bar{d}_{pq}\right) \qquad 0 \le \Omega \le 1, \forall p \in P, \forall q \in Q \tag{3-48}$$

$$\sum_{m \in M} \bar{x}_a^m = \sum_{p \in P} \sum_{q \in Q} \sum_{r \in R_{pq}} \bar{d}_{pq} \gamma_{pqr} \delta_{pqra} \quad \forall a \in A \tag{3-49}$$

$$\textstyle\sum_{m \in M} \sigma_a^m = \sum_{p \in P} \sum_{q \in Q} \sum_{\acute{r} \in \acute{R}_{pq}} \sum_{r \in R_{pq}} \sigma_{pq} \gamma_{pqr} \gamma_{pq\acute{r}} \delta_{pqra} \delta_{pq\acute{r}a} \qquad \forall a \in A \tag{3-50}$$

$$\sigma_a^m \le \bar{x}_a^m \ \ \forall m \in M, \qquad \forall a \in A \tag{3-51}$$

$$\sigma_a^{rail} \le M\, y_a^{rail} \ \ \forall a \in A \tag{3-52}$$

$$x_a^{rail} \le f_{max}^{rail}\, y_a^{rail} \ \ \forall a \in A \tag{3-53}$$

$$\bar{x}_a^{bus} \le f_{max}^{bus}\, y_a^{bus} \ \ \forall a \in A \tag{3-54}$$

$$\sigma_a^{bus} \le M\, y_a^{bus} \ \forall a \in A \tag{3-55}$$

$$\bar{x}_a = \frac{\bar{x}_a^{car}}{\pi} + \omega \frac{\bar{x}_a^{bus}}{\theta} \quad \forall a \in A \tag{3-56}$$

$$\sigma_a = \frac{\sigma_a^{car}}{\pi^2} + \omega^2 \frac{\sigma_a^{bus}}{\theta^2} \quad \forall a \in A \tag{3-57}$$

$$\bar{x}_a^m \ge 0 \ \ \forall m \in M, \forall a \in A \tag{3-58}$$

$$\sigma_a^m \ge 0 \ \ \forall m \in M, \forall a \in A \tag{3-59}$$

$$\gamma_{pqr} \ge 0 \ \ \forall p \in P, \forall q \in Q, \forall r \in R_{pq} \tag{3-60}$$

The presented mathematical model, Eq. (3-34)-(3-60), is a bi-level MINLP problem. There are several possible reformulations of the bi-level programming problem into ordinary one-level problem. One level programming problem clearly can be used to derive necessary and sufficient optimality conditions for the bi-level programming problem. One of the possible reformulation approaches to change the problem to one-level is using the Karush-Kuhn-Tucker (KKT) conditions of the lower level model. The single level problem is equivalent to the bi-level programming problem provided that the lower level problem is convex (Dempe, 2002).

The objective function of the lower level problem is convex as proven in *lemma 1* but the feasible region is non-convex due to the bi-linear term ($\gamma_{pq\acute{r}}\ \gamma_{pqr}$) in Eq. (3-50). In this study, McCormick envelopes are employed to relax the bi-linear term into a convex term. Using the McCormick envelopes, the Eq. (3-50) is replaced by the Eqs.

(3-61)-(3-65). You can refer to the Appendix for more information about the McCormick envelopes to relax bi-linear terms.

$$\sum_{m\in M}\sigma_a^m = \sum_{p\in P}\sum_{q\in Q}\sum_{\acute{r}\in \acute{R}_{pq}}\sum_{r\in R_{pq}}\sigma_{pq}\,\Lambda_{pqr\acute{r}}\,\delta_{pqra}\delta_{pq\acute{r}a} \qquad \forall a\in A \tag{3-61}$$

$$\Lambda_{pqr\acute{r}} \geq 0 \quad \forall p\in P, \forall q\in Q, \forall r\in R_{pq}, \forall \acute{r}\in \acute{R}_{pq} \tag{3-62}$$

$$\Lambda_{pqr\acute{r}} \geq \gamma_{pqr} + \gamma_{pq\acute{r}} - 1 \quad \forall p\in P, \forall q\in Q, \forall r\in R_{pq}, \forall \acute{r}\in \acute{R}_{pq} \tag{3-63}$$

$$\Lambda_{pqr\acute{r}} \leq \gamma_{pqr} \quad \forall p\in P, \forall q\in Q, \forall r\in R_{pq}, \forall \acute{r}\in \acute{R}_{pq} \tag{3-64}$$

$$\Lambda_{pqr\acute{r}} \leq \gamma_{pq\acute{r}} \quad \forall p\in P, \forall q\in Q, \forall r\in R_{pq}, \forall \acute{r}\in \acute{R}_{pq} \tag{3-65}$$

Lemma 1. The objective function of lower level problem is convex.

Proof. If we prove $E(t_a^m)$ in Eq. (3-24) is convex, we can claim that the objective function is convex. Showing Eq. (3-22) is convex is sufficient to conclude that $E(t_a^m)$ is also convex. In order to prove convexity, we need to show that Eq. (3-66), (3-67) and (3-68) are convex.

$$AA = \left(\frac{\bar{x}_a^{car}}{\pi} + \omega\frac{\bar{x}_a^{bus}}{\theta}\right)^4 \tag{3-66}$$

$$BB = 6\left(\frac{\sigma_a^{car}}{\pi^2} + \omega^2\frac{\sigma_a^{bus}}{\theta^2}\right)\left(\frac{\bar{x}_a^{car}}{\pi} + \omega\frac{\bar{x}_a^{bus}}{\theta}\right)^2 \tag{3-67}$$

$$CC = 3\left(\frac{\sigma_a^{car}}{\pi^2} + \omega^2\frac{\sigma_a^{bus}}{\theta^2}\right)^2 \tag{3-68}$$

The Hessian of Eq. (3-66), (3-67) and (3-68) are positive semi-definite (as shown in appendix A), so the objective function is convex.

As seen in Eq. (3-45)-(3-60) the objective function and the constraints are continuously differentiable at a point $({\gamma_{pqr}}^*, \bar{x}_a^{m*}, \sigma_a^{m*})$. If $({\gamma_{pqr}}^*, \bar{x}_a^{m*}, \sigma_a^{m*})$ is a global minimum, then the solution satisfies some regularity conditions (see Eq. (3-69)-(3-110)). Constants $\mu_.^{\,i}$ ($i=1, \ldots, 8$) and, $\lambda_.^{\,j}$ ($j=1, \ldots, 5$) are the KKT multipliers.

Closed form expressions for the optimality condition of the lower level problem (Eq. (3-45)-(3-60)) are formulated in Eq. (3-69)- (3-110) by using KKT optimality conditions. $\mu_.^{\,1}$ to $\mu_.^{\,8}$ are lagrangian multipliers of Eq. (3-51)-(3-55) and Eq. (3-63)-(3-65). $\lambda_.^{\,1}$ to $\lambda_.^{\,5}$ are lagrangian multipliers of Eq. (3-46), Eq. (3-49)-(3-50) and Eq. (3-56)-(3-57).

Eq. (3-69)-(3-85) show primal feasibility. Eq. (3-86)-(3-93) are complementary slackness. Eq. (3-94)-(3-100) show dual feasibility. Eq. (3-101)-(3-110) present stationary conditions.

	Lagrangian multipliers	
$\sum_{r\in R_{pq}}\gamma_{pqr} = 1$	$\boldsymbol{\lambda_{pq}^1}$	(3-69)
$\sum_{p\in P}\sum_{q\in Q}\sum_{r\in R_{pq}}\bar{d}_{pq}\gamma_{pqr}\delta_{pqra} - \sum_{m\in M}\bar{x}_a^m = 0 \;\; \forall a\in A$	$\boldsymbol{\lambda_{am}^2}$	(3-70)
$\sum_{p\in P}\sum_{q\in Q}\sum_{\acute{r}\in \acute{R}_{pq}}\sum_{r\in R_{pq}}\sigma_{pq}\,\Lambda_{pqr\acute{r}}\,\delta_{pqra}\delta_{pq\acute{r}a} - \sum_{m\in M}\sigma_a^m = 0 \;\; \forall a\in A$	$\boldsymbol{\lambda_{am}^3}$	(3-71)
$\bar{x}_a - \frac{\bar{x}_a^{car}}{\pi} - \omega\frac{\bar{x}_a^{bus}}{\theta} = 0 \;\; \forall a\in A$	$\boldsymbol{\lambda_{a}^4}$	(3-72)

$$\sigma_a - \frac{\sigma_a^{car}}{\pi^2} - \omega^2 \frac{\sigma_a^{bus}}{\theta^2} = 0 \quad \forall a \in A \qquad \boldsymbol{\lambda_a^5} \tag{3-73}$$

$$\bar{x}_a^{rail} \le f_{max}^{rail}\, y_a^{rail} \quad \forall a \in A \qquad \boldsymbol{\mu_a^1} \tag{3-74}$$

$$\sigma_a^{rail} \le M\, y_a^{rail} \quad \forall a \in A \qquad \boldsymbol{\mu_a^2} \tag{3-75}$$

$$\bar{x}_a^{bus} \le f_{max}^{bus}\, y_a^{bus} \quad \forall a \in A \qquad \boldsymbol{\mu_a^3} \tag{3-76}$$

$$\sigma_a^{bus} \le M\, y_a^{bus} \quad \forall a \in A \qquad \boldsymbol{\mu_a^4} \tag{3-77}$$

$$\gamma_{pqr} + \gamma_{pq\acute{r}} - 1 - \Lambda_{pqr\acute{r}} \le 0 \quad \forall p \in P, \forall q \in Q, \forall r \in R_{pq}, \forall \acute{r} \in \acute{R}_{pq} \qquad \boldsymbol{\mu_{pqr\acute{r}}^5} \tag{3-78}$$

$$\Lambda_{pqr\acute{r}} - \gamma_{pqr} \le 0 \quad \forall p \in P, \forall q \in Q, \forall r \in R_{pq}, \forall \acute{r} \in \acute{R}_{pq} \qquad \boldsymbol{\mu_{pqr\acute{r}}^6} \tag{3-79}$$

$$\Lambda_{pqr\acute{r}} - \gamma_{pq\acute{r}} \le 0 \quad \forall p \in P, \forall q \in Q, \forall r \in R_{pq}, \forall \acute{r} \in \acute{R}_{pq} \qquad \boldsymbol{\mu_{pqr\acute{r}}^7} \tag{3-80}$$

$$\sigma_a^m - \bar{x}_a^m \le 0 \quad \forall m \in M, \qquad \forall a \in A \qquad \boldsymbol{\mu_{am}^8} \tag{3-81}$$

$$\bar{x}_a^m \ge 0 \quad \forall m \in M, \forall a \in A \tag{3-82}$$

$$\gamma_{pqr} \ge 0 \quad \forall p \in P, \forall q \in Q, \forall r \in R \tag{3-83}$$

$$\sigma_a^m \ge 0 \quad \forall m \in M, \qquad \forall a \in A \tag{3-84}$$

$$\Lambda_{pqr\acute{r}} \ge 0 \quad \forall p \in P, \forall q \in Q, \forall r \in R_{pq}, \forall \acute{r} \in \acute{R}_{pq} \tag{3-85}$$

$$\mu_a^1 \left(\bar{x}_a^{rail} - f_{max}^{rail}\, y_a^{rail}\right) = 0 \quad \forall a \in A \tag{3-86}$$

$$\mu_a^2\left(\sigma_a^{rail} - M\, y_a^{rail}\right) = 0 \quad \forall a \in A \tag{3-87}$$

$$\mu_a^3 \left(\bar{x}_a^{bus} - f_{max}^{bus}\, y_a^{bus}\right) = 0 \quad \forall a \in A \tag{3-88}$$

$$\mu_a^4 \left(\sigma_a^{bus} - M\, y_a^{bus}\right) = 0 \quad \forall a \in A \tag{3-89}$$

$$\mu_{pqr\acute{r}}^5 \left(\gamma_{pqr} + \gamma_{pq\acute{r}} - 1 - \Lambda_{pqr\acute{r}}\right) = 0 \quad \forall p \in P, \forall q \in Q, \forall r \in R_{pq}, \forall \acute{r} \in \acute{R}_{pq} \tag{3-90}$$

$$\mu_{pqr\acute{r}}^6 \left(\Lambda_{pqr\acute{r}} - \gamma_{pqr}\right) = 0 \quad \forall p \in P, \forall q \in Q, \forall r \in R_{pq}, \forall \acute{r} \in \acute{R}_{pq} \tag{3-91}$$

$$\mu_{pqr\acute{r}}^7 \left(\Lambda_{pqr\acute{r}} - \gamma_{pq\acute{r}}\right) = 0 \quad \forall p \in P, \forall q \in Q, \forall r \in R_{pq}, \forall \acute{r} \in \acute{R}_{pq} \tag{3-92}$$

$$\mu_{a\,m}^8 \left(\sigma_a^m - \bar{x}_a^m\right) = 0 \quad \forall a \in A, \forall m \in M \tag{3-93}$$

$$\mu_a^1 \ge 0 \quad \forall a \in A \tag{3-94}$$

$$\mu_a^2 \ge 0 \quad \forall a \in A \tag{3-95}$$

$$\mu_a^3 \ge 0 \quad \forall a \in A \tag{3-96}$$

$$\mu_a^4 \ge 0 \quad \forall a \in A \tag{3-97}$$

$$\mu_{pqr\acute{r}}^5 \ge 0 \quad \forall p \in P, \forall q \in Q, \forall r \in R_{pq}, \forall \acute{r} \in \acute{R}_{pq} \tag{3-98}$$

$$\mu_{pqr\acute{r}}^6 \ge 0, \qquad \mu_{pqr\acute{r}}^7 \ge 0 \quad \forall p \in P, \forall q \in Q, \forall r \in R_{pq}, \forall \acute{r} \in \acute{R}_{pq} \tag{3-99}$$

$$\mu_{a\,m}^8 \ge 0 \quad \forall a \in A, \forall m \in M \tag{3-100}$$

Stationary point

$$\sum_{a \in A} \sum_{m \in M} \lambda_{am}^2 \bar{d}_{pq} \delta_{pqra} + \lambda_{pq}^1 + \mu_{pqr\acute{r}}^5 - \mu_{pqr\acute{r}}^6 - \mu_{pqr\acute{r}}^7 = 0 \quad \forall p \in P, \forall q \in Q, \forall r \in R_{pq} \qquad \boldsymbol{\gamma_{pqr}} \tag{3-101}$$

$$\sum_{a \in A} \sum_{m \in M} \lambda_{am}^3\, \sigma_{pq}\, \delta_{pqra}\, \delta_{pq\acute{r}\acute{a}} - \mu_{pqr\acute{r}}^5 + \mu_{pqr\acute{r}}^6 + \mu_{pqr\acute{r}}^7 = 0 \quad \forall p \in P, \forall q \in Q, \forall r \in R_{pq}, \forall \acute{r} \in \acute{R}_{pq} \qquad \boldsymbol{\Lambda_{pqr\acute{r}}} \tag{3-102}$$

$$-\frac{(\omega \lambda_a^4)}{\pi} - \lambda_{a\,bus}^2 + \mu_a^3 - \mu_{a\,bus}^8 = 0 \quad \forall a \in A \qquad \boldsymbol{\bar{x}_a^{bus}} \tag{3-103}$$

$$-\frac{(\lambda_a^4)}{\pi} - \lambda_{a\,car}^2 - \mu_{a\,car}^8 = 0 \quad \forall a \in A \qquad \boldsymbol{\bar{x}_a^{auto}} \tag{3-104}$$

$$\mu_a^1 - \lambda_{a\,rail}^2 - \mu_{a\,rail}^8 = 0 \quad \forall a \in A \qquad \boldsymbol{\bar{x}_a^{metro}} \tag{3-105}$$

$$-\frac{(\omega^2 \lambda_a^5)}{\pi^2} - \lambda_{a\,bus}^3 + \mu_a^4 + \mu_{a\,bus}^8 = 0 \quad \forall a \in A \qquad \boldsymbol{\sigma_a^{bus}} \tag{3-106}$$

$$-\frac{(\lambda_a^5)}{\pi^2} - \lambda_{a\,car}^3 + \mu_{a\,car}^8 = 0 \quad \forall a \in A \qquad \boldsymbol{\sigma_a^{auto}} \tag{3-107}$$

$$\mu_a^2 - \lambda_{a\,rail}^3 + \mu_{a\,rail}^8 = 0 \quad \forall a \in A \qquad \boldsymbol{\sigma_a^{metro}} \tag{3-108}$$

$$\lambda_a^4 + \sum_{p \in P} \sum_{q \in Q} \sum_{r \in R_{pq}} \left(\left(\sum_{k \in K} vot^k \left(\frac{0.15 \check{t}_a^0 (4\bar{x}_a^3 + 12\bar{x}_a \sigma_a)}{(Ca_a + e_a)^4} \right) \delta_{pqra} \right) + \left(\sum_{k \in K} vot^k \left(\frac{0.15 \hat{t}_a^0 (4\bar{x}_a^3 + 12\bar{x}_a \sigma_a) y_a^{bus}}{(Ca_a + e_a)^4} \right) \delta_{pqra} \right) \right) = 0 \quad \forall a \in A \qquad \boldsymbol{\bar{x}_a} \tag{3-109}$$

$$\lambda_a^5 + \sum_{p \in P} \sum_{q \in Q} \sum_{r \in R_{pq}} \left(\left(\sum_{k \in K} vot^k \left(\frac{0.15 \check{t}_a^0 (6\bar{x}_a^2 + 6\sigma_a)}{(Ca_a + e_a)^4} \right) \delta_{pqra} \right) + \left(\sum_{k \in K} vot^k \left(\frac{0.15 \hat{t}_a^0 (6\bar{x}_a^2 + 6\sigma_a) y_a^{bus}}{(Ca_a + e_a)^4} \right) \delta_{pqra} \right) \right) = 0 \quad \forall a \in A \qquad \boldsymbol{\sigma_a} \tag{3-110}$$

Therefore, an integrated single level for the bi-level problem, Eq. (3-34)-(3-60), can be formulated by considering Eq. (3-34) and (3-35) as the objective functions and Eq. (3-36)-(3-44) and Eq. (3-69)-(3-110) as the constraints. The reformulated model is a single level MINLP problem.

3.5 Solution Algorithm

Major methods for solving MINLP problems include branch-and-cut, which is a generalization of the linear case (Stubbs and Mehrotra, 1999), Generalized Benders Decomposition (GBD) (Geoffrion, 1972), Outer Approximation (OA) (Duran and Grossmann, 1986; Fletcher and Leyffer, 1994) and Extended Cutting Plane (ECP) method (Westerlund and Pettersson, 1995). GBD and OA are iterative methods that solve a sequence of alternate NLP sub problems with all the discrete variables fixed, and MILP master problems that perform the optimization in the discrete space. The ECP method relies on successive linearization to build MILP approximation problems. The OA algorithm requires the solution of NLP sub problems, which are obtained by fixing the binary variables, and MILP master problems. The master problem is formulated by using hyper planes that replace the non-linear functions.

In this study, ϵ-constraint method for generating set of Pareto solutions and Outer Approximation method for solving each MINLP problem are used to develop a solution algorithm for the bi-objective MINLP problem. The implemented algorithm is presented in Figure 10.

Input: Bi-objective MINLP problem
Output: efficient solutions

Begin
Set $z_1^{UB}=bigM$ and $z_1^{LB}=-bigM$
Set $z_2^{UB}=bigM$ and $z_2^{LB}=-bigM$

Calculate the pay-off table……………………………………………………
Consider z_1 as the objective function (minimization)
Solve single objective MINLP problems by DICOPT solver
While $z_1^{UB}- z_1^{LB} \geq \vartheta$ ***do***
Fix $y = y^{Opt}$ (binary variables)
Solve NLP subproblem
$z_1^{UB} = z_1^{opt}$
Approximate non-linear terms by linear terms in point cx^{opt}
Solve MILP master problem
$z_1^{LB} = z_1^{opt}$
End
$z_1^{LO} = z_1^{opt}$
$z_2^{LO} = z_2(cx^{opt},y^{opt})$

Consider z_2 as the objective function (maximization)
Solve single objective MINLP problems by DICOPT solver
While $z_2^{UB}- z_2^{LB} \geq \vartheta$ ***do***

Fix $y = y^{opt}$
Solve NLP subproblem
$z_2^{LB} = z_2^{opt}$
Approximate non-linear terms by linear terms in point cx^{opt}
Solve MILP master problem
$z_2^{UB} = z_2^{opt}$
End
$z_2^{UP} = z_2^{opt}$
$z_1^{UP} = z_1(cx^{opt}, y^{opt})$

Display z_1^{LO}, z_1^{UP}, z_2^{LO}, z_2^{UP}

Calculate efficient solutions……………………………………………………………………
Set $z_1^{UB}=big\text{-}M$ and $z_1^{LB}=-big\text{-}M$
Set $z_2^{UB}=big\text{-}M$ and $z_2^{LB}=-big\text{-}M$

$$\varepsilon = (z_2^{UP} - z_2^{LO})/n \tag{3-111}$$

For $j = 1$ *to* n ***do***

$$z_2 = z_2^{UP} - j\,\varepsilon \tag{3-112}$$

Solve single objective MINLP problems considering z_1 as the objective function, by DICOPT solver
While $z_1^{UB} - z_1^{LB} \geq \vartheta$ ***do***
Fix $y = y^{opt}$
Solve NLP sub-problem
$z_1^{UB} = z_1^{opt}$
Approximate non-linear terms by linear terms in cx^{opt} point
Solve MILP master problem
$z_1^{LB} = z_1^{opt}$
End
Display z_1^{opt}, z_2, cx^{opt} and y^{opt}

End

End

Figure 10. ϵ-Constraint Outer Approximation Algorithm

In the first step of the algorithm the pay-off table generates. The elements of this table are the upper bound and lower bound of the first objective function (z_1^{UP} and z_1^{LO}) and the second objective function (z_2^{UP} and z_2^{LO}). In the second step, by considering the first objective function as the main objective and changing the values of the second objective function from its best value to its worst value using Eq.(3-111) and (3-112), Pareto solutions generate.

The optimal solution for each Pareto solution is obtained using OA algorithm. As shown in the last “while-do” parts of Figure 10, the NLP and MILP sub problems generates iteratively until the gap between the lower bound (z_1^{LB}) and upper bound (z_1^{UB}) for the first objective function for each Pareto solution becomes less than ϑ. ϑ is a small value set to 0.01 in our setting. $z_1^{opt}$and z_2^{opt} show the optimal values for the first and second objectives in Eq. (3-34) and (3-35), respectively. cx^{opt} and y^{opt} show the optimal values for the continues and binary variables, respectively.

The detail information about the formulations of NLP and MILP sub problems are provided in the Appendix. The non-linear terms of the single level model, Eq. (3-34)-(3-35), Eq. (3-36)- (3-44) and Eq. (3-69)-(3-110) are listed in Table 1 of Appendix. In addition, the closed form expressions of the derivatives used for estimating the non-linear terms with linear terms are formulated in Table 1 of Appendix.

3.6 Illustrative Example

Figure 11 shows the layout of the example network consisting of six nodes, seven links, two origins, and two destinations. As shown in Figure 11 there are two routes to travel from origin 1 to destination 3 (route 1: link 1, route 2: links 2-5-6), one route from origin 1 to destination 4 (links 2-5-7), one route from origin 2 to destination 3 (links 4-5-6) and two routes from origin 2 to destination 4 (route 1: links 4-5-7, route 2: link 3). The characteristics of links, zones and income groups are listed in Table 5. The capacity of network links is allowed to expand up to 10% of the existing link capacity as shown in Eq. (3-113).

$$0 \leq y_a \leq 0.1Ca_a \tag{3-113}$$

We assume that there are no railway and bus lines in the network and there is budget to install three bus lines and three railway lines in three roads. Correlation coefficients of travel demand among links are considered according to

Table **6**. The values of parameters ω, π and θ are considered 3, 2 and 6 respectively. The minimum travel demand for railway vehicles (f_{min}^{rail}) and buses (f_{min}^{bus}) are considered equal to 30 and 9 respectively. In addition, the maximum travel demand for railway vehicles (f_{max}^{rail}) and buses (f_{max}^{bus}) are considered equal to 100 and 50 passengers per hour, respectively. The population in each origin and destination nodes is equal to 100. The average values for waiting and walking times are considered equal to zero (Davis et al 2011; Miandoabchi et al 2011b; Yim et al 2011; Ma and Lo 2012; Ng and Lo 2013). The coefficients for the mean (τ) and variance (Ω) of total travel demand are considered equal to 0.5 and 0.5, respectively.

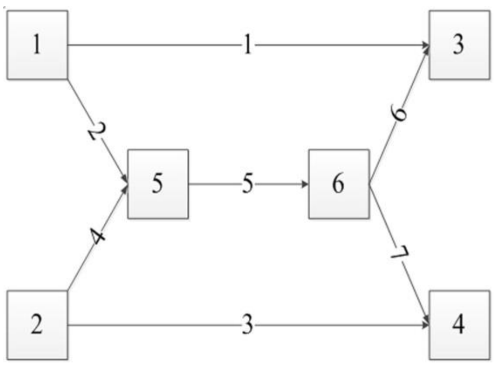

Figure 11. The schematic drawing of the numerical example

Table 5. The characteristics of the illustrative example

Link number	$\check{t}_0^a$	$\hat{t}_0^a$	$\acute{t}_0^a$	Ca_a(veh/h)	p_a^{auto}	p_a^{bus}	p_a^{rail}	l_a (km)
1	0.13	0.13	0.1	78	0.053	0.25(monetary unit)	0.25(monetary unit)	8
2	0.03	0.03	0.025	23	0.013	0.25	0.25	2
3	0.15	0.15	0.1125	23	0.06	0.25	0.25	9
4	0.05	0.05	0.0375	43	0.02	0.25	0.25	3
5	0.1	0.1	0.075	93	0.04	0.25	0.25	6
6	0.05	0.05	0.0375	43	0.02	0.25	0.25	3
7	0.067	0.067	0.05	43	0.027	0.25	0.25	4

Income group	vot^k
High	5
Low	4

Table 6. Correlation coefficients of travel demand among links

link	1	2	3	4	5	6	7
1	1	0	0.2	0.3	0.05	0.1	0.2
2	0	1	0	0.1	0.2	0.3	0.2
3	.2	0	1	0	0.4	0	1
4	0.3	0.1	0	1	0	0	0.1
5	0.05	0.2	0.4	0	1	0	0.2
6	0.1	0.3	0	0	0	1	0.15
7	0.2	0.2	0.1	0.1	0.2	0.15	1

The optimization model is coded in in GAMS (Generalized Algebraic Modeling System) (Rosenthal, 2012) and all runs were performed on a PC Intel(R), Xeon(R), CPU 3.33GHz dual-core, 32 GB RAM running Windows 7.

The results of solving the illustrative example are shown in

Table **7**. The best solution by considering the emission index as the objective function is shown in column 1 of

Table **7** and the best solution by considering the reliability index as the objective function is shown in column 4. In addition the optimal solutions for two more Pareto solutions are shown in columns 2 and 3. The optimal solutions show the capacities of the links are expanded as much as possible to reduce emissions, traffic congestion and the travel cost. Besides, the results show different values for emissions, the reliability index and the travel cost are obtained by selecting different links for installing bus and railway facilities. The results also show the optimal route choices of the travelers to minimize the total travel cost.

The efficient frontier of optimal solutions is plotted in Figure 12. In UTOPIA point, both objectives have their best values while in NADIR point the objectives have the worst values. By moving in the efficient frontier from left to right the reliability improves but the emission increases.

Table 7. The results of the illustrative example

		1	2	3	4
Emission index		3.693	4.203	4.334	5.88
Reliability index		0.662	0.795	0.836	0.8564
Travel cost		16.197	15.33	15.43	16.76
Capacity expansion	1	7.800	7.800	7.800	7.800
	2	2.300	2.300	2.300	2.300
	3	2.300	2.300	2.300	2.300
	4	4.300	4.300	4.300	4.300
	5	9.300	9.300	9.300	9.300
	6	4.300	4.300	4.300	4.300
	7	4.300	4.300	4.300	4.300
Link travel demand for railway vehicles (passenger per hour)	1	100.000	99.908		
	2		99.805	99.799	85.756
	3	100.000	99.928	100.000	85.574
	4				
	5	100.000		100.000	
	6				
	7				95.903
Link travel demand for buses (passenger per hour	1			30.000	
	2	30.000			
	3				
	4	30.000	30.000	30.000	30.000
	5		30.000		30.000
	6			30.000	30.000
	7	30.000	30.000		
Link travel demand for cars (passenger per hour)	1		0.092	70.00	100.000
	2	70.000	0.195	0.201	14.236
	3		0.072		14.433
	4	70.000	70.000	70.00	70.000
	5	100.000	170.000	100.00	170.000
	6	100.000	100.000	70.000	70.000
	7	70.000	70.000	100.00	4.097
On road demand (number of passenger cars per hour)	1		0.046	45.00	50.000
	2	45.000	0.098	0.100	7.118
	3		0.036		7.216
	4	45.000	45.000	45.00	45.000
	5	50.000	95.000	50.00	95.000
	6	50.000	50.000	45.00	45.000
	7	45.000	45.000	50.00	2.048
Optimal route choice	Zone 1- Zone 3	100 % from route 1(link 1)	100 % from route 1	100 % from route 1	100 % from route 1
	Zone	100 % from	100 % from	100 %	100 %

1-Zone 4	route 1(links 2-5-7)	route 1	from route 1	from route 1
Zone 2-Zone 3	100 % from route 1(links 4-5-6)	100 % from route 1	100 % from route 1	100 % from route 1
Zone 2-Zone 4	100 % from route 2 (link 3)	100 % from route 2	100 % from route 2	100 % from route 2

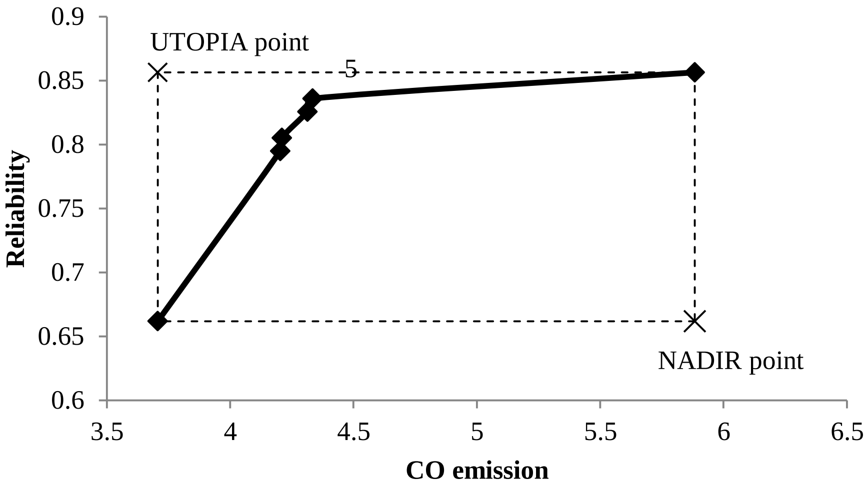

Figure 12. Efficient frontier of solutions

The number of variables and constraints of the MINLP problem and its NLP and MINLP sub problems are presented in Table 8. In addition in this table the total CPU time for 10 runs that find 6 efficient solutions is shown. Obviously CPU time increase by increasing number of runs to have more accurate representation of the efficient frontier.

Table 8. Problem Complexity

#	MINLP			NLP			MILP			# of efficient solutions generated	Total CPU time (s)
	# of variables	# of 0-1 variables	# of constraints	# of variables	# of 0-1 variables	# of constraints	# of variables	# of 0-1 variables	# of constraints		
1	578	21	642	557	0	642	565	21	4,711	6	4806.72

Table 9 shows average CPU time and number of iterations to solve NLP and MILP sub problems. In addition the number of branch and bound nodes and the number of sub problems solved for each efficient solution are presented in Table 9.

Table 9. Computational Statistics

#	NLP sub problems		MILP sub problems			# of sub problems solved
	Average CPU time	# of iterations	Average CPU time	# of iterations	# of Branch and bound nodes	
1	7.02	227926	0.17	54393	162	138
2	0.3	925	0.22	5815	37	7
3	0.34	450	0.24	3397	6	4
4	0.45	50427	0.57	997922	359	300

5	1.07	9895	0.24	26961	72	43
6	0.39	23892	0.25	124941	35	130

3.7 Sensitivity Analysis

In this section, the impacts of changing a set of parameters on the values of the objective functions and optimal solutions are analyzed. These parameters are the number of bus and railway lines can be installed in Eq. (3-36), the capacity expansions in Eq. (3-113), the correlation coefficients in Eq. (3-33), the maximum travel demands in Eq. (3-40) and (3-42), the coefficients for the mean and variance of total travel demand in Eq. (3-3) and (3-4), and the waiting time and walking time in Eq. (3-26) and (3-27).

3.7.1 Impact of changing the number of installed bus and railway lines

We test the sensitivity of the model to the number of installed bus and railway lines. The Pareto solutions of four scenarios are shown in Figure 13 (a). The scenario named "Base" show the Pareto solutions of the illustrative example in the previous section. The scenario named "only bus" represents the case that we do not have any budget to install any railway facilities but we can install bus facilities in all roads. And for the scenario named "only railway vehicles" we can install railway facilities in all roads but we cannot install any bus lines. Finally the scenario named "no bus-no rail" represents the case when there is no budget to install any public transports. As we expect the Pareto solutions of "only railway vehicle" case have better values for the two objective functions compare to the other three cases. While the Pareto solutions of "no bus-no rail" case show the worst values for the two objective functions.
In addition as shown in Figure 13 (b), the "only bus" case and the "only railway vehicle" have the highest and lowest values for the travel cost, respectively.

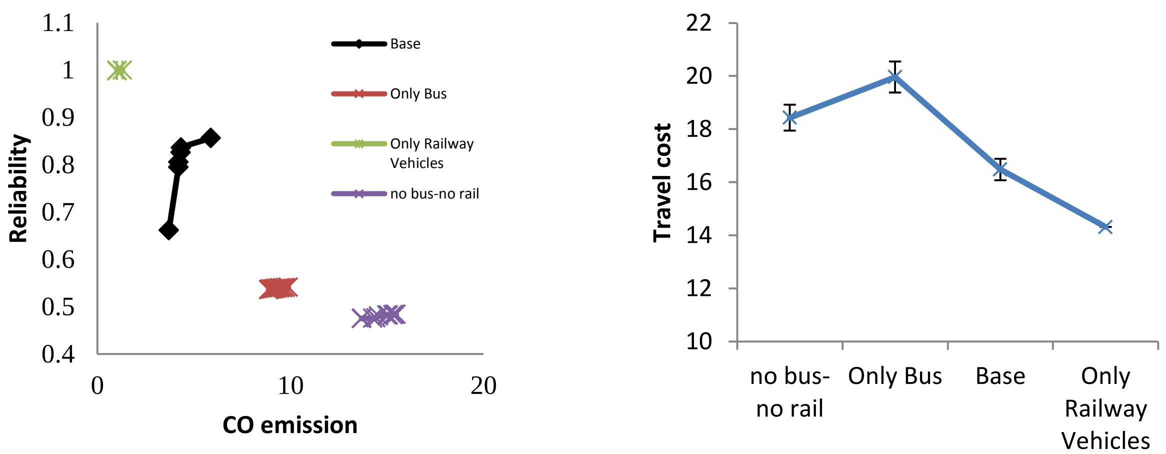

(a) (b)

Figure 13. The behavior of the objective functions by changing the number of installed bus and rail lines

3.7.2 Impacts of changing capacity expansion

Here, the behavior of the objective functions is analyzed by changing the upper bound for the amount of expansions from 0.1 in Eq. (3-113) to 0.3 and 0.5. The results show increasing the upper bound helps to improve the three objective functions as shown in Figure 14(a) and (b).

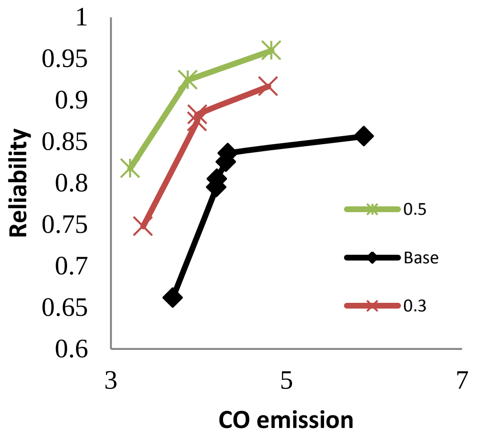

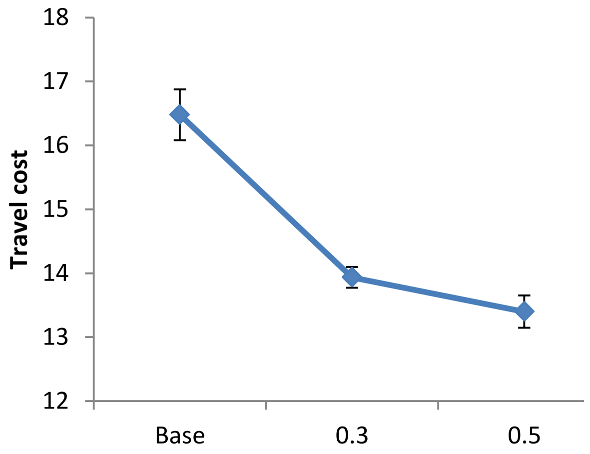

(a) (b)

Figure 14. The behaivior of the objective functions by increasing the capacity of the links

3.7.3 Impact of changing the correlation coefficients

Two scenarios are designed to analyze the impact of increasing the correlation coefficients on the behavior of objective functions and optimal solutions. Scenarios named “0.1” and “0.3” have the same setting as the illustrative example but the elements of the correlation coefficient matrix are summed by 0.1 and 0.3, respectively. The results show the stronger correlation among links does not help to improve the three objective functions: the reliability index, emissions and the travel cost, as shown in Figure 15(a) and (b).

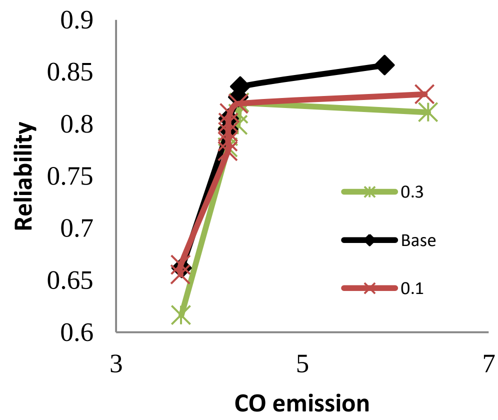

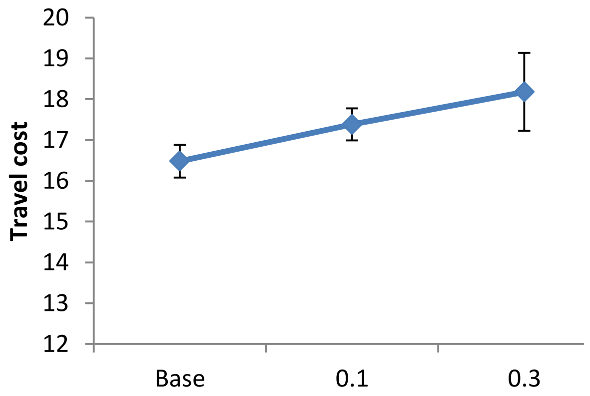

(a) (b)

Figure 15. The behaivior of the objective functions by increasing the correlations among the links

3.7.4 Impact of changing the maximum number of passengers can carried by buses and railway vehicles

As shown in Eq. (3-40) and (3-42), there is a limitation on the maximum number of passengers can carried by buses and railway vehicles per hour. Based on the setting of the illustrative example, railway vehicles and buses can carry maximum 100 and 30 passengers per hour. In this sub sections we change these values for buses and railway vehicles to 110 and 40 for the scenario named “110&40” and to 140 and 70 for the scenario named “140&70”, respectively. The results show increasing this upper bound improves the three objective functions as shown in Figure 16 (a) and (b).

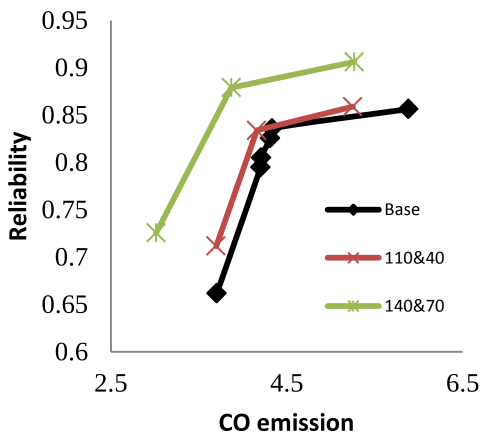

(a)

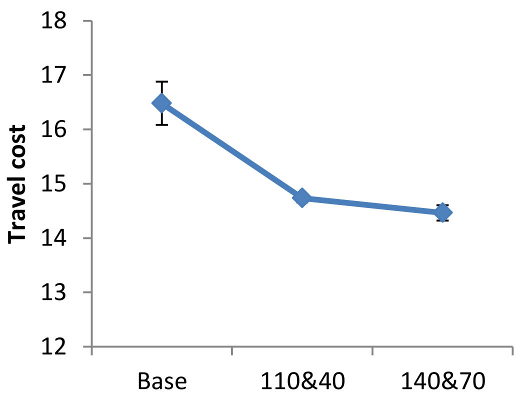

(b)

Figure 16. The behaivior of the objective functions by increasing the maximum number of passengers can carried by buses and railway vehicles

3.7.5 Impact of changing the coefficients for the mean and variance of total travel demand

The coefficients for mean (τ) and variance (Ω) of total travel demand are set to 0.5 and 0.5 for the illustrative example, respectively. Here we design two scenarios and we evaluate the impact of increasing these coefficients. The scenario named “0.6&0.6” shows the case when these two coefficients are set to 0.6 and for the scenario “0.7&0.7” they are set to 0.7. As shown in Figure 17, increasing the values of these coefficients does not help to improve the three objective functions. When the coefficients for the mean and variance of total travel demand increase, the number of travelers and uncertainty increase in the system, which are not favorable for improving the three objective functions.

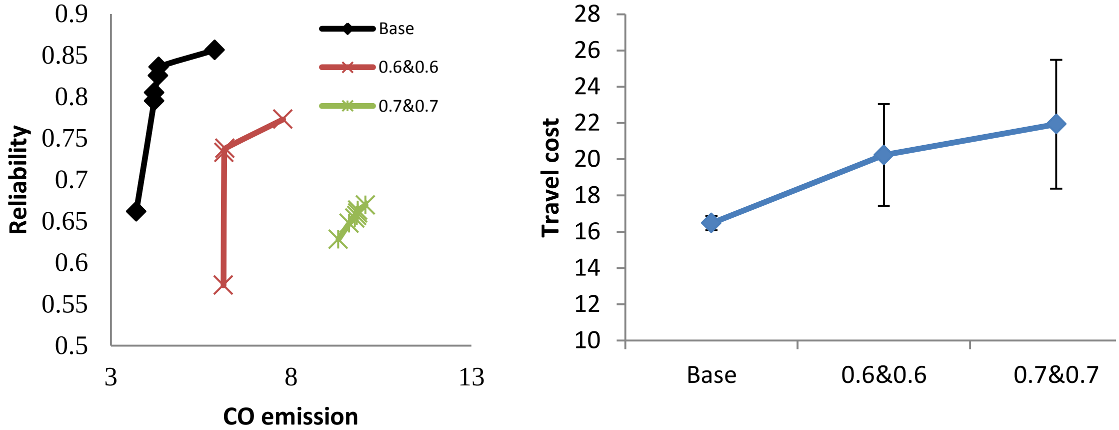

(a) (b)

Figure 17. The behaivior of the objective functions by increasing the coefficients for mean and variance of total travel demand

3.7.6 Impact of changing the average values for waiting and walking times

The average values for waiting and walking times are set to zero in the illustrative example. Here we adjust the average values for waiting and walking times to 6 min and 6 min for the scenario "6 min" and to 12 min and 12 min for the scenario "12 min". As shown in Figure 18, by increasing these values the three objective functions become worse. However just the travel cost is the function of these values but the objective functions of the upper level also change. The reason is we consider the optimality conditions of the lower level through the single level formulation.

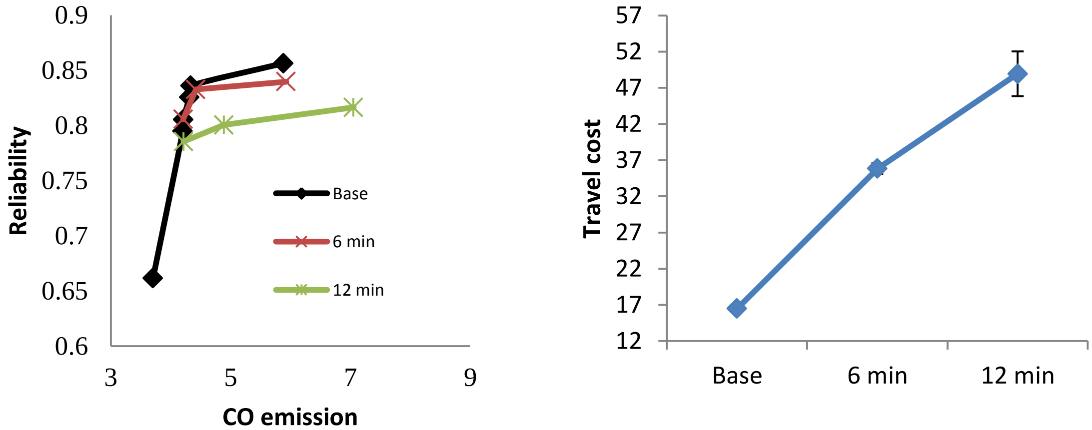

(a) (b)

Figure 18. The behaivior of the objective functions by increasing the average values for waiting and walking times

3.8 Results for Benchmark Problems

In this subsection, we evaluate the performance of our presented model on 9 different benchmark problems. Different city network layouts are developed by using JAVA programming language and their models are solved in GAMS environment. We change 4 parameters, *p*, *q*, *s* and *n*, which show, respectively, the number of origin nodes, the number of destination nodes, the number of echelons and the number of nodes in the intermediate echelons to generate different feasible layouts. After determining the values for *p*, *q*, *s* and *n,* links will connect all nodes in each echelon to all nodes in the previous and subsequent echelons. The number of routes that connect each origin node to each destination node is counted and it is considered in the models. By changing the values of *p* and *q* between 2 and 4, the value of s between 3 and 4 and the value of n between 1 and 5, we create 9 scenarios of which are labeled by vector (*p*,*q*,*s*,*n*). These 9 scenarios are selected because they have different numbers of nodes and links and we can analyze the relation between the number of nodes and links of a network with CPU time, the reliability index, the emission, and the travel cost.

For these examples, we consider 100 existing population units for each origin and destination nodes. The coefficients for the mean (τ) and variance (Ω) of total travel demand are set to 0.5 and 0.5, respectively. The data related to links and income groups are considered equal to the average values for each parameter in Table 5. The networks structures of these nine problems are given in Appendix B.

Table 10. Complexity of the problem

No	Network characteristics	# of nodes	# of links	# of variables	# of equations	# of efficient solutions	CPU time (s)
S1	(2,2,3,1)	5	4	232	240	3	350.03
S2	(2,2,3,2)	6	8	693	742	3	1112.17
S3	(2,2,3,3)	7	12	971	1,084	1	1047.31
S4	(2,2,3,4)	8	16	1,453	1,666	1	10126.43
S5	(3,3,3,3)	9	18	1,738	2,004	3	68.85
S6	(3,3,3,4)	10	24	2,864	3,363	4	1147.55
S7	(4,4,3,3)	11	24	2,693	3,178	7	355.63
S8	(3,3,4,3)	12	27	5,437	8,223	1	409.72
S9	(4,4,4,3)	14	33	8,612	13,591	1	1697.05

The results presented in Table 10 show the problem complexity, model statistics and the CPU time required to obtain the optimal solutions for each problem. The set of 9 scenarios are successfully optimized in reasonable CPU times since the problem is a network planning problem.

We group these nine examples into three categories based on having the same number of origin and destination nodes. The first four examples (S1, S2, S3 and S4) are in the category 1. The example S5, S6, and S8 are in the second category and the example S7 and S9 are in the third group. By moving from the first example to the last example of each group, the number of links in the networks increases.

The efficient frontiers of optimal solutions of the first four examples are shown in Figure 19(a). The results show by increasing the links without changing the number of echelons in the network the three objective functions improve for these examples as shown in Figure 19 (a) and (b).

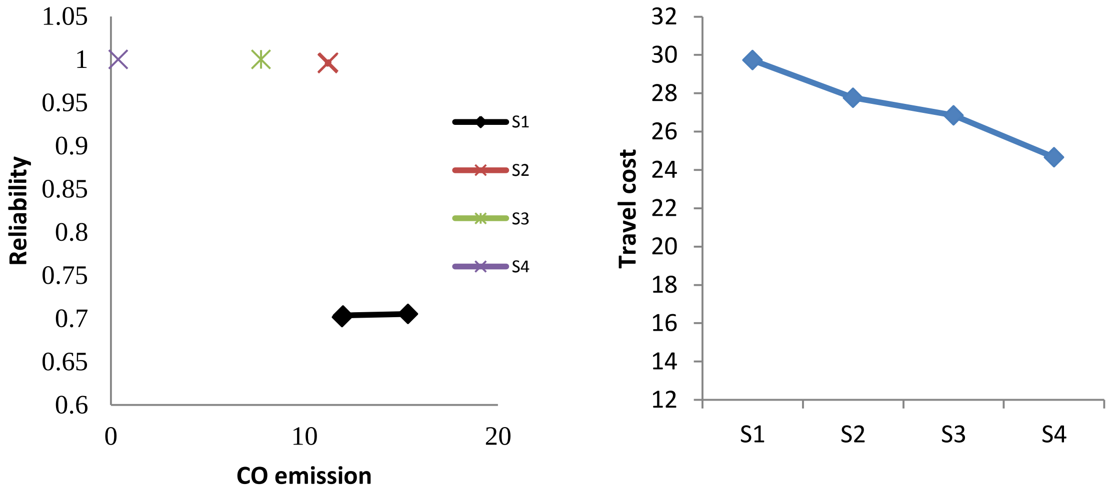

(a) (b)

Figure 19. Results for the examples of group 1

As shown in Figure 20(a) and (b), from the first example to the second example of the second category, the three objective functions improve. But for the last example all objective functions become worse compare to the first and the second example since the number of echelons increases in the network. In addition, If we consider a scenario that we can install rail way facilities in all roads of the example 5, all three objective functions are set to better values compared to other scenarios as shown in Figure 20(a) and (b).

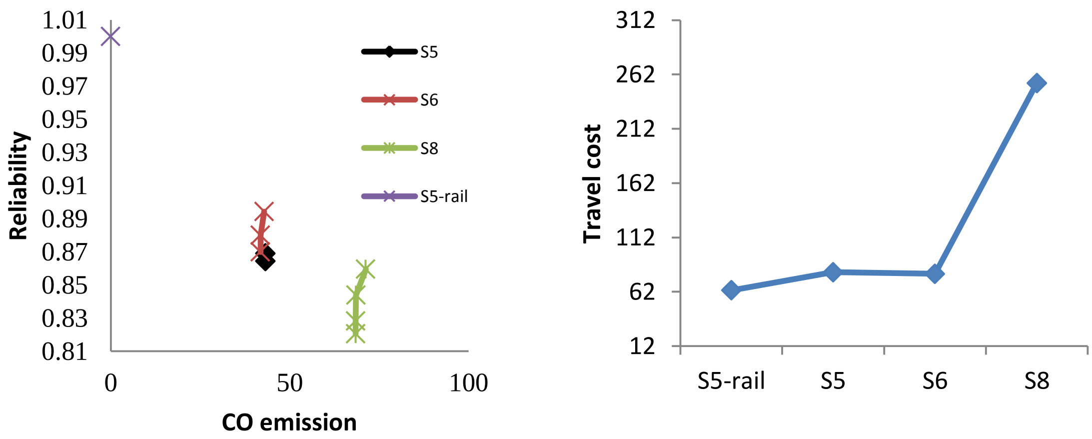

(a) (b)

Figure 20. Results for the examples of group 2

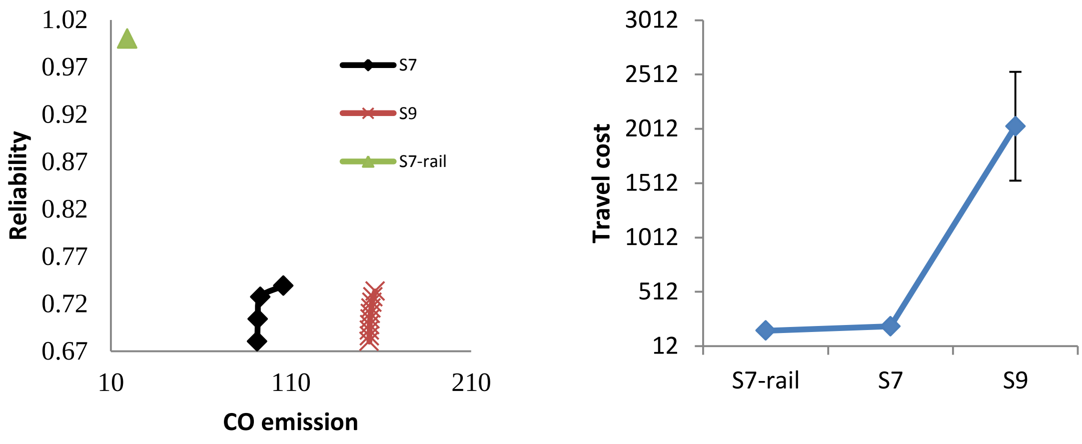

(a) (b)

Figure 21. Results for the examples of group 3

For the examples in group 3, the numbers of links and echelons from the first (S7) to the last example (S9) increase. As shown in Figure 21(a) and (b), from the first to the last one, the probability of traffic congestion changes almost in a same range but the emissions and travel cost increase by expanding the network. As shown in Figure 21 (a) and (b), if we consider a scenario with installed railway facilities in all roads, all three objective functions improve.

3.9 Conclusions

In this paper, we present a bi-level stochastic sustainable transportation model: the lower level problem is a network design problem with an objective to minimize the total travel cost and the upper level problem is a transport allocation problem with two objective functions to minimize CO emissions from transportation and minimize the probability of traffic congestion in the network. The travel cost is formulated by using BPR link impedance function for on road vehicles. The amount of CO emission production is considered as a function of the average travel time and speed of each transport in each link. In addition, the probability of traffic congestion is calculated by using multivariate normal distribution. This probability calculates the probability that travel demand in each link is less than capacity of the links plus amount of expansions.

The lower level problem is non-convex due to a bi-linear term in a constraint. McCormick envelopes are employed to relax the non-linear term into a convex term, and KKT conditions are used to formulate the closed form expressions of the optimality conditions of the lower level problem. These optimality conditions are considered as a set of constraints in the upper level model. In this manner, we formulate a single level bi-objective model that is an MINLP problem. We implement outer approximation algorithm and ϵ-constraint method to solve the problem. Outer approximation algorithm is based on generating the NLP and MILP sub problems and solving them iteratively till the optimality gap is within tolerance limits.

In this paper, the impact of changing different parameters on the behavior of the model is analyzed. In addition, we solve nine examples with different structures to analyze the relation between the structure of the network with the problem complexity and CPU time required to obtain optimal solutions. The results show the optimal solutions are obtained in reasonable CPU times, and we expect to solve larger examples using the proposed solution algorithm. Additionally, the results show the amount of emission productions, traffic congestion and travel cost highly depend on the network structures. In addition, it is shown, allocating more budgets for constructing railway lines than constructing new on-road links is a better strategy to reduce the probability of traffic congestion, travel cost, and emissions in urban areas. Constructing more railway lines helps to decrease on-road travel demands and improve the three objective values while constructing new roads may increase the travel time and emissions.

Appendix is given in Annex II

4 Chapter IV

Optimal Transportation Network Structure to Reduce Emissions, a Case Study in Istanbul Metropolitan Area

In this chapter, we formulate optimization models to minimize the emissions produced by vehicles in each main road of Istanbul metropolitan area. The amount of emissions is calculated as a function of the real average speed in each road based on traffic congestion. In this study, the travel production and attraction of 38 districts and detail information of 17,663 Istanbul main roads such as numbers of lanes, length and maximum speed limit in each main road are implemented as the input to the optimization model. The large data set is successfully handled and the formulated models are solved optimally. The optimal results show the selected roads for capacity expansion and installing additional shared public vehicles. The result shows specific roads have significant effect on emission production and traffic congestion in Istanbul metropolitan area. Furthermore, we analyze the reason of traffic congestion and pollution in these roads. In addition, in this study we analyze the effect of different fuel type on different emission production. This chapter presents the first optimization framework at micro scale level to analyze traffic emission problem in Istanbul metropolitan area.

4.1 Introduction

Transportation sector is one of the major sources for energy consumption and pollutants emissions. Road transport produces around 20% of the European Union (EU)'s total emissions of carbon dioxide (CO_2) and the main greenhouse gas (GHG) (European Commission, 2015a). In additions cars are responsible for about 12% of total EU emissions of CO_2 (European Commission, 2015b). In Turkey, 69% of carbon monoxide (CO), and 89% of mono-nitrogen oxides (NOx) are traffic originated emissions (IMM, 2009). TurkStat, (2011) reported GHG emissions as CO_2 equivalent increased 124% in 2011 compared to the 1990's emission, in Turkey. According to International Sustainable Systems Research Center (ISSRC) emissions from vehicles in developing countries are not well understood, and the ability to make accurate emissions estimates is critical for air quality management planning (Lents et al., 2007).

Quantifying the pollutant emissions contributed by the transportation sector is the initial step in developing effective policies for improving environmental sustainability in urban areas. There are two approaches for calculating emissions, micro scale and macro scale (Ryu et al., 2013). Majority of studies implement macro scale models for estimating emissions (Aggarwal and Jain, 2014; Cheng et al., 2015; Hao et al., 2014; D. He et al., 2013; J. Javid et al., 2014; Melo and Ramli, 2014; Sookun et al., 2014; Tongwane et al., 2015). These studies use the bottom-up models to calculate emissions based on energy and fuel consumption. ASIF (Activity Structure Energy Intensity Fuel Mix) (Khanna et al., 2011) and LEAP (Long-range Energy Alternatives Planning System) are two macro scale bottom-up models widely used in emission analysis (Peng et al., 2015). ASIF model estimates CO_2 emission based on vehicle-kilometer-traveled (VKT), modes of vehicles, technology, type of fuel and vintage, and amount of fuel consumption. LEAP model estimate GHG and pollutant emissions using fuel consumption, emission factor of different fuel types and vehicle travel mile-age of different vehicle types (Peng et al., 2015).

The macro scale bottom-up approaches have been widely used in emission analysis since the data requirement is generally available and simple. These approaches calculate emissions using energy and fuel consumption based on average speed limit and traveled distances for each vehicle type. However, vehicle speed is different based on traffic congestion on the different roads of a city. Therefore, macro scale approaches do not help decision makers to know about the amount of pollution in different parts of a city and its roads. Recognizing the most polluted roads and areas is very important in finding a solution to improve environmental sustainability in transportation systems.

In micro scale models, the amount of emissions is calculated using passenger travel behavior, vehicle data and road network information. This approach allows the decision maker to analyze the emissions in each road. It means this approach needs the detail information of the transportation network which is not only difficult to collect, but also makes the analysis more difficult.

By increasing traffic congestion, fuel consumption and CO_2 emission increase. There are some studies in micro scale level, which estimates emissions as a function of traffic volume in each road (Affum et al., 2003; Nejadkoorki et al., 2008; Ryu et al., 2013). Ryu et al., (2013) implement multiple linear regression analysis for developing the relation between traffic volume in each road, and number of vehicles, number of lanes and time slots in each road. Using this approach traffic volume is estimated and the emission in calculated in each road (Ryu et al., 2013). In addition, Affum et al., (2003) and Nejadkoorki et al., (2008) use simulation to estimate the traffic volume and then amount of emission in each road.

There are a number of studies to analyze emission produced by transport in Turkey. Soylu, (2007) and Muneer et al., (2011) investigate the effect of different vehicle and fuel types on emission in Turkey in macro scale. From the macro scale emission calculation perspective specific for Istanbul, ISSRC, Istanbul Metropolitan Municipality (IMM) and Embarq, conducted a study of the emissions from diesel vehicles operating in Istanbul in 2006. In the study a series of 42 diesel vehicles tested and International Vehicle Emissions (IVE) model applied to estimate emissions from diesel vehicles under different driving and control scenarios (Lents et al., 2007). At wider regional scale, Kanakidou et al., (2011) developed a comprehensive overview of the actual knowledge on the atmospheric pollution sources, transport, transformation and levels in the East Mediterranean by combining ground-based observations with satellite data and atmospheric modeling in Istanbul, Cairo and the Athens shows the urban pollution influence to the larger region beyond those individual cities.

At micro scale, IMM completed "A GIS Based Decision Support System for Urban Air Quality Management in the City of Istanbul (LIFE06-TCY/TR/000283)" within the EU's LIFE Program focused on broader air quality domain. Five major pollutants consisting of Particulate Matter up to 10 micrometers in size (PM_{10}), sulfur dioxide (SO_2), CO, NO_x, and non-methane volatile organic compounds (NMVOCs) emitted through these sources were identified at the metropolitan scale. The results shows 20% of PM_{10}, 1% of SO_2, 69% of CO, and 89% of NO_x are traffic originated emissions (IMM, 2009). Based on that study, the first policy paper at urban scale focused Air Quality Strategy of Istanbul developed. After that, a number of planning frameworks and urban policy papers at micro scale addressed emissions caused by congestion directly and indirectly by their decisions. First, Istanbul Environmental Plan that draws the sustainable development framework for the entire metropolis at EU's Nomenclature of Territorial Units for Statistics 2 (NUTS2) level approved in 2006 revised in 2009, and started to be revise in 2015. Second, the fifth generation Istanbul Integrated Urban Transport Master Plan focused on minimizing the congestion by motor vehicles to enable livable urban environment (IMM, 2011). Third, the corporate Strategic Plan 2015-2019 of IMM strategized several transport and emission related decisions and measures at different levels. For instance, strategic aim AHA02 on "Transport Services Management" has a strategic objective SA02SH05 states "increasing the number of motor vehicles with low emissions" is for entire metropolis (IMM, 2014). Strategic objective SA04SH02 focuses on decreasing the negative impact on environment created by wholesale markets, where emission figures stated as an indicator for performance measures. Likewise SA02SH05's indicator specifically focuses on the increasing the number of low emission motor vehicles of non-mass-public transport (minibus, taxi, etc.) in the metropolis (IMM, 2014).

However, there are a number of studies focused on finding solutions to reduce transport emission in Istanbul at micro scale, but there are no optimization frameworks to analyze the traffic emission problem in Istanbul.

A number of optimization models are developed to minimize the amount of CO emission based on traffic volume, but the developed optimization models are not applied for large scale problems (Ferguson et al., 2010; Huang, Ke, Jin Zhang, Meiling He, 2010; Li et al., 2012a; Shahraki and Turkay, 2014; Yin and Lu, 1999; Zhou et al., 2008). Sharma and Mathew, (2011) have formulated an optimization model based on minimizing CO and NO_X emissions and the model is applied for Indian city of Pune.

Istanbul ranks 16th out of 30 European cities, for overall CO_2 emissions, it scores strongly on CO_2 emissions per head; ranking second in this subcategory (Siemens, 2009). According to (IMM, 2009) number of motor vehicles has increased by 8.2 times while population has increased 2.5 times in the last three decades, and the numbers of motor vehicles are bigger than total population of average European cities.

It is highly relevant need to focus on transport related emissions calculations and modeling in order to reach the planning objectives, to increase the performance and to fine-tune inter-related the urban policy and planning frameworks. In this study, using micro scale approach, the amount of emission in each road of Istanbul transportation network is calculated based on the actual travel behaviors and road network structure. We investigate the production amount of four emission pollutent CO_2, CO, NO_X and Volatile Organic Compound (VOC) in Istanbul main roads. The emissions are calculated using the average real speed limit and travel times in each road, therfore traffic congasion in each road directly considered for emission calculations.

In this study, we developed optimization models to minimize CO_2 emission produced by transports which has not studied indepth at micro scale in the literture. In this study we used the travel production and attraction of 38 districts and detail information of 17,663 Istanbul main roads such as numbers of lanes, length and maximum speed limit in each road. This work is the first comprehensive study for exploring the emission production in each main road of Istanbul. In addition, in this study we analyze the affact of different fuel types on different emission production in Istanbul.

The results are expected to contribute the scientific debate and provide input for integrated urban policy with crosscutting dimensions on air quality, traffic emissions, environmental protection, and quality of life aspects. Also optimization approaches proposed in this study could provide knowledge based for key performance indicators for urban policy on emissions, as well as further research combines different models such as International Vehicle Emissions (IVE).

4.2 Methodology

4.2.1 Study area

Istanbul Metropolitan Area as a regional economic and demographic magnet (OECD, 2008) is the largest energy consuming metropolitan area in Turkey. Located at 41 N 29 E, on the Bosporus strait connects the Black Sea to the Aegean Sea via Marmara Sea. Administrative boundaries at both on the European and on the Asian side cover 39 districts that constitute a metropolitan government IMM. This area is NUTS1, NUTS2, and NUTS2 level region according to EUROSTAT standards.

Within the EU accession chapters, Turkey issued regulation on air quality assessment and management defined the measures on emissions. Not only for CO_2 but 13 pollutant particles including sulfur dioxide (SO_2), Particulate Matter up to 10 micrometers in size (PM_{10}), mono-nitrogen oxides (NO_x) measures defined by the Ministry of Environment and Urbanism.

4.2.2 Traffic emissions in Istanbul

The transportation network in Istanbul, Turkey is used as a case study to apply the optimization models. Although the case study is specific, the models can be generally applied to other cities as well.

In this study, the existing 17,663 main roads in Istanbul shown in Figure 22 with blue lines are considered for traffic emission analysis. The Istanbul road network containing information such as, road lengths, maximum speed limit in roads, the number of lanes in each road and directions, is used for the analyses. Out of 39 districts 38 zones selected in Istanbul as shown in Figure 22 (Prince Islands District excluded due to non-connection to the road network). The travel behavior data used in this study is collected over a period of one week (March 3 to 7, 2014). The collected data shows the average number of passengers that travel between origin and destination districts per hour. The analysis shows districts 21 and 22 have highest attractions and productions compare with other zones.

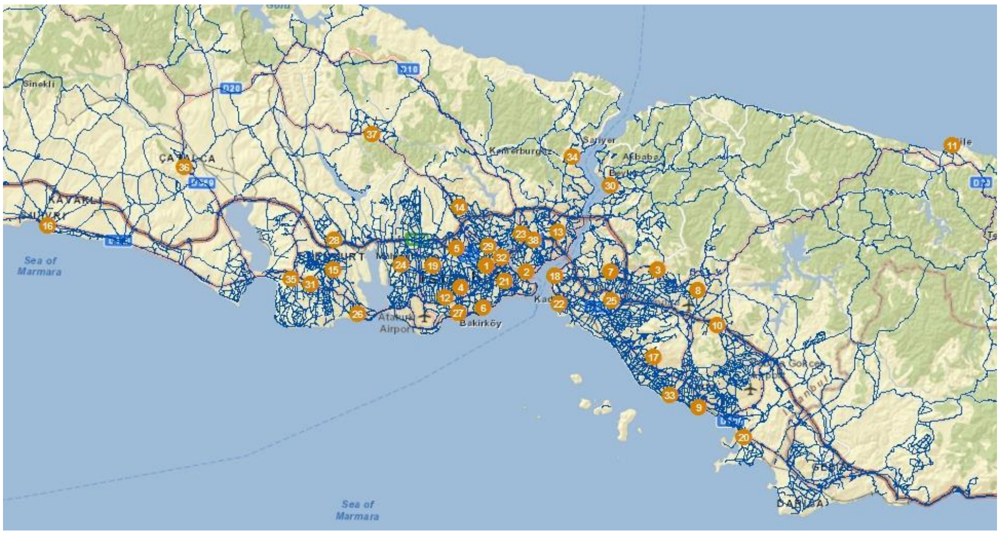

Figure 22. The location of 38 districts and the road network in Istanbul.

The average flow per hour in different roads is calculated using Eq. (4-1). $\bar{d}_{pq}$ is the average number of passengers travel per hour between origin p and destination q. δ_{pqa} is the link-path incidence matrix that is equal to 1 if the shortest path connects pair p and q, passes through road a otherwise it is equal to 0. The incidence matrix has 105,695 elements equal to one, means considering road inter sections, there are 105,696 road segments in the network. Assuming whole travel demand is on road, the total overloaded travel distance is equal to 877,158 meters while total length of main roads in Istanbul is 8,178,686 meters. Therefore, approximately 11% of traveled distances have flows more than their capacities. The overloaded roads are highlighted with pink color in Figure 23.

$$\bar{x}_a = \sum_{p \in P} \sum_{q \in Q} \bar{d}_{pq} \delta_{pqa} \quad \forall a \in A \tag{4-1}$$

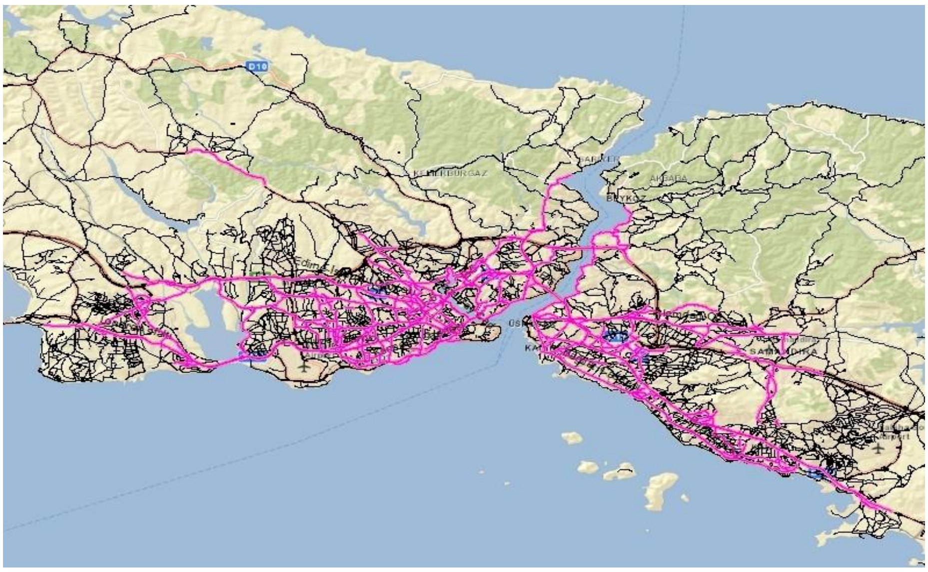

Figure 23. Overloaded roads in Istanbul

The average emissions over a trip vary according to the average speed of the trip (Hickman et al., 1999) Additionally, they vary somewhat depending on the type of vehicle and the pollutant. The relation between the average speed and CO_2, NO_X, VOC and CO emissions produced by gasoline, diesel and LPG vehicles, is formulated in Table 11, Table 12, Table 13 and Table 14, respectively (Hickman et al., 1999). Generally, high emissions are produced at slow average speeds when the vehicle operation is inefficient - because of stops, starts and delays -, and at high speeds because of the high power demand on the engine. Minimum emissions are produced in the middle speed range (Hickman et al., 1999).

Table 11. Speed dependency of emission factors for gasoline passenger cars complying with the EURO I directive

Pollutant	Cylinder capacity	Speed range	Emission factor (g/km)
CO_2	1.41 < CC < 2.01	5-130	$231 - 3.62V + 0.0263V^2 + 2526/V$
NO_X	1.41 < CC < 2.01	10-130	0.526 - 0.0085V + 8.54E-05V^2
VOC	1.41 < CC < 2.01	10-130	0.4494 - 0.00888V + 5.21E-05V^2
CO	1.41 < CC < 2.01	10-130	$9.617 - 0.245V + 0.001729V^2$

Table 12. Speed dependency of emission factors for diesel vehicles <2.5 t, complying with the EURO I directive

Pollutant	Cylinder capacity	Speed range	Emission factor (g/km)
CO_2	All categories	10-130	$286 - 4.07V + 0.0271V^2$
NO_X	All categories	10-120	1.4335 - 0.026V + 1.785E-04V^2
VOC	All categories	10-130	0.1978 - 0.003925V + 2.24E-05V^2
CO	All categories	10-120	1.4497 - 0.03385V + 2.1E-04V^2

Table 13. Speed dependency of emission factors for LPG vehicles <2.5 t, complying with the EURO I directive

Pollutant	Cylinder capacity	Speed range	Emission factor (g/km)
CO_2	All categories	10-130	$228 - 2.70V + 0.0208V^2$
NO_X	All categories	10-130	$0.5278 - 0.0063V + 0.00004\ V^2$
VOC	All categories	10-130	$0.7431 - 0.0166V + 0.00010V^2$
CO	All categories	10-130	$4.2098 - 0.1165V + 0.00110V^2$

Table 14. Speed dependency of emission factors for urban buses

Pollutant	Speed range	Emission factor (g/km)
CO_2	10-90	$679 – 0.00268V^3 + 9635/V$
NO_X	10-90	$16.3 - 0.173V + 111/V$
VOC	10-90	$0.0778 + 41.2/V + 184/V^3$
CO	10-90	$1.64 + 132/V$

In the formulas in Table 11, Table 12, Table 13 and Table 14, V shows the real vehicle speed (km/h). V_a , the real vehicle speed in road a, is calculated using Eq. (4-2). l_a is the length of road a and t_a is the average travel time in road a, calculated using the BPR function in Eq. (4-3).

$$V_a = \frac{l_a}{t_a} \qquad \forall a \in A \tag{4-2}$$

$$t_a = t_0^a \left(1 + \beta \left(\frac{\bar{x}_a}{Ca_a}\right)^{\alpha}\right) \qquad \forall a \in A \tag{4-3}$$

In Eq. (4-3), β and α are the model parameters. The values for β and α are typically considered equal to 0.15 and 4.0 respectively (Sheffi, 1985). $\bar{x}_a$ is the average amount of flow in road a. Ca_a is the practical capacity of road a. The practical capacity of the roads is calculated using the number of lanes in each road. The capacity of a single lane is the maximum number of vehicles that can pass the stop line of a lane which is 1800 pce/h (Rijn, 2004). PCE stands for passenger car equivalent. t_0^a is the free-flow travel time of link a calculated in Eq. (4-4). s_a is the maximum speed limit in road a.

$$t_0^a = \frac{l_a}{s_a} \tag{4-4}$$

In Turkey, 41% of total cars are LPG-fuelled, while 30% and 29% of total cars are diesel and gasoline, respectively. Within the total vehicles, cars represented 52.5 percent, followed by small trucks 16.3 percent, motorcycles 14.9 percent, tractors 8.6 percent, trucks 4.1 percent, minibuses 2.3 percent, buses 1.1 percent and special purpose vehicles 0.2 percent (TurkStat, 2015). Using the formulas in Table 11, Table 12 and Table 13, if we assume whole travel demand satisfy by passenger cars, average amount of CO_2, NO_X, VOC and CO gram per kilometer are 344.573, 0.55, 0.28 and 2.62, respectively. The relations between different emission types and average speed for passenger cars in Turkey are plotted in Figure 24. Figure 25 shows the roads with different CO_2 production in Istanbul.

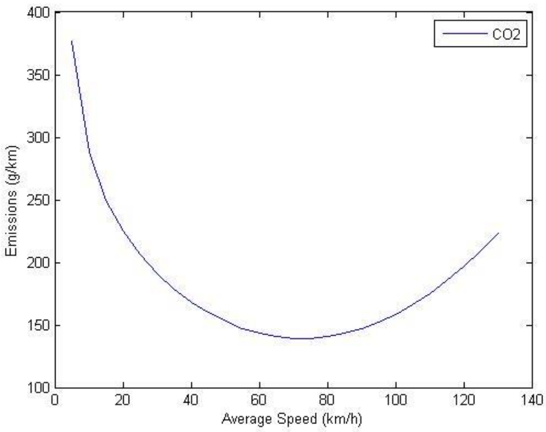

(a)

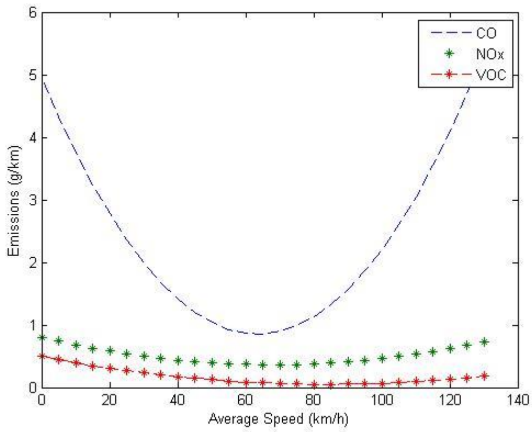

(b)

Figure 24. Emission diagram for passenger cars in Turkey

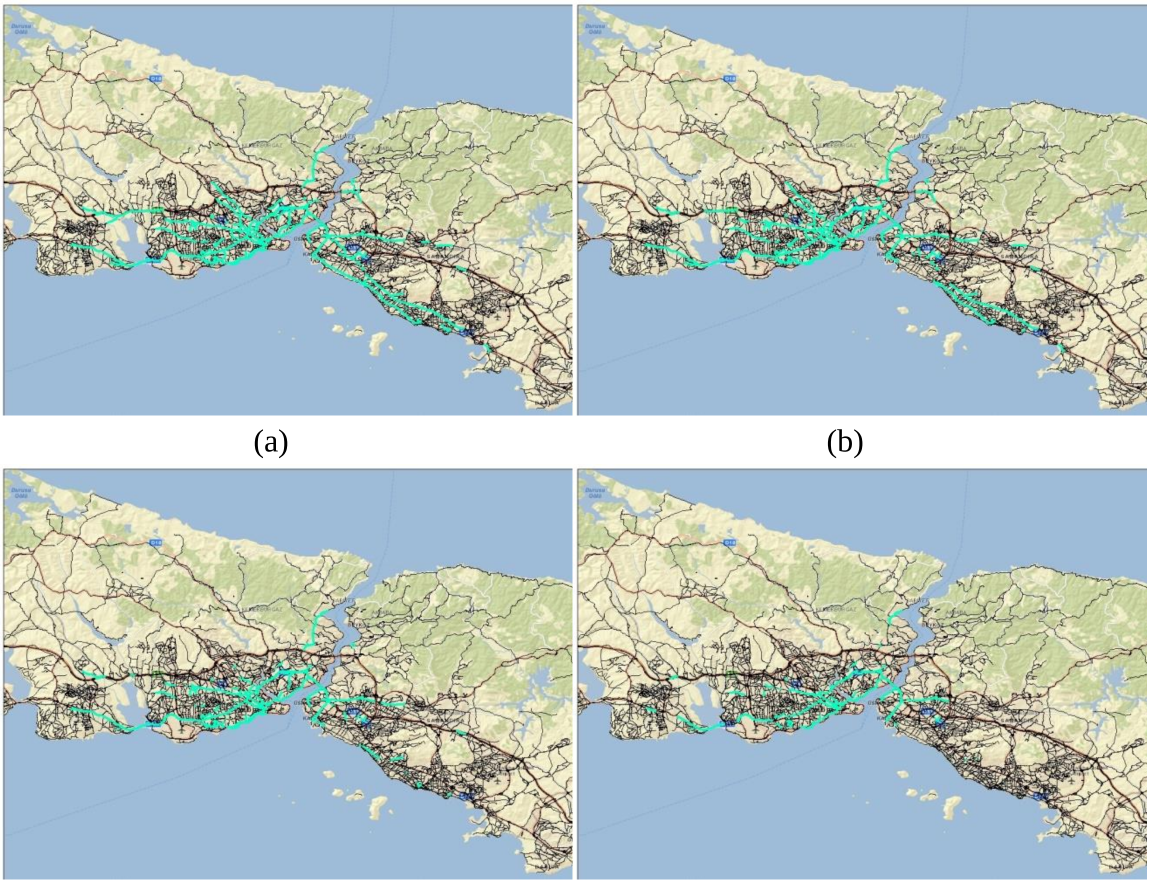

(a) (b)

(c) (d)

Figure 25. Roads with more than (a) 650 CO_2 production (g/km), (b) 750 CO_2 production (g/km), (c) 850 CO_2 production (g/km), and (d) 950 CO_2 production (g/km)

4.3 Three scenarios for emission reduction for Istanbul

In this section, three scenarios are designed to reduce emission values. Based on these three scenarios, we develop three optimization models and we analyze the optimal results.

4.3.1 Scenario 1

As mentioned, in Turkey, 41% of total cars are LPG-fuelled, while 30% and 29% of total cars are diesel and gasoline, respectively. The first scenario is developed to recognize the optimal combination of these three categories to minimize different emission types CO_2, NO_X, VOC and CO, presented in Eq. (4-11), (4-12), (4-13), and (4-14), respectively. Eq. (4-5) is represented as the objective function to minimize the emissions produced by different fuel types. α, β and γ represent the percentage of vehicles powered by gasoline, diesel and LPG fuel, respectively. As explained in previous section, in Eq. (4-6), (4-7) and (4-8), average flow, real travel time and real speed level in each link are calculated respectively. Eq. (4-9) shows the summation of α, β and γ which should be one. In addition, α, β and γ should be positive as shown in Eq. (4-10).

$$Min\ E_{em} \qquad \forall em \in \{\mathrm{CO_2}, \mathrm{NO_X}, \mathrm{VOC\ and\ CO}\} \tag{4-5}$$

subject to

$$\bar{x}_a = \sum_{p\in P}\sum_{q\in Q}\bar{d}_{pq}\delta_{pqa} \qquad \forall a \in A \tag{4-6}$$

$$t_a = t_0^a\left(1+\beta\left(\frac{\bar{x}_a}{Ca_a}\right)^{\alpha}\right) \qquad \forall a \in A \tag{4-7}$$

$$V_a = \frac{l_a}{t_a} \qquad \forall a \in A \tag{4-8}$$

$$\alpha+\beta+\gamma = 1 \tag{4-9}$$

$$\alpha,\ \beta,\ \gamma \geq 0 \tag{4-10}$$

where,

$$E_{\mathrm{CO2}} = \sum_{a\in A}\alpha(231 - 3.62\mathrm{V}_a + 0.0263\mathrm{V}_a^2 + 2526/\mathrm{V}_a) + \beta(286 - 4.07\mathrm{V}_a + 0.0271\mathrm{V}_a^2) + \gamma(228 - 2.70\mathrm{V}_a + 0.0208\mathrm{V}_a^2) \tag{4-11}$$

$$E_{\mathrm{NOX}} = \sum_{a\in A}\alpha(0.526 - 0.0085\mathrm{V} + 8.54\mathrm{E}-05\mathrm{V}^2) + \beta(1.4335 - 0.026\mathrm{V} + 1.785\mathrm{E}-04\mathrm{V}^2) + \gamma(0.5278 - 0.0063\mathrm{V} + 0.00004\,\mathrm{V}^2) \tag{4-12}$$

$$E_{\mathrm{VOC}} = \sum_{a\in A}\alpha(0.4494 - 0.00888\mathrm{V} + 5.21\mathrm{E}-05\mathrm{V}^2) + \beta(0.1978 - 0.003925\mathrm{V} + 2.24\mathrm{E}-05\mathrm{V}^2) + \gamma(0.7431 - 0.0166\mathrm{V} + 0.00010\mathrm{V}^2) \tag{4-13}$$

$$E_{\mathrm{CO}} = \sum_{a\in A}\alpha(9.617 - 0.245\mathrm{V} + 0.001729\mathrm{V}^2) + \beta(1.4497 - 0.03385\mathrm{V} + 2.1\mathrm{E}-04\mathrm{V}^2) + \gamma(4.2098 - 0.1165\mathrm{V} + 0.00110\mathrm{V}^2) \tag{4-14}$$

4.3.2 Scenario 2

An optimization model is developed for the second scenario to find the priority of the roads for installing public shared vehicles considering limited budget. Two categories considered for shared vehicles, buses and railway vehicles. We assume buses are non-electric vehicles while railway vehicles are electric which are either underground or on-road with separate lines. Electric vehicles have zero tailpipe emissions, but emissions may be produced by the source of electrical power, such as a power plant which is not considered in this study. We consider the existing combination of different vehicle fuel types for on road vehicles. Eq. (4-15) shows the objective function which is minimizing CO_2 emissions. In Eq. (4-16), M shows the set of vehicles, passenger cars, buses and railway vehicles. The average on road flow, in Eq. (4-17), is formulated as the summation of average passenger car flow and bus flow. $\bar{x}_a^1$ and $\bar{x}_a^2$ are based on passenger per hour. On road flows are defined based on the number of passenger cars. π and θ are average number of passengers in one car and in one bus respectively and, μ is a parameter to convert the bus flow to the equivalent car flow. The values of parameters μ, π and θ are considered 3, 2 and 9 respectively (Miandoabchi et al., 2011). Eq. (4-18) and (4-19) calculate the expected travel time in each road and the real speed level in each link. Eq. (4-20) and (4-21) represent the budget limitation for providing buses and railway facilities respectively. Amount of flow in each link should be positive as shown in Eq. (4-22).

Budget constraints, Eq. (4-20) and (4-21), are formulated without using binary variables since we are dealing with a large data set of Istanbul road network. If we formulate the problem using binary variables, the problem will change to Mixed Integer Nonlinear Programming (MINLP) problem. MINLP models are much more difficult than both Mixed Integer Linear Programming (MIP) and Nonlinear Programming (NLP) models. Even small MINLP problems generate many sub problems, making it very computationally intensive and requiring significant amount of physical memory (Solutions et al., 2012).

$$Min \sum_{a\in A}\Big((1-b_u)\big(.29(231 - 3.62\mathrm{V}_a + 0.0263\mathrm{V}_a^2 + 2526/\mathrm{V}_a) + .3(286 - 4.07\mathrm{V}_a + 0.0271\mathrm{V}_a^2) + .41(228 - 2.70\mathrm{V}_a + 0.0208\mathrm{V}_a^2)\big) + b_u(679 - 0.00268V_a^3 + 9635/V_a)\Big) \tag{4-15}$$

subject to

$$\sum_{m\in M}\bar{x}_a^m = \sum_{p\in P}\sum_{q\in Q}\bar{d}_{pq}\delta_{pqa} \quad \forall a\in A \tag{4-16}$$

$$\bar{x}_a = \bar{x}_a^1/\pi + \mu(\bar{x}_a^2/\theta) \tag{4-17}$$

$$t_a = t_0^a\left(1+\beta\left(\frac{\bar{x}_a}{Ca_a}\right)^\alpha\right) \tag{4-18}$$

$$V_a = \frac{l_a}{t_a} \tag{4-19}$$

$$\sum_{a\in A}\bar{x}_a^2 \le b_u\sum_{a\in A}(\bar{x}_a^1+\bar{x}_a^2+\bar{x}_a^3) \tag{4-20}$$

$$\sum_{a\in A}\bar{x}_a^3 \le b_m\sum_{a\in A}(\bar{x}_a^1+\bar{x}_a^2+\bar{x}_a^3) \tag{4-21}$$

$$\bar{x}_a^m \ge 0 \tag{4-22}$$

4.3.3 Scenario 3

An optimization model, Eq. (4-23)-(4-26), is designed for the third scenario to minimize the total overloading flows, Eq. (4-23). The goal is recognizing the priority of the roads for capacity expansions to minimize the total overloaded roads. y_a shows the expansion amount of road *a*. Eq. (4-24) calculates the amount of flow in each road. In addition, there is a limited budget for expanding the capacity of the roads equal to *B*, as shown in Eq. (4-25). Eq. (4-26) shows the amount of expansions and flows in each link, should be positive.

$$Min \sum_{a\in A}\bar{x}_a/(Ca_a+y_a) \tag{4-23}$$

subject to

$$\bar{x}_a = \sum_{p\in P}\sum_{q\in Q}\bar{d}_{pq}\delta_{pqa} \qquad \forall a\in A \tag{4-24}$$

$$\sum_{a\in A}y_a \le B \qquad \forall a\in A \tag{4-25}$$

$$y_a \ge 0,\ \bar{x}_a \ge 0 \qquad \forall a\in A \tag{4-26}$$

4.4 Results and discussion

The results of solving the optimization models formulated for scenario 1, 2 and 3 are presented in section 4.4.1, 4.4.2 and 4.4.3 respectively. All runs were performed on a PC Intel(R), Xeon(R), central processing unit (CPU) 3.33GHz dual-core, 32 GB RAM running Windows 7 using CONOPT (Drud, 1994) in GAMS (Generalized Algebraic Modeling System) (Rosenthal, 2012). The formulated models are nonlinear programming (NLP). GAMS has a number of solvers to solve a NLP problem, CONOPT is one of these solvers which is designed for large and sparse models. CONOPT may not find a global solution for non-convex models. However, the solvers designed for finding a global solution can not usually solve large and complex models (Drud, 1994).

The data are prepared into four input matrixes, $D(d_{pq})$, $V(v_a)$, $L(l_a)$, and δ (δ_{pqa}), with p equals to 38, q equals to 38, and a equals to 17,663. D, V and L are demand, speed and number of lane matrixes. δ_{pqa} is a 0-1 matrix with 1 indicating that the shortest path connecting origin p to destination q passes through road a and 0 indicating that the path does not pass through road a. δ matrix has over 150 million elements which is time-consuming to read them for optimization. To overcome this computational obstacle, we use a specific feature from the optimization software GAMS. If we do not set any value for a parameter In GAMS, its default value is set to zero. The δ matrix contains many zeros. We simply extract the non-zero δ_{pqa}. Reading only the non-zero elements will reduce data size dramatically.

4.4.1 Result for scenario 1

The optimization model is convex, therefore the optimal solution is global optimal. In optimal situation for Istanbul, if the whole passenger cars powered by LPG-fuelled, we will have the minimum level of CO_2 emission. If we set γ=0, then we have diesel and gasoline options. In this case whole percentage of the vehicles should be powered by diesel, in optimal solution. We can conclude LPG, diesel and gasoline passenger cars are ranked first, second and third respectively, in terms of producing less CO_2 emissions.

If we optimize the model respect to minimizing CO emission, diesel, LPG, and gasoline are selected as the first, second and third choice for passenger cars respectively, in terms of producing less CO emissions. In the case we optimize the model base on VOC emission, diesel, gasoline, and LPG passenger cars are ranked first, second and third respectively, in terms of producing less VOC emissions. Finally if we minimize NO_X emission level, gasoline, LPG, and diesel passenger cars are ranked first, second and third respectively.

4.4.2 Result for scenario 2 through 12 examinations

As mentioned, in this scenario, we would like to recognize the optimal roads for installing shared public facilities based on the limited budget.

4.4.2.1 12 examinations

We design 12 examinations as shown in Table 15 with different values for b_u and b_m representing limitations on the budget for installing bus and railway facilities respectively.

Table 15. 12 examinations

Examination	0	1	2	3	4	5	6
b_u	0	0.01	0.1	0.2	0.3	0.4	0
b_m	0	0	0	0	0	0	0.01
Examination	7	8	9	10	11	12	
b_u	0	0	0	0	0.4	0.1	
b_m	0.1	0.2	0.3	0.4	0.1	0.4	

Table 16 and Figure 26 show the objective function values for each examination. The results show using shared railway vehicles have significantly effect on reducing the emissions.

Table 16. Average CO_2 production (g/km) for each examination

Examination	0	1	2	3	4	5	6
CO_2 emission	344.573	344.559	344.148	340.926	334.982	322.787	344.516
Examination	7	8	9	10	11	12	
CO_2 emission	336.593	305.826	262.464	221.263	298.303	209.925	

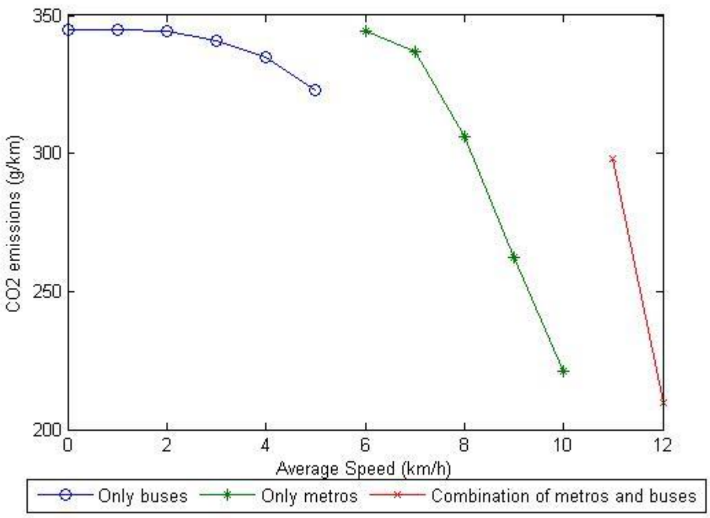

Figure 26. CO_2 emission production (g/km) for each examination

Figure 27 shows the optimal roads for installing bus facilities to minimize CO_2 emissions for examination 1, 2, 3, 4 and 5. The roads highlighted in Figure 27 (a) have the highest priority for installing bus facilities and they have significant effect on reducing CO_2 emission. By increasing budget from Figure 27 (a) to (e), more roads will be selected as the candidates for providing buses facilities on them. We have same trend for installing railway facilities as shown in Figure 28 for examinations 6 to 10. The priority of the selected roads will be increased for installing additional public shared facilities by moving from part (e) to (a) in Figure 27 and Figure 28. It also means that the effect of selected roads on producing CO_2 emission increases by moving from part (e) to (a) in Figure 27 and Figure 28.

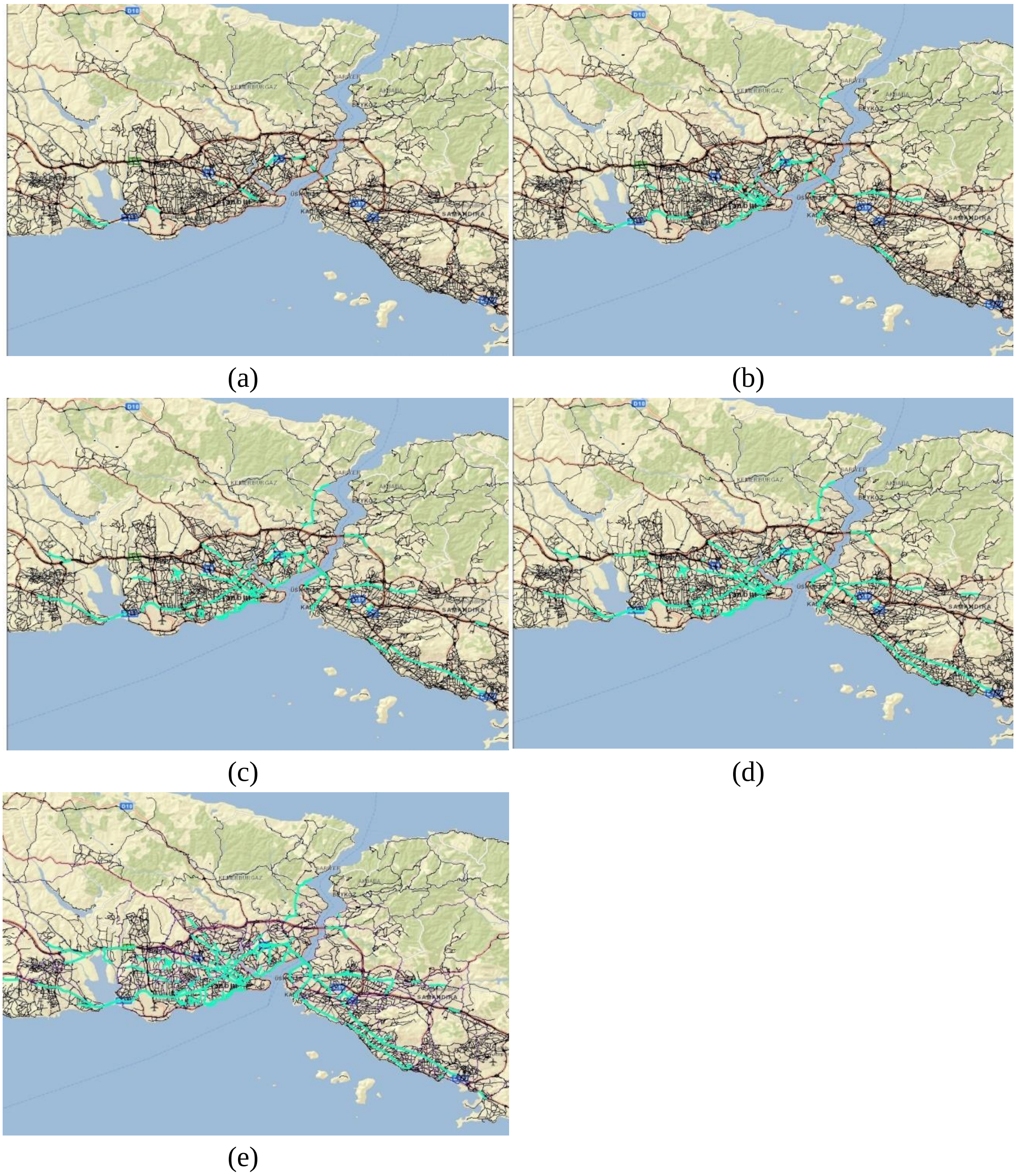

Figure 27. (a) Optimal roads for installing bus facilities for (a) examination 1, (b) examination 2, (c) examination 3, (d) examination 4, and (e) examination 5

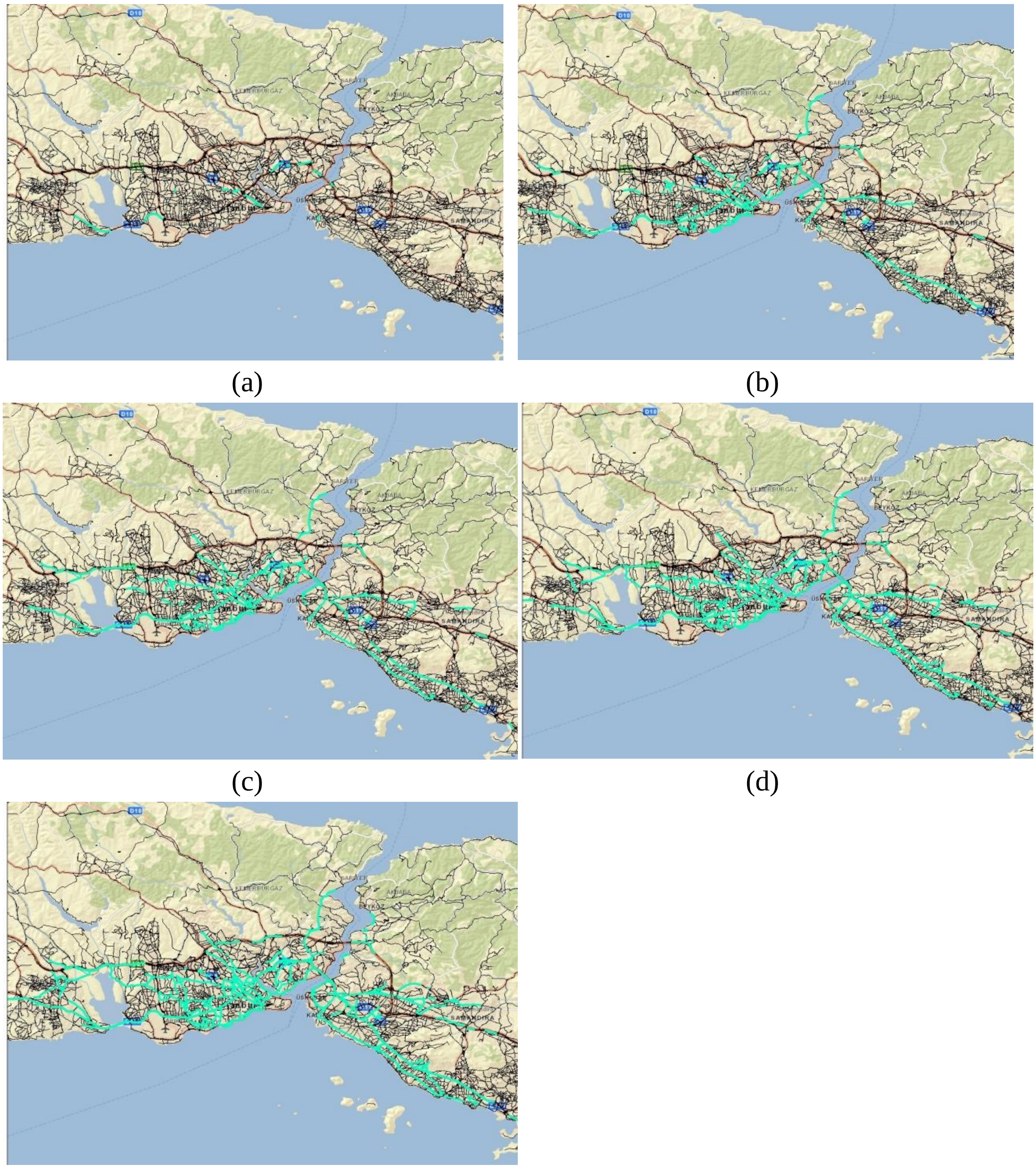

(a) (b) (c) (d) (e)

Figure 28. Optimal roads for installing railway vehicles facilities for (a) examination 6, (b) examination 7, (c) examination 8, (d) examination 9, and (e) examination 10

In addition, the optimal solutions for examinations 11 and 12 are shown in Figure 29 and Figure 30, respectively. By comparing the selected roads in part (c) of Figure 29 and Figure 30, with their part (a) and (b), we can conclude using more share vehicles in specific roads has significantly effect on reducing emissions. The results of all examinations of this scenario show almost same conclusion for the priority of the roads for installing shared vehicles.

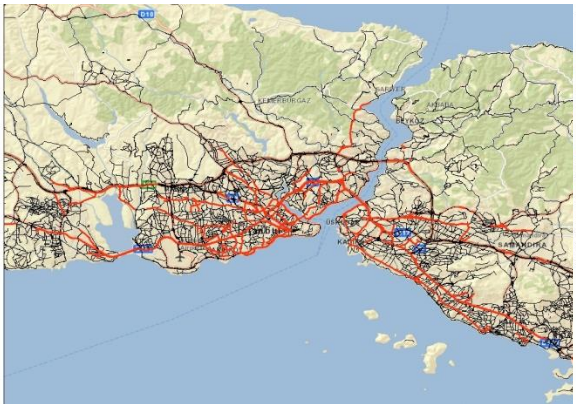
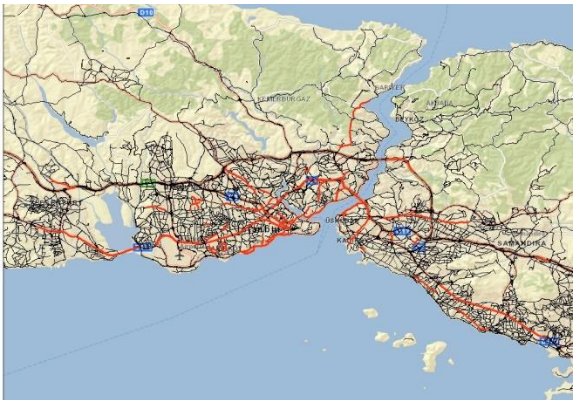

(a) (b)

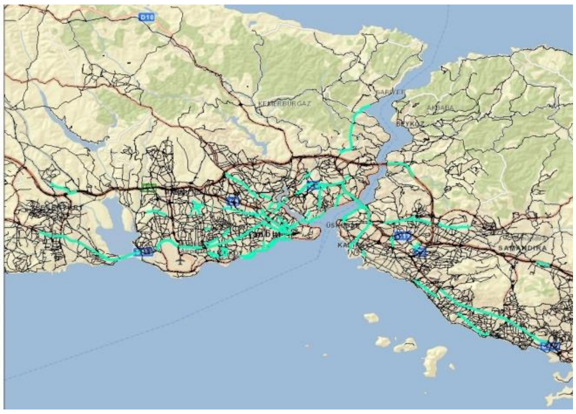

(c)

Figure 29. Optimal roads for examination 11 for installing (a) buses, (b) railway vehicles, (c) common roads for installing railway vehicles and bus facilities

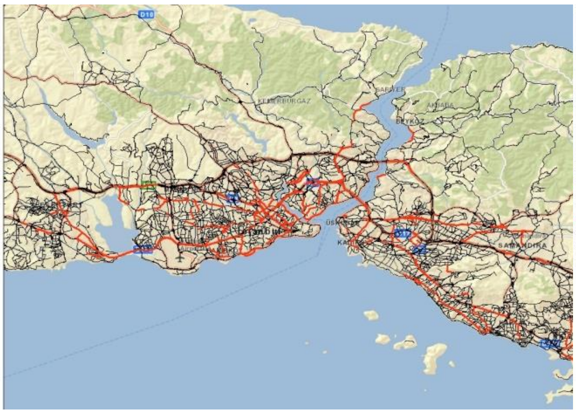
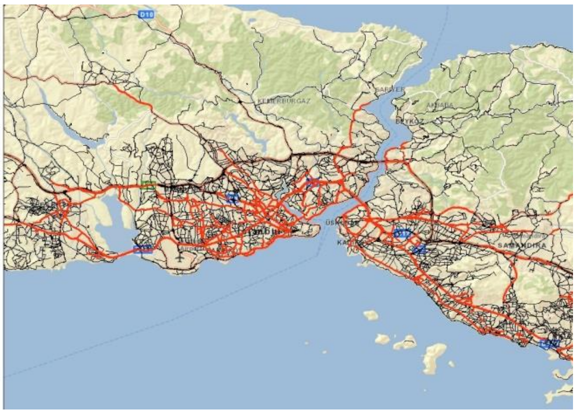

(a) (b)

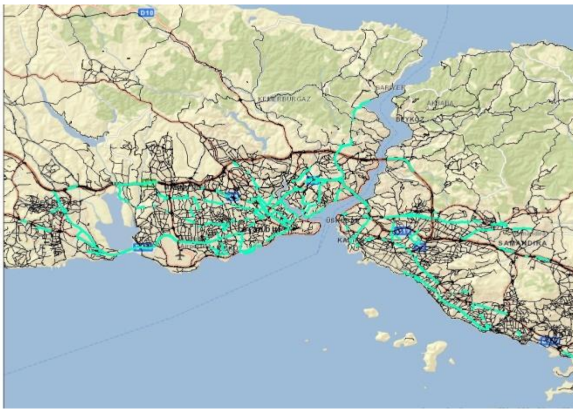

(c)

Figure 30. Optimal roads for examination 12 for installing (a) buses, (b) railway vehicles, (c) common roads for installing railway vehicles and bus facilities

4.4.3 Result for scenario 3 through 4 examinations

We would like to recognize the priority of the roads for capacity expansions by designing the scenario 3.

4.4.3.1 4 examinations

The optimization model is convex, therefore the optimal solution is global. Based on the allocated budget we have limitation on the amount of capacity expansion. Different examinations based on maximum amount of capacity expansion (*B*) are designed in Table 17. The optimal roads based on examination 1, 2, 3 and 4 are shown in Figure 31 (a), (b), (c) and (d), respectively. Moving from (d) to (a) in Figure 31, the priority of the selected roads for capacity expansions increases.

Table 17. Examinations for capacity expansions

Examination	1	2	3	4
B (pce/h)	180000	585000	990000	1800000
CO_2 (g/km)	344.186	341.286	336.285	320.300

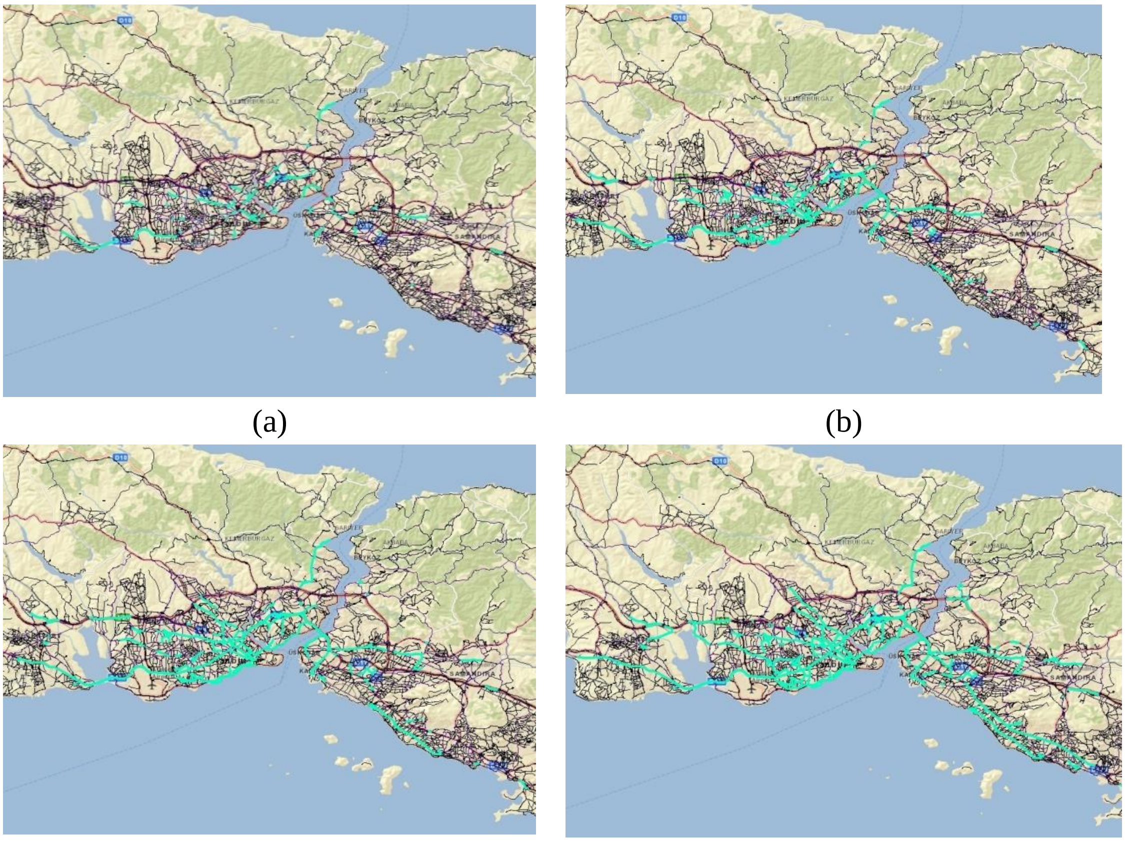

(a) (b) (c) (d)

Figure 31.(a) Optimal roads for capacity expansion based on examination 1,(b) examination 2 ,(c) examination 3 and (d) examination 4

4.4.4 Discussion

In this section we discuss about the optimal solutions obtained through the examinations for scenario 1, scenario 2 and scenario 3.

4.4.4.1 Discussion about the results of Scenario 1

The optimal solutions of scenario 1 are summarized in Table 18. Considering the ranking, LPG, and gasoline produce low CO_2 and NO_X emissions, respectively, while diesel fuel produces low CO and VOC emissions.

Table 18. Summary of results of scenario 1

	Rank 1	Rank 2	Rank 3
Minimizing respect to CO_2	LPG	Diesel	Gasoline
Minimizing respect to CO	Diesel	LPG	Gasoline
Minimizing respect to VOC	Diesel	Gasoline	LPG
Minimizing respect to NO_X	Gasoline	LPG	Diesel

With respect to minimizing the total CO, VOC and NO_X emission production, diesel and LPG are selected as the optimal choices in the first and second places, respectively, as shown in Table 19.

Table 19. Summary of the results based on two categories minimizing CO_2 and the other emission types

	Rank 1	Rank 2	Rank 3
Minimizing respect to CO_2	LPG	Diesel	Gasoline
Minimizing respect to summation of CO, VOC and NO_X	Diesel	LPG	Gasoline

Furthermore, Using LPG for passenger cars is expected to minimize the total emissions for the entire Istanbul metropolitan area as shown in Table 20. According to the analysis, average production rate of CO_2 is much higher than CO, VOC, and NO_X.

Table 20. Results respect to minimizing total emission

	Rank 1	Rank 2	Rank 3
Minimizing respect to summation of CO_2 , CO, VOC and NO_X	LPG	Diesel	Gasoline

As mentioned, based on the report released in early 2015, 41% of total cars are LPG-fuelled, while 30% and 29% of total cars are diesel and gasoline (TurkStat, 2015). However the percentage of total cars fuelled by LPG is higher than diesel and gasoline cars, but it is not significant. Making strategies for increasing the number of cars fueled by LPG and decreasing the number of cars fueled by gasoline is recommended to reduce air pollution.

4.4.4.2 Discussion about the results of Scenario 2 and Scenario 3

If we look at the results of the analyses for recognizing the overloaded roads (Figure 23), the polluted roads (Figure 25), the priority of roads for installing public shared vehicles (Figure 27-Figure 30), and the priority of roads for capacity expansions (Figure 31), we can conclude almost same conclusion. It means the roads overloaded, they are also polluted and we need to define strategies to reduce emissions like installing additional shared public vehicles and expanding their capacities analyzed in scenario 2 and scenario 3.

Figure 32 is prepared to show the results of the analysis at a glance. There are some common roads which are selected because they are overloaded, polluted, they need expansions, and installing shared public vehicle to reduce emissions. In this discussion we debate about these specific roads and area shown in the red circles. It is concluded from the analyses that there are traffic congestions on them and they are also recognized as the polluted roads or area. In the selected roads installing shared vehicle or capacity expansion is recommended to reduce air pollution based on the results of scenario 2 and scenario 3.

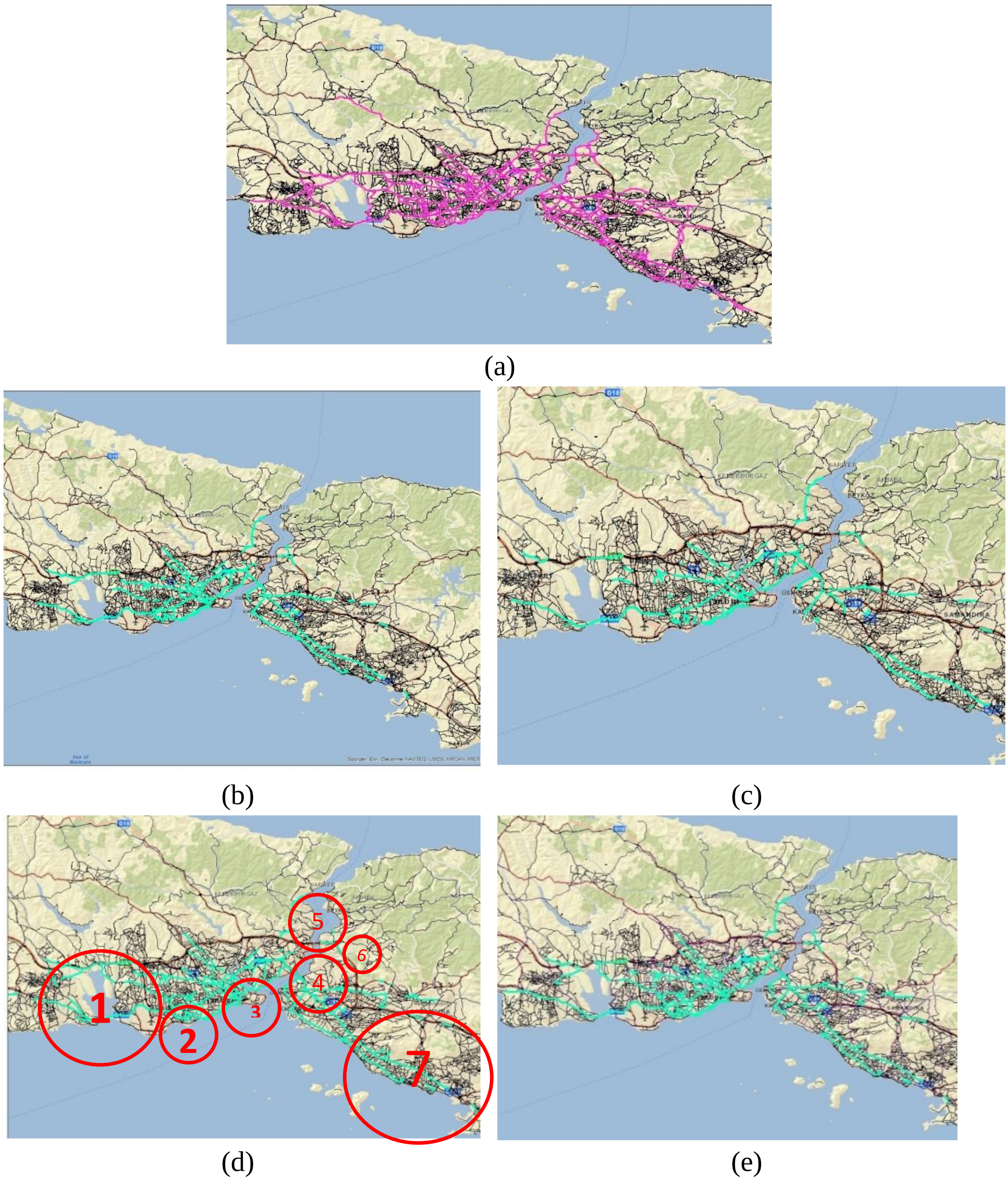

Figure 32. (a) Overloaded roads, (b) roads with more than 650 CO_2 (g/km) production, (c) the selected roads to install bus facilities to satisfy 40% of travel demand by buses, (d) the selected roads to install railway vehicle facilities to satisfy 30% of travel demand by railway vehicles, (e) the selected roads for capacity expansion based on examination 4 of scenario 3

Figure 32 (d) is shown in Figure 33 with a high resolution to illustrate the selected roads more clearly with 7 high emission areas came up with the results.

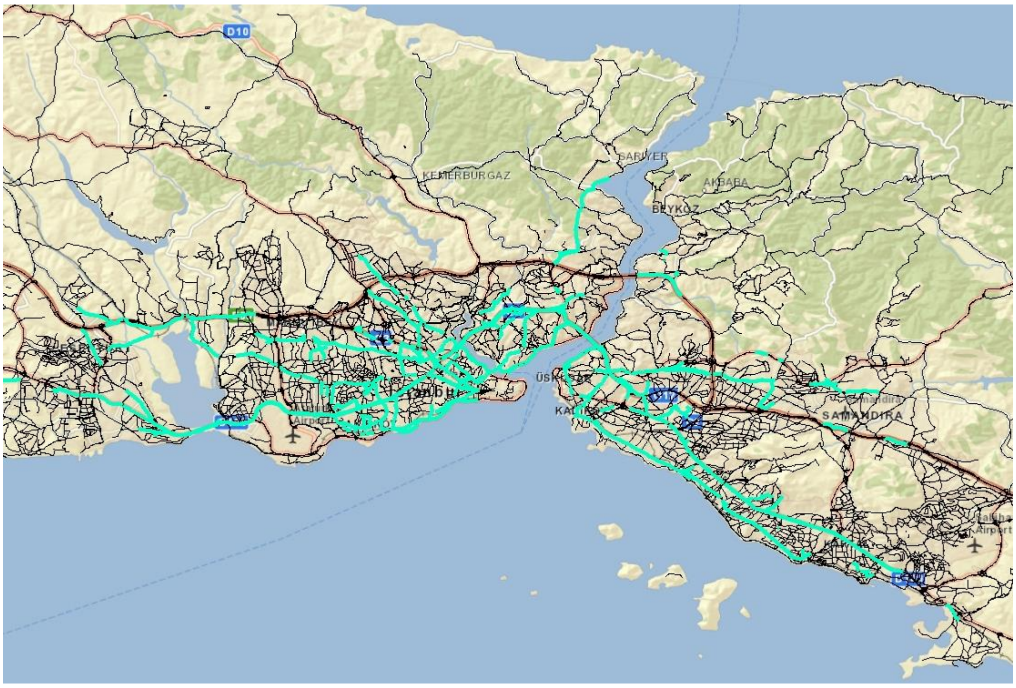

Figure 33. Figure 32(d) with higher resolutions

The most polluted roads based on the analysis, are the concentration of business districts, and mixed-use development with housing and jobs in area 7 located in the Asian part of Istanbul. The northern intercontinental bridge does not have high emissions but the Asian connection of that bridge performed high emission production in area 6, could be explained with the clustering of office development located.

Whereas the southern transit in area 4 has a continuous high emission figures on the coastal roads to the airport. Another higher emission locations are area 3 and area 2 where dense urban development in the periphery of the Historical Peninsula as well as alongside D-100 highway in European part. In addition, the first bridge that is recognized as a much polluted road as illustrated in area 4, shows the dense use of D-100 highway.

For the historic sites of Istanbul, the analysis shows the former Eminonu part of the Historic Peninsula has significantly low emissions, comparing the northeastern part. Some years ago strict pedestrianization policy resulted the low emissions results whereas clustering of hotels, business areas and major roads resulted with high emissions at the northeastern part of the Historic Peninsula shown as area 3.

The highway intersections of Kucuk Cekmece, Beylikduzu and Esenyurt districts shown as area 1 performed high emission results in the western edge of the metropolitan area according to the analysis. This could be explained with booming high urban development areas in those districts have more than 1.5 million inhabitants plus new high-rise office uses.

Another high emission results out of the analysis shown as area 5, the Maslak area of Sariyer district located in northern European part of the metropolitan area. This zone has one of the most dense shopping centers and offices where commuting creates the high emissions cause by motor vehicles.

Based on these results, several suggestions could be proposed in order to reduce the emission in these seven areas. The first one is improving the public transport with railway systems as discussed on the optimal results in scenario 2. Second one is promoting the private use of electric cars and vehicles in the long-term transport policy. Third one is expanding the capacity of the selected roads as discussed through the examinations in scenario 3. Fourth suggestion is about urban planning that particularly deals with the distribution of urban centers, major mixed-use real estate investments including offices, residential units and shopping centers together.

4.5 Conclusion

In this paper, we developed an optimization framework to recognize the polluted roads and analysis the solutions for reducing traffic pollution in Istanbul metropolitan area. Using large data set of Istanbul metropolitan transportation network the amount of emission and flow in each main road of Istanbul is analyzed. This large data set contains the travel production and attraction of 38 districts and the detail information of 17,663 roads. The emission is calculated as a function of the real speed level in each road. Real speed level is calculated based on the road length and the actual travel time in each link, and travel time calculated using BPR link impedance function which is a function of flow and the capacity of each road. The optimal results identify the priority of roads for capacity expansion and installing public shared vehicles, which directly shows the polluted and congested roads. In addition the result shows specific roads have significant effect on increasing air pollution in Istanbul. Some of the main reasons of pollution in these roads which was discussed are intercontinental and inter-district commuting and logistics activities with motor vehicles.

In addition, in this study we analyzed the effect of different fuel types for passenger cars on emission production. The results show making strategies to increase the proportion of LPG-fueled cars helps to reduce the emission in Istanbul.

The optimization models in this study provide a base for examining the existing, developing and planned transport network for Istanbul. Furthermore, the optimization framework developed would provide a scientific insight and a potential indication on city development strategies and urban planning with an integrated approach with cross-cutting dimensions referenced by several urban policy papers.

5 Chapter V

Optimal Locations of Electric Public Charging Stations Using Real World Vehicle Travel Patterns

We propose an optimization model based on vehicle travel patterns to capture public charging demand and select the locations of public charging stations to maximize the amount of vehicle miles traveled (VMT) being electrified. The formulated model is applied to Beijing, China as a case study using vehicle trajectory data of 11,880 taxis over a period of three weeks. The mathematical problem is formulated in GAMS modeling environment and Cplex optimizer is used to find the optimal solutions. Formulating mathematical model properly, input data transformation, and Cplex option adjustment are considered for accommodating large-scale data. We show that, comparing to the 40 existing public charging stations, the 40 optimal ones selected by the model can increase electrified fleet VMT by 59% and 88% for slow and fast charging, respectively. Charging demand for the taxi fleet concentrates in the inner city. When the total number of charging stations increase, the locations of the optimal stations expand outward from the inner city. While more charging stations increase the electrified fleet VMT, the marginal gain diminishes quickly regardless of charging speed.

5.1 Introduction

Fossil fuel-based road transportation has instigated increasing global demand for oil and air pollution, especially in urban areas (Hoogma et al., 2005). Emerging vehicle technologies that can utilize alternative fuels are considered as potential solutions for these issues, such as electric vehicles (EVs). Although the life cycle environmental implications of EVs depends on the fuel mix of electricity generation (Torchio and Santarelli, 2010), using electricity instead of liquid fossil-based fuels for road transportation can relocate tailpipe emissions from mobile vehicular sources to stack emissions in power plants which are more concentrated and easier to control. Many countries have set goals for EV adoption. For example, the U.S. plans to adopt a total of one million plug-in hybrid electric vehicles (PHEVs); and China hopes to put 500,000 hybrid and electric vehicles on the road by 2015 (Murphy, 2014; U.S. Department of Energy, 2008).

One of the factors that significantly impact the growth of the EV market is access to public charging infrastructure (Morrow, 2008). Many governments are investing in the deployment of public charging stations. For example, California has announced to build 200 public fast-charging stations; and British Columbia, Canada has set goals for building 570 charging stations across the province (City of Surrey, 2012; JR, 2012). While the deployment of charging infrastructure has been moving forward in many cities, research on developing mathematical models for charging infrastructure siting is also growing. Xi et al., (2013) have formulated an optimization framework for charging station siting to maximize the amount of energy and the expected EVs recharged, by estimating charging demand as a function of household demographic variables (e.g. average total mileage driven) and macroeconomic variables (e.g. gasoline and electricity prices). Sathaye and Kelley (2013) estimate charging demand using a linear function of two terms—traffic and population—to minimize total distances between demand locations and charging stations. Sadeghi-Barzani et al., (2014) predict the charging demand based on number of EV owners to minimize the total cost associated with charging which includes travel cost to stations and electricity cost. He et al., (2013) predict charging demand based on travel time, charging expenses, availability, and attractions to maximize total social welfare. Dong et al., (2014) use multiday travel data of 275 household in the Seattle metropolitan area to minimize the number of trips which cannot be completed using electricity. Despite the difference on scope and goals, these studies use non-exact algorithms to find local optimal solutions to our knowledge.

Two research gaps exist in the literature on siting public charging stations. First, methods currently used in estimating charging demand may not reflect the real world situation. Unlike refueling liquid fuels which only takes a few minutes to fill the tank, fully recharging the battery on an EV can take a much longer time, from 30 minutes to several hours depending on the charger power, battery size, and the state of charge of the battery (Dong et al., 2014). Therefore, EV charging is more likely to happen at the end of a trip instead of in the middle of a trip. In addition, EV owners can charge their vehicles at home during the night. As a result, using traffic flow volume or vehicle ownership density to estimate charging demand as predominately used in previous studies may not be valid. Secondly, few studies considered environmental impacts of EV charging as the objective function for global optimal solution. The ultimate goal of EV system deployment is to fulfill more travel needs using electricity instead of fossil-based liquid fuels. We aim to address both gaps in this study by 1) using large-scale real world vehicle travel data to better model charging demand and 2) maximizing electrified fleet VMT as the objective function to find the global optimal solution. Our previous work has demonstrated that collective public parking lots “hotspots” extracted from real world vehicle trajectory data are good indicators of public charging demand (Cai et al., 2014). This research expands upon Cai et al., (2014) to develop an optimization model to solve for global optimization solutions for public charging station siting using large-scale real world vehicle travel data. In addition, the goal of our optimization model is to maximize electrified fleet VMT, which directly links to the environmental benefits of vehicle electrification.

Using Beijing, China as a case study, this chapter presents an optimization framework which utilizes large-scale real world vehicle trajectory data for selecting the location of public charging stations to maximize electrified fleet VMT. The demonstrated optimization framework can be applied to other fleets in other cities using similar data. The case study also has its own policy relevance because Beijing plans to deploy 100,000 electric vehicles on road by 2015 and build 466 public charging stations (Shuwen, 2011). Results from this study can help future decisions on developing public charging stations in Beijing. The proposed optimization model is implemented in GAMS with Cplex solver. In order to accommodate for the large-scale vehicle trajectory data in the model, we identify factors in model formulation, input data format, and settings of Cplex options that need to be adjusted to solve the model efficiently. In summary, major contributions of this chapter include 1) formulating an optimization model which selects the location of public charging stations to maximize electrified fleet VMT; 2) incorporating vehicle travel patterns by using large-scale individual-based vehicle trajectory data to model public charging demand; 3) studying public charging infrastructure planning in Beijing as a case study; and 4) providing suggestions in model formulation and execution to handle large-scale data.

5.2 Mathematical Formulation

EVs include battery electric vehicles (BEV) and plug-in hybrid electric vehicles (PHEV). BEVs use electricity as the sole power source while PHEV has the flexibility of using both electricity and liquid fuels (Markel, 2010). In this chapter we focus on PHEVs to allow drivers finishing trips on liquid fuels when batteries are depleted, because it is unclear how limited driving range of BEVs will affect the behavior of drivers.

Let $G(i,j,k)$ be a network with i candidate locations for installing public charging stations, j individual PHEVs, and k trips for each vehicle in the examined period. The time spent between two consecutive trips is defined as the dwell time.

Each vehicle (j) has a remained battery charge (R_{jk}) at the end of each trip (k) before starting its dwell time. For the convenience of modeling, R_{jk} is measured as the mileage that the vehicle can travel with the remaining electricity (battery range). R_{jk} can be formulated as shown in Eq. (5-1) (Dong et al., 2014). Negative values of R_{jk} represent the mileage that cannot be powered by electricity (i.e., powered by liquid fuels) in trip k. Eq. (5-2) shows the real remaining battery range ($\hat{R}_{jk}$) of vehicle j at the end of trip k, which is forced to be non-negative.

$$R_{jk} = \hat{R}_{jk-1} + E_{jk-1} - d_{jk} \quad \forall j \in J, \forall k \in K \tag{5-1}$$

$$\hat{R}_{jk-1} = max\{R_{jk-1}, 0\} \qquad \forall j \in J, \forall k \in K \tag{5-2}$$

where R_{jk} is the remaining battery range of vehicle j at the end of trip k (mile), E_{jk-1} is electricity recharged (measured in miles) for vehicle j during the dwell time between trip k-1 and trip k; and d_{jk} is the travel distance (miles) of vehicle j during trip k.

This model differentiates home charging and public charging. If vehicle j does not park at home after trip k (h_{jk} = 0), the vehicle seeks public charging opportunities. Electricity recharged for vehicle j after trip k (E_{jk}), as shown in Eq. (5-3), equals to the difference between the full battery range and the remaining battery range if the dwell time is longer than what is required to fully charge the battery, or the exact amount of electricity that can be charged if a full charge cannot be achieved within the dwell time. E_{jk} equals to 0 if no charging station is available for vehicle j at the end of trip k. If vehicle j parks at home after trip k (h_{jk} = 1), home charging is utilized. Recharged electricity at home, as shown in Eq. (**5-4**), equals to the difference between the full battery range and the remaining battery charge if the home parking time is longer than what is required to fully charge the battery, or the exact amount of electricity that can be charged during home dwell time.

$$E_{jk} = \min\left\{E_j - \hat{R}_{jk}, \frac{Le\, t_{jk}}{r_j}, M \textstyle\sum_{i\in I} P_{ijk}\right\} \qquad if\ h_{jk} = 0 \tag{5-3}$$

$$E_{jk} = \min\left\{E_j - \hat{R}_{jk}, \frac{Lh\, t_{jk}}{r_j}\right\} \qquad if\ h_{jk} = 1 \tag{5-4}$$

where h_{jk} equals to 1 if vehicle j is parked at home after trip k and 0 otherwise; E_j is the effective all-electric-range (AER) of vehicle j's battery (measured in miles); Le is the charging power level (kW) at each of the public charging stations (assuming same for all public charging stations); Lh is home charging power level; t_{jk} is dwell time of vehicle j at the end of trip k (hour); r_j is the average electricity consumption rate of vehicle j in charge depletion (CD) mode (kWh/mile); M is a large number greater than

E_j; and P_{ijk} is the availability of charging station for vehicle j at location i after trip k. P_{ijk} equals to 1 if candidate location i is accessible for vehicle j at the end of trip k and a charging station is installed at location i. Accessibility of charging station at location i by vehicle j is measured by the distance between location i and vehicle j at the end of trip k. If this distance is less than the service range of charging stations, location i is accessible.

5.3 Optimization Model

The optimal selection of charging station locations in a geographical area using the travel patterns of individual vehicles defined in this chapter is given by Eqs. (5-5) - (5-14). The objective function, as shown in Eq. (5-5), minimizes the total travel distances that cannot be fulfilled by electricity. This is equivalent as maximizing the electrified fleet VMT. Eqs. (5-6), (5-7) and (5-8) formulate the remaining battery range of vehicle j at the end of trip k. In Eq. (5-7), R_j is the remaining battery range of vehicle j at the beginning of trip 1. Recharged electricity of vehicle j at the end of trip k is shown in Eqs. (5-9) and (5-10). Eq. (5-11) shows the budget constraint, limiting the maximum number of public charging stations as B. Charging opportunity is available at candidate location i for vehicle j at the end of trip k if two conditions are satisfied simultaneously, as shown in Eq. (5-12). The first condition is that the distance between candidate location i and the location of vehicle j at the end of trip k is less than the specified charging station service range. If vehicle j at the end of trip k is within the service range of candidate location i, Z_{ijk} equals to 1, otherwise zero. The second condition is that a charging station is installed at location i (y_i = 1). The model solves y_i for the optimal solutions. Eq. (5-13) and (5-14) show the binary and positive variables, respectively.

$$\min \sum_{k\in K}\sum_{j\in J}\left(\hat{R}_{jk} - R_{jk}\right) \tag{5-5}$$

Subject to:

$$R_{jk} = \hat{R}_{jk-1} + E_{jk-1} - d_{jk} \qquad \forall j \in J, \forall k \in K/\{1\} \tag{5-6}$$

$$R_{j1} = R_j - d_{j1} \qquad \forall j \in J \tag{5-7}$$

$$\hat{R}_{jk} = max\{R_{jk}, 0\} \qquad \forall j \in J, \forall k \in K \tag{5-8}$$

$$E_{jk} = \min\left\{E_j - \hat{R}_{jk}\,, \frac{Le\,t_{jk}}{r_j}, M\sum_{i\in I} P_{ijk}\right\} \quad if\ h_{jk} = 0,\ \forall j \in J, \forall k \in K \tag{5-9}$$

$$E_{jk} = \min\left\{E_j - \hat{R}_{jk}\,, \frac{Lh\,t_{jk}}{r_j}\right\} \qquad if\ h_{jk} = 1,\ \forall j \in J, \forall k \in K \tag{5-10}$$

$$\sum_{i\in I} y_i \le B \tag{5-11}$$

$$P_{ijk} = Z_{ijk}\, y_i \qquad \forall j \in J, \forall k \in K, \forall i \in I \tag{5-12}$$

$$P_{ijk}, y_i \in \{0,1\} \qquad \forall j \in J, \forall k \in K, \forall i \in I \tag{5-13}$$

$$\hat{R}_{jk}, E_{jk} \ge 0 \qquad \forall j \in J, \forall k \in K \tag{5-14}$$

where the decision variables of the problem are as follows:

R_{jk}: The remaining battery range of vehicle *j* at the end of trip k (mile)
$\hat{R}_{jk}$: The real remaining battery range of vehicle *j* at the end of trip *k* (mile)
P_{ijk}: Binary variable which shows the availability of public charging for vehicle *j* at the end of trip *k* at location *i*, with 1 indicating available and otherwise 0
y_i: Binary variable which shows whether a charging station is installed at location *i*, with 1 indicating present and otherwise 0
E_{jk}: Battery electricity recharged for vehicle *j* at the end of trip *k* (mile)

The formulated optimization model is a Mixed Integer Non-Linear Programming (MINLP) model due to *max* and *min* operators in Eqs. (**5-8**), (**5-9**) and (**5-10**). Since solving MINLP problem is much more computationally challenging than solving a Mixed Integer Linear Programming (MILP) problem, we transform the MINLP to MILP in next section.

5.3.1 Linearization

By substituting Eq. (**5-6**) and (**5-7**) in Eq. (5-5), the objective function can be written in Eq. (**5-15**) which is equal to Eq. (**5-16**) and for specific *j*. Therefore, the objective function can be written as in Eq. (**5-17**).

$$\sum_{k\in K}\sum_{j\in J}\left(\hat{R}_{jk}-R_{jk}\right)= \sum_{k=1}\sum_{j\in J}\left(\hat{R}_{jk}-E_j+d_{jk}\right) +\sum_{k>1\&\,k\in K}\sum_{j\in J}\left(\hat{R}_{jk}-\hat{R}_{jk-1}-E_{jk-1}+d_{jk}\right) \tag{5-15}$$

$$\sum_{k\in K}\left(\hat{R}_{jk}-R_{jk}\right)= \hat{R}_{j1}-E_j+d_{j1}+\hat{R}_{j2}-\hat{R}_{j1}-E_{j1}+d_{j2}+\hat{R}_{j3}-\hat{R}_{j2}-E_{j2}+d_{j3}+\cdots+ \hat{R}_{jk}-\hat{R}_{jk-1}-E_{jk-1}+d_{jk}=\hat{R}_{jk}-E_j+d_{j1}+\sum_{k>1\&\,k\in K}\left(-E_{jk-1}+d_{jk}\right) \tag{5-16}$$

$$\sum_{k\in K}\sum_{j\in J}\left(\hat{R}_{jk}-R_{jk}\right)= \sum_{j\in J}\left(\hat{R}_{jk}-E_j+d_{j1}+\sum_{k>1\&\,k\in K}\left(-E_{jk-1}+d_{jk}\right)\right) \tag{5-17}$$

According to Eqs. (5-17) and (5-5), we maximize the amount of recharged electricity (E_{jk}). Therefore, Eqs. (5-18), (5-19), (5-20) and (5-21) show the linear formulation of Eqs. (5-9) and (5-10). To linearize Eq. (5-8), we add Eqs. (5-22) and (5-23) as constraints to the model and penalty function, Eq. (5-24), to the objective function with μ=1. In addition, we multiply Eq. (5-5) by a coefficient (*M*) which is a large number greater than μ. Therefore, the objective function is changed to Eq. (5-25).

Adding the penalty function with μ=1, Eq. (5-24), does not affect the optimal solution, since the value of $\left(\hat{R}_{jk}-R_{jk}\right)$ depends directly on the amount of recharged electricity (E_{jk}) which objective function aims to maximize. Eqs. (5-6), (5-7) and (5-8) calculates the remaining battery range (R_{jk}) at the end of each trip based on the amount of recharge electricity (E_{jk}). The penalty function adjusts the value of $\hat{R}_{jk}$ to its minimum value which is R_{jk}. When R_{jk} is negative, $\hat{R}_{jk}$ is set to zero, leading to that the penalty function will be zero. When R_{jk} is positive, $\hat{R}_{jk}$ is set to its minimum value which is R_{jk} according to Eq. (5-22). In addition, the large number M guarantees that adding the penalty function does not have any effect on the optimal solution.

$$E_{jk} \leq E_j - \hat{R}_{jk} \qquad \forall j \in J, \forall k \in K \tag{5-18}$$

$$E_{jk} \leq \frac{Le\ t_{jk}}{r_j} \qquad if\ h_{jk} = 0,\ \forall j \in J, \forall k \in K \tag{5-19}$$

$$E_{jk} \leq M \textstyle\sum_{i\in I} P_{ijk} \qquad if\ h_{jk} = 0,\ \forall j \in J, \forall k \in K \tag{5-20}$$

$$E_{jk} \leq \frac{Lh\ t_{jk}}{r_j} \qquad if\ h_{jk} = 1,\ \forall j \in J, \forall k \in K \tag{5-21}$$

$$\hat{R}_{jk} \geq R_{jk} \qquad \forall j \in J, \forall k \in K \tag{5-22}$$

$$\hat{R}_{jk} \geq 0 \qquad \forall j \in J, \forall k \in K \tag{5-23}$$

$$\mu \textstyle\sum_{k\in K} \sum_{j\in J} \hat{R}_{jk} \tag{5-24}$$

$$\min \ M \textstyle\sum_{k\in K} \sum_{j\in J} \left(\hat{R}_{jk} - R_{jk}\right) + \mu \sum_{k\in K} \sum_{j\in J} \hat{R}_{jk} \tag{5-25}$$

5.3.2 Extensions on the Optimization Model

In the case that a mix of charging stations with different charging power (e.g., fast charging and slow charging) need to be installed, the model can be extended by replacing Eqs. (**5-9**), (**5-11**) and (5-12) with Eqs. (5-26)-(5-33). Eq. (5-26) calculates the amount of electricity that vehicle *j* can gain from recharge at either fast or slow charging stations at the end of trip *k*. Eqs. (5-27) and (5-28) show the limitation on the number of fast and slow charging stations, respectively. The amount of electricity that vehicle *j* can get from a slow or fast charging station at the end of trip *k* is formulated in Eqs. (5-29) and (5-30), respectively. Eq. (5-31) shows that at each candidate location, we can either install a fast charging station or a slow charging station, but not both. Eqs. (5-32) and (5-33) assure that each vehicle can only charge at one station at the end of each trip, with le^s and le^f representing the power level at a slow and fast charging stations, respectively.

$$E_{jk} = \min\left\{E_j - \hat{R}_{jk}, \textstyle\sum_{i\in I}(E^s_{jki} + E^f_{jki})\right\} \quad if\ h_{jk} = 0, \quad \forall j \in J, \forall k \in K \tag{5-26}$$

$$\textstyle\sum_{i\in I} y^f_i \leq B_f \tag{5-27}$$

$$\textstyle\sum_{i\in I} y^s_i \leq B_s \tag{5-28}$$

$$E^s_{jki} = min\left\{\frac{le^s\ t_{jk}}{r_j}, M\ Z_{ijk}\ y^s_i\right\} \qquad if\ h_{jk} = 0, \quad \forall j \in J, \forall k \in K, \forall i \in I \tag{5-29}$$

$$E^f_{jki} = min\left\{\frac{le^f\ t_{jk}}{r_j}, M\ Z_{ijk}\ y^f_i\right\} \qquad if\ h_{jk} = 0, \quad \forall j \in J, \forall k \in K, \forall i \in I \tag{5-30}$$

$$y_i^f + y_i^s \le 1 \qquad \forall i \in I \qquad (5\text{-}31)$$

$$\sum_{i\in I} E_{jki}^s \le \frac{le^s\, t_{jk}}{r_j} \qquad \forall j \in J, \forall k \in K \qquad (5\text{-}32)$$

$$\sum_{i\in I} E_{jki}^f \le \frac{le^f\, t_{jk}}{r_j} \qquad \forall j \in J, \forall k \in K \qquad (5\text{-}33)$$

In this formulation, the binary variable y_i is replaced by the two binary variable sets to separate slow and fast charging stations. Similarly, E_{ijk} is replaced by E_{jki}^s and E_{jki}^f.

y_i^f: Binary variable which shows whether a fast charging station is installed at location i, with 1 indicating presence and 0 indicating absence.

y_i^s: Binary variable which shows if a slow charging station is installed at location i, with 1 indicating presence and 0 indicating absence.

E_{jki}^s: Electricity recharged for vehicle j at the end of trip k from a slow charging station at location i (mile)

E_{jki}^f: Electricity recharged for vehicle j at the end of trip k from a fast charging station i (mile)

Constraints (5-26), (5-29) and (5-30) can be replaced by Eqs. (5-34)-(5-39) to obtain a linear formulation.

$$E_{jk} \le E_j - \hat{R}_{jk} \qquad \forall j \in J, \forall k \in K \qquad (5\text{-}34)$$

$$E_{jk} \le \sum_{i\in I}(E_{jki}^s + E_{jki}^f) \qquad if\ h_{jk} = 0,\ \forall j \in J, \forall k \in K \qquad (5\text{-}35)$$

$$E_{jki}^s \le \frac{le^s\, t_{jk}}{r_j} \qquad if\ h_{jk} = 0,\ \ \forall j \in J, \forall k \in K, \forall i \in I \qquad (5\text{-}36)$$

$$E_{jki}^s \le M\, Z_{ijk}\, y_i^s \qquad if\ h_{jk} = 0,\ \forall j \in J, \forall k \in K, \forall i \in I \qquad (5\text{-}37)$$

$$E_{jki}^f \le \frac{le^f t_{jk}}{r_j} \qquad if\ h_{jk} = 0,\ \forall j \in J, \forall k \in K, \forall i \in I \qquad (5\text{-}38)$$

$$E_{jki}^f \le M\, Z_{ijk}\, y_i^f \qquad if\ h_{jk} = 0,\ \forall j \in J, \forall k \in K, \forall i \in I \qquad (5\text{-}39)$$

5.4 Data

The taxi fleet in Beijing, China is used as a case study to apply the optimization model. Public fleets (i.e., taxis and buses) are likely early adopters for electric vehicles (A Krieger, L Wang, P Radtke, 2012). Although the case study is specific, the model can be generally applied to other fleets as well.

The vehicle trajectory data used in this study include 11,880 taxis (18% of the fleet) in Beijing over a period of three weeks (March 2 to 25, 2009). The data were recorded by geographic positioning systems (GPS) devices and consist of vehicle id, time stamps up to the seconds, and position of the vehicle at the recorded time (longitude and latitude). A total of 255 million data points are included in the data, covering over 2 million trips and 34 million miles of travel. The trajectory data are used to evaluate vehicle travel behaviors and extract trip chains (a series of driving and parking events). A threshold of fifteen minutes parking is used to separate trips. This threshold is set with the consideration that drivers are not likely to go through the hassle of charging if they have less than 15 minutes of parking time. More information about this data set can be found in (Cai et al., 2014).

The existing 1,737 gas stations in Beijing are considered as candidate locations to build public charging stations. Want et al. (2010) shows that gas stations with charging capability may lead to more efficient long-term infrastructure use when EVs gradually replace conventional gasoline vehicles. Beijing currently has 40 charging stations built. To compare how charging station sites optimized with vehicle travel patterns can increase electrified fleet VMT, our baseline model selects 40 locations among the 1,737 candidates to build charging stations. The impacts of the total number of charging stations on electrified fleet VMT are also examined. The service range of each charging station is set at 1 mile with the assumption that drivers are not willing to significantly revise their travel behavior to accommodate for charging.

Vehicle travel behavior varies from day to day. To capture this variation and examine model sensitivity, we separate the trajectory data into three weekly data sets and apply model to each. For each week, the data are prepared into four input matrixes, $D(d_{jk})$, $T(t_{jk})$, $H(h_{jk})$, and DIS (dis_{ijk}), with j equals to 11,881, i equals to 1,737, and k ranges from 83 to 125 depending on the week. Thus, each d_{jk}, t_{jk} and h_{jk} has at least 986,123 elements, where d_{jk} is the travel distance of vehicle j during trip k (mile), t_{jk} is dwell time of vehicle j at the end of trip k and before trip $k+1$ (hour), h_{jk} is a 0-1 matrix with 1 indicating that vehicle j parks at home during its dwell time at the end of trip k and 0 indicating that it does not park at home during the dwell time, and dis_{ijk} is the distance between candidate location i and the location of vehicle j at the end of trip k (mile). Given the size of the data set, the DIS matrix has over one billion elements. If directly considering DIS matrix elements as inputs to our optimization model, we have to define a set of binary variables with over one billion elements and parameters to indicate the accessibility of DIS elements by each vehicle, which makes solving the problem computationally intractable. To make the problem solvable, the elements of the DIS matrix are translated into binary elements in a Z matrix, where Z_{ijk} is 1 if vehicle j is parked within the service range of candidate location i at the end of trip k, and zero otherwise. Using Z matrix instead of DIS matrix reduces not only the data size but also the complexity of the problem by reducing the number of binary variables. However, reading Z matrix with over one billion elements is still time-consuming. To overcome this computational obstacle, we use a specific feature from the optimization software GAMS. In GAMS if we do not set any value for a parameter, its default value is set to zero. Because the Z matrix contains many zeros, we simply extract the non-zero Z_{ijk} and store the i, j, and k information in a series of vectors. Reading only the non-zero elements will reduce data size dramatically. In short, instead of directly using the *DIS* matrix, the information is translated into the position locations of non-zero Z_{ijk} as vectors before reading into the model.

We use 37.5kW and 7.04 kW for power outputs of public fast charging and slow charging stations, respectively (State Grid Corporation of China, 2010; Tong, 2014). Home charging is assumed to use residential power outlet at 2.2 kW. We assume all vehicles have access to home charging when they park at home. The effective all-electric-range (E_j) of all PHEVs is assumed to be 100 miles. Electricity consumption rate of PHEV is assumed to be constant at 0.35kWh/mile during the charging-depleting mode (USA.gov, 2013). Variation of fuel economy due to different driving condition is not considered in this study. Charging efficiency is considered as 88% (Kelly et al., 2012). We assume that all vehicles start with fully charged battery at the beginning of each week, meaning that R_j is set to 100 miles.

5.5 Results and Discussions

The optimization model is implemented in the GAMS environment using Cplex solver to solve the optimization problem. For solving MILP problems, Cplex uses a branch and cut algorithm which generates and solves a series of LP subproblems. The most common difficulty for solving MIP problems is running out of memory. Even small MILP problems generate many subproblems, making it very computationally intensive and requiring significant amount of physical memory. This problem arises when the branch and bound tree becomes so large that insufficient memory is available to solve an LP subproblem. The branch and bound tree can contain as large as 2^n terminal nodes, where n equals the number of binary variables. A problem containing only 30 binary variables could produce a tree having over one billion terminal nodes (Solutions et al., 2012).

In our problem, we have 1,737 binary variables and three set of variables with $j \times k$ dimension, with j equal to 11,881 and k ranging from 83 to 125. There are at least 3×11,881×83 = 2,958,369 general variables. When using GAMS/Cplex to find the global optimal solutions, the solution process using this dataset terminates with an unrecoverable integer failure message with 100 GB of physical memory that is highly demanding in terms of computing infrastructure. To overcome this problem, the values of following Cplex options are changed: reinv, varsel, cuts, nodesel, nodefileind, workmem, memoryemphasis, names, threads, and lpmethod. Justifying these options carefully can have dramatic effects on improving the computing speed and reducing memory usage.

5.5.1 The 40-Station Scenario

At the time of this study, Beijing has 40 charging stations and posts already built. The 40-station scenario implemented in our model finds the 40 optimal locations from the candidate gas stations based on weekly data. As shown in Figure 34 (a), while existing charging stations can electrify 29±3% and 35±2% of the fleet VMT with slow charging and fast charging respectively, location-optimized stations can effectively increase electrified fleet VMT to 46±4% and 66±2%, on average an 59% and 88% improvement. Comparing to the locations of the existing stations, the optimized stations are concentrated in the inner city (Figure 34b). Here only the stations optimized with data for week 1 are presented for illustration. Location maps with other weekly data are included in the Appendix (Figure A. 12). Similar patterns exist across all weeks. It is notable that, while the location of optimized stations in the suburban area varies from week to week, selection of optimized stations in the inner city is quite consistent (Figure A. 12d). By zooming into the inner city, it is clear that the locations of the optimized stations are quite different from those existing ones (Figure 35a-c). Significant charging demand near the Beijing Capital International Airport has not currently been covered by the existing stations (Figure 35d).

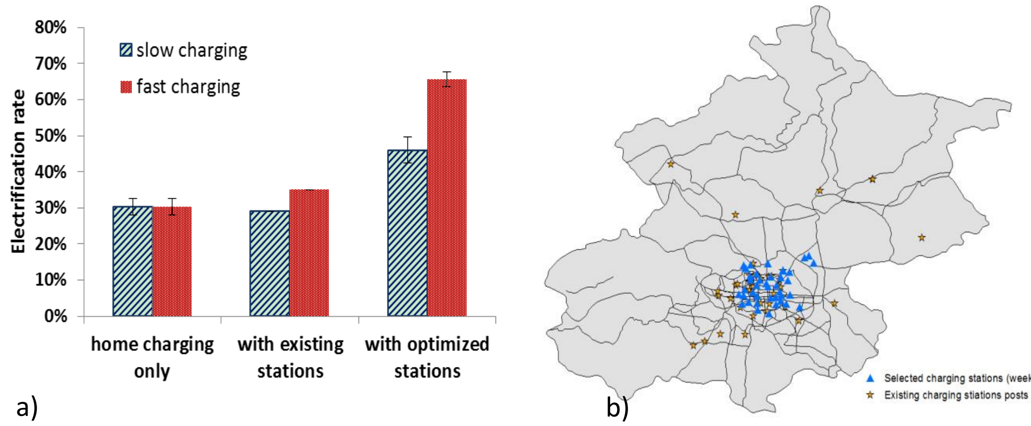

Figure 34. Electrified fleet VMT as percentage of total fleet VMT (electrification rate) (a) and optimal public charging stations (b) of the 40-station scenario comparing to the existing 40 built charging stations.

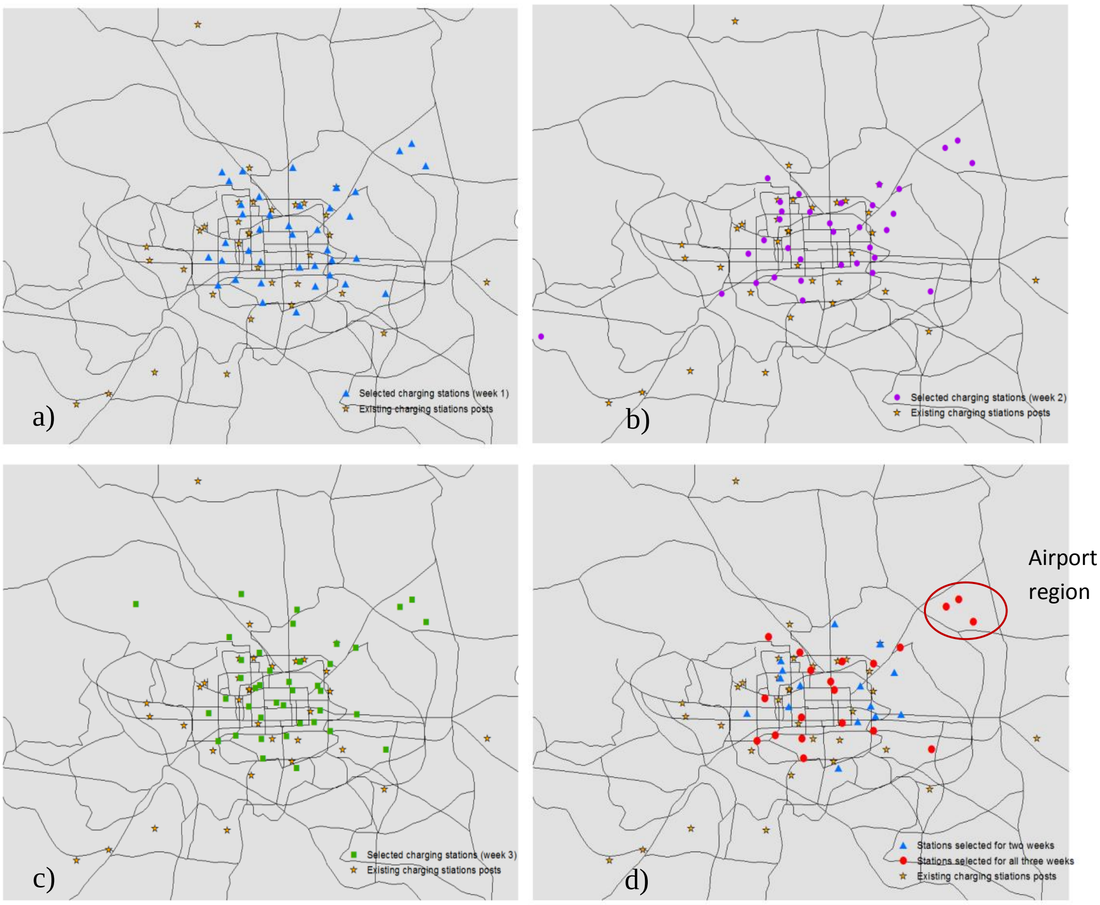

Figure 35. Location comparison of optimized stations and existing stations in the inner city of Beijing: a) optimization results with data for week 1; b) optimization results with data for week 2; c) optimization results with data for week; and d) optimal locations selected in two or three weeks.

5.5.2 Impacts of increased number of charging stations

To evaluate the impact of the total number of stations that can be installed (*B*) on the optimization results, we ran models ranging *B* from 20 to 500. The results show that, while increasing the total number of charging stations increases electrified fleet VMT regardless of charging speed, the marginal electrified fleet VMT for both type of charging stations quickly diminishes (Figure 36). The difference in electrified fleet VMT between installing the same number of fast and slow charging stations diverges initially but stays stable at about 20% when there are 40 or more charging stations. Considering solely gas stations as the candidate locations cannot achieve 100% electrified fleet VMT. Therefore, other locations such as parking lots should also be considered as the candidate locations for higher electrified fleet VMT.

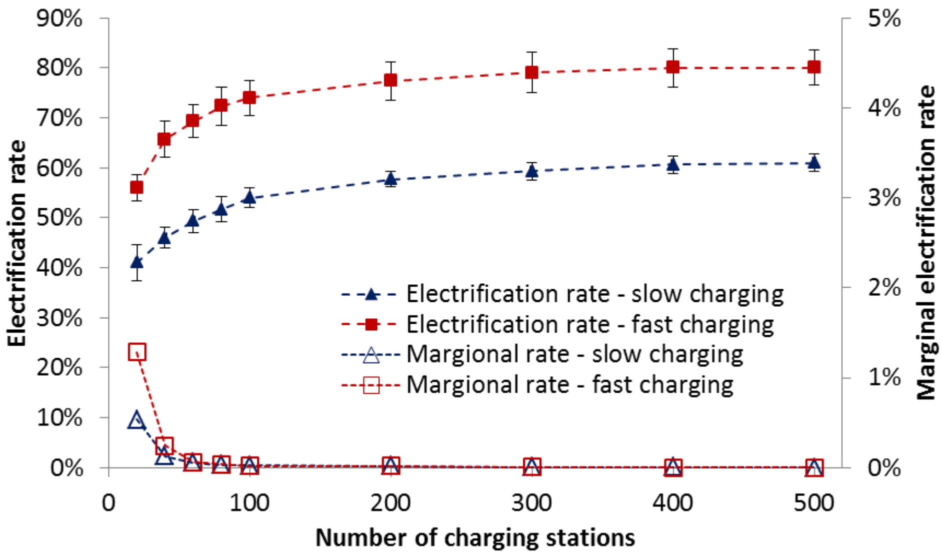

Figure 36. Change of electrified fleet VMT as the percentage of total fleet VMT (electrification rate) and marginal electrification rate with increasing number of charging stations

The locations of optimized stations concentrate in the inner city in all scenarios, gradually expanding to the suburban area with increasing number of charging stations (Figure 37 a-d). Zoomed-in maps for the inner city are included in the Appendix (Figure A. 13). To measure how many of the selected stations stay as the optimal choice when the total number of charging stations is increased, we define retention rate as the percentage of selected stations in a scenario with smaller number of stations remains as the optimal choices in a scenario with greater number of stations. As shown in Figure 38, on average, the overall retention rate is 70% to 88% for slow charging and 67% to 88% for fast charging, which indicates that the majority of the optimal stations are consistently selected even when the total number of charging stations are increased by 25 times. In general, the optimal slow charging stations have higher retention rate than the fast charging ones, showing that slow charging stations selected for short term planning (i.e. scenarios with less total number of stations) are more likely to stay as the optimal choices for long term planning (i.e. scenarios with larger total number of stations). Additionally, the standard deviation of the retention rate reduces with increasing total number of charging stations, showing that the variation of travel pattern among different weeks can be better covered with more charging stations. With 200 charging stations, the standard deviation of retention rate can be effectively reduced to less than 3%.

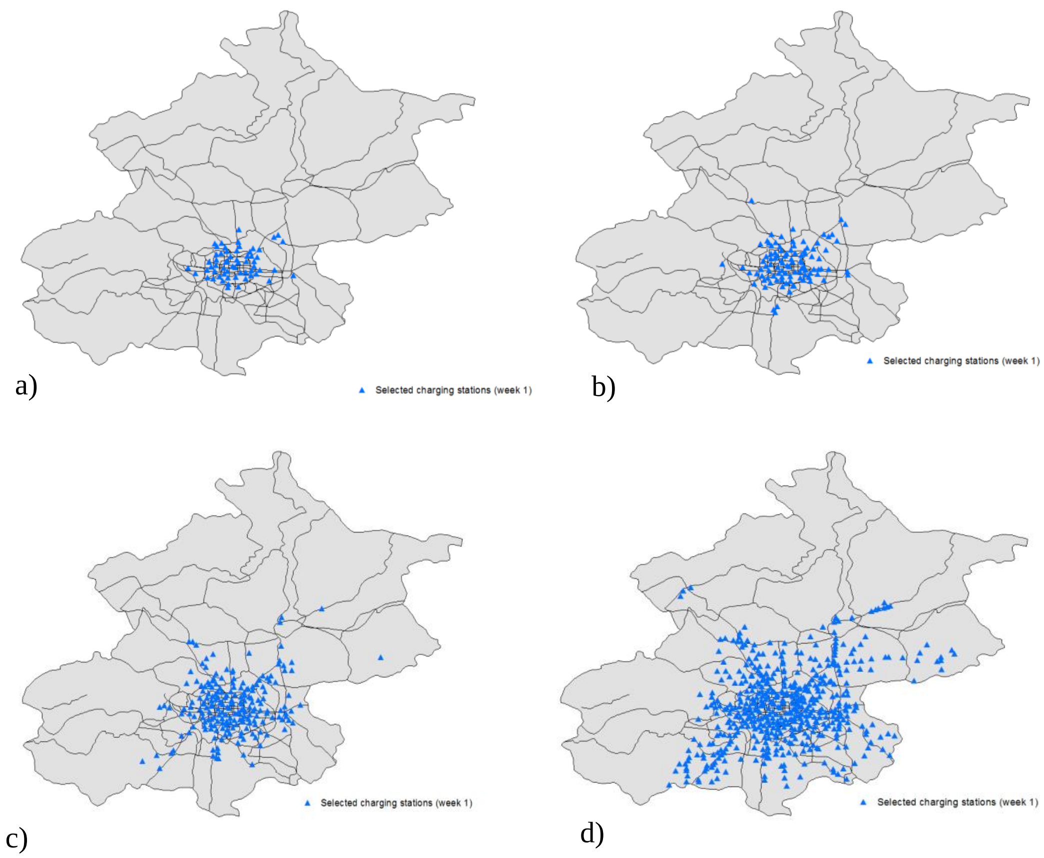

Figure 37. Locations of optimized stations in scenarios with different total number of charging stations: a) 60 stations, b) 100 stations, c) 200 stations, and d) 500 stations.

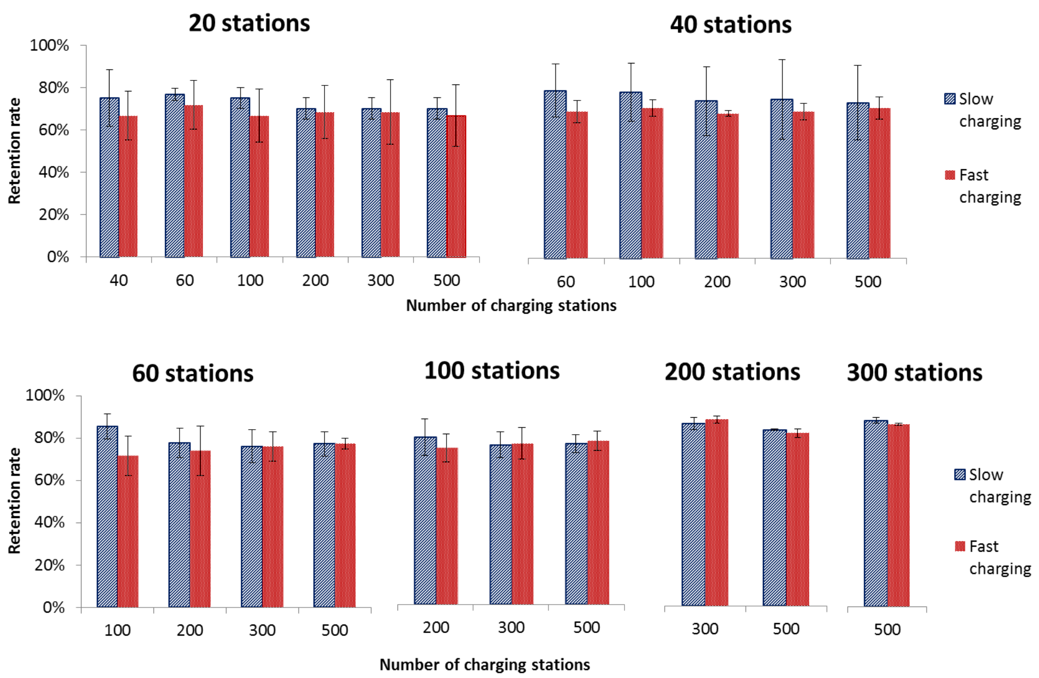

Figure 38. Retention rate of selected stations when increasing total number of charging stations

5.6 Impacts of AER

AER is also a key factor in determining overall electrification rate. To test the model's sensitivity to AER, we conducted a sensitivity analysis ranging AER from 60 miles to 120 miles. The results show that, in the tested range, greater AER can lead to higher electrification rate (Figure 6). On average, increasing AER by 1 mile can gain 0.15% to 0.4% of electrification rate improvement with fast charging, and 0.15% to 0.25% with slow charging. It is notable that PHEVs with greater AER could be more expensive and as a result have lower adoption rates (Cai and Xu, 2013). The economics consideration is not included in this analysis. With the same number of charging stations, the locations of the selected stations are not significantly affected by AER (Figure 7). With fast charging, 63% to 80% of the selected stations are consistent regardless of different AER; while with slow charging, the rate is higher at 75% to 82%.

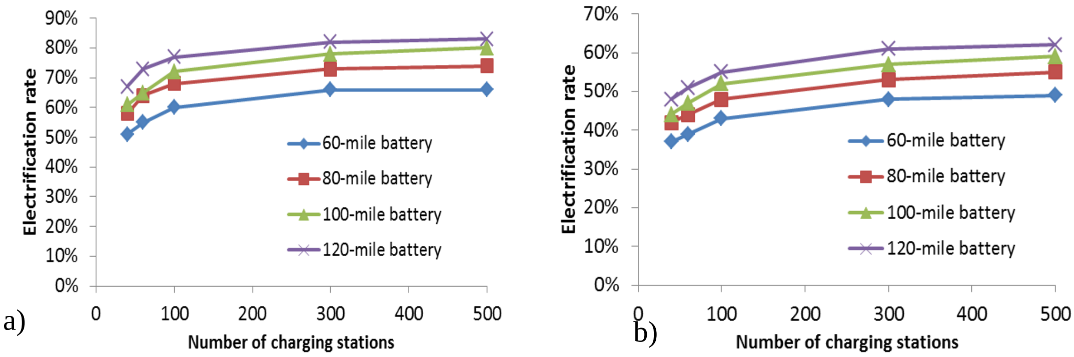

Figure 6. Electrification rates with different battery all-electric-range and different numbers of charging stations: a) fast charging; b) slow charging.

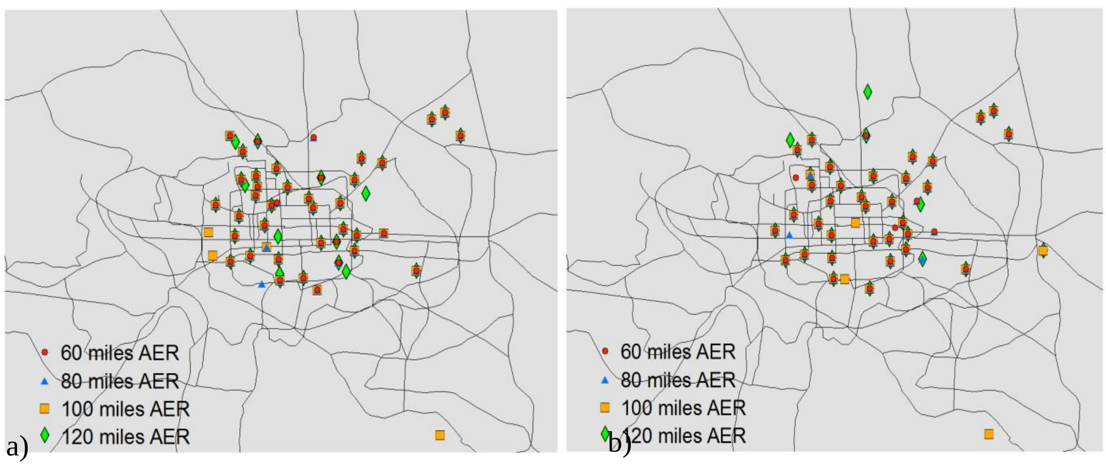

Figure 7. Locations of selected stations in 40-station scenario using different AER: a) fast charging; b) slow charging.

5.7 Conclusion

In this study, an optimization model is formulated to find the optimal locations for installing charging stations to maximize electrified fleet VMT based on vehicle travel behaviors. The formulated model is implemented for Beijing, China as a case study using vehicle trajectory data of 11,880 taxis over a period of three weeks. The large scale data is handled by formulating the mathematical model properly, transforming input data, and adjusting Cplex options. The results show that the optimal locations of charging stations can have significant improvements. The Majority of the optimal locations are selected in the inner city. By increasing the total number of charging stations, the locations of the optimal stations expand outward from the inner city. While more charging stations increase electrified fleet VMT, the marginal gain diminishes quickly regardless of charging speed. With more than 40 charging stations, the difference of electrified fleet VMT between the same number of slow and fast charging stations stays constantly at 20%. The majority of the stations selected in a model with smaller number of charging stations remain as the optimal choices when the total number of charging stations increases. Slow charging stations generally have higher retention rates.

Appendix is given in Annex IV

6 Chapter VI
Synoptic Discussion and Outlook

Conclusion and Future Directions

The sustainable transportation system design problem in urban areas is one of the most important sustainability challenges in the 21st century considering the fact that more than 50% of the world population lives in urban areas. This trend will continue into the future. The main problem is to provide a sustainable transportation infrastructure for travel between housing/work/commerce. This problem was addressed in the literature after the WWII in order to accommodate urban influx of industry and service workers in North America and Western Europe from cost effectiveness perspective only. However, main challenge nowadays is to look at this problem from sustainability perspectives including environmental and social considerations in addition to classical economic consideration.

Urban network design problems are complex since different groups are involved in decision-making process. In addition, considering sustainability also makes the problem even more complex, since we usually deal with more than one objective functions. In this dissertation, I successfully developed models for transportation network and location design problems to improve sustainability in urban regions.

An important modeling assumption of transportation network design problems in this dissertation is that travel demand is stochastic, which is ignored in previous studies. In this dissertation I successfully formulated the urban transportation network by considering demand as a random variable. In addition, I captured three aspects of sustainability in the formulations. Environmental aspect is considered by minimizing the amount of emissions, while social aspect is captured in model formulation by minimizing the probability of traffic congestion. The probability of traffic congestion is successfully formulated using multi-variant normal distribution. In addition, a novel solution algorithm based on outer approximation and ε-constraint is developed to find the optimal solution for the MINLP formulation for the urban transportation networks. I applied the model for Istanbul, Turkey using travel production and attraction of 38 zones and detail information of 17,663 Istanbul main roads. This large data set is successfully handled and the formulated model is solved optimally.

In addition I successfully formulated a novel optimization model to find optimal locations to build electric vehicle charging stations. I applied the model for Beijing, China using travel behaviors of 11,880 taxis over a period of three weeks. I could successfully handle this large data set and find the optimal solutions by applying three techniques; formulating the mathematical model properly, transforming input data, and adjusting Cplex options.

Four manuscripts are written based on the mentioned ideas for urban transportation networks and location design problems presented in chapter 2, 3, 4 and 5. The main findings are explained as follows.

In chapter 1, I formulated two bi-objective models to minimize the amount of traffic congestion and amount of CO emission produced by transport, and maximize the utility function of the residence. Objective functions of the first model are maximizing the utility function and minimizing the probability of traffic congestion, and the objective functions of the second model are maximizing the utility function and minimizing the amount of CO emission. Therefore, the relation between different land use and transport structure and amount of CO emission is analyzed.

I formulated a closed form expression to calculate the Cholesky factorization matrix that is implemented as a set of constraints in the optimization model, to estimate the probability of traffic congestion by multivariate normal distribution. The utility function captures travel time and attractiveness of each zone as a cost function. I use BPR link impedance function to estimate average travel time. In addition I consider zonal attractiveness as a function of intensity or congestion of each zone and travel cost. And, CO emission is considered as the function of travel time and speed in each link.

I proposed ϵ-constraint method as the solution algorithm, and I analyzed model behavior through several experiments. I tested our approach on ten different problems with different sizes. By analyzing the model behavior, I found that expanding the capacity of existing links instead of constructing the new links can be a better policy. By augmenting the link capacities, both amount of traffic congestion and utility improve, while by constructing the new links just the amount of traffic congestion improve. In addition amount of CO emission reduces by augmenting the link capacities. Besides, distributing the population more symmetrically in the origin and destination zones can help to improve the reliability and the utility of the network and reducing CO emission. Considering CO emission as the objective function instead of reliability index effects on the distribution of flow in the network and improves the utility value.

In chapter 2, I formulated a bi-level stochastic sustainable transportation model. Lower level problem is a network design problem and its objective function is minimizing travel cost. The travel cost is formulated by using BPR link impedance function for on road vehicles. The upper level problem is transport allocation problem where it has two objective functions minimizing transport pollutions and minimizing probability of traffic congestion in the network. Transport pollution is formulated by calculating amount of CO emissions produced by each transport in each link. In addition probability of traffic congestion is calculated by using multivariate normal distribution. This probability calculates probability that flow in each link is less than capacity of the links plus amount of expansions.

In this study I present closed form expressions of KKT optimality conditions of lower level problem and I consider them as a set of constraints in the upper level model. In this manner I formulate a single level bi-objective model which is MINLP problem. I implement outer approximation algorithm and ε-constraint method to solve the problem. Outer approximation algorithm is based on generating NLP sub problems and Master problems and solving them iteratively till the optimality gap is within tolerance limits. In addition, the designed algorithm guarantees the optimal solution is a global solution for the lower problem.

The results show that the use of subway is the best solution to minimize travel cost, emission and traffic congestion in urban areas. Allocating more budgets for subway construction lines helps to decrease on road flows and improve the two objective values. In addition distributing on road flow more balance in the network helps to reduce probability of traffic congestion but it increases amount of CO emissions. So designing strategies to make trade off between these two conditions can be the best solution to minimize emissions and traffic congestion. In addition allocating more budget for constructing subway lines than constructing new on road links can be a good strategy for reduce probability of traffic congestion and emission in urban areas.

In chapter 4, I calculated the amount of different emission productions of each road of the Istanbul transportation network. The emission is calculated as a function of the real speed level in each road. Real speed level is calculated based on the road length and the actual travel time in each link, and travel time is calculated using BPR link impedance function which is a function of flow and the capacity of each road. Using large data set of the Istanbul transportation network, flow in each road and the capacity of the main roads is estimated. Flow is calculated using travel attraction and production in 38 districts, while also considering the shortest path connecting them. Capacity is calculated using the number of lanes in each road. In addition, optimization models are developed to minimize CO_2 emissions and overloading flows. The optimal results identify the priority of roads for capacity expansion and installing public shared vehicles. The result shows specific roads have significant effect on increasing air pollution in Istanbul.

In chapter 5, I formulated an optimization model to find the optimal locations for installing charging stations to maximize electrified fleet VMT based on vehicle travel behaviors. The formulated model is implemented for Beijing, China as a case study using vehicle trajectory data of 11,880 taxis over a period of three weeks. The large scale data is handled by formulating the mathematical model properly, transforming input data, and adjusting Cplex options.

The results show that the optimal locations of charging stations can have significant improvements. The Majority of the optimal locations are selected in the inner city. By increasing the total number of charging stations, the locations of the optimal stations expand outward from the inner city. While more charging stations increase electrified fleet VMT, the marginal gain diminishes quickly regardless of charging speed. With more than 40 charging stations, the difference of electrified fleet VMT between the same number of slow and fast charging stations stays constantly at 20%. The majority of the stations selected in a model with smaller number of charging stations remain as the optimal choices when the total number of charging stations increases. Slow charging stations generally have higher retention rates.

Perspective and future directions

Passenger flows are studied in this dissertation for urban transportation network design problems. While freight vehicle movements in urban areas contribute to congestion, in total passenger vehicles usually have a more significant impact on congestion levels. Freight vehicles typically represent 8-15% of total traffic flow in urban areas. Almost all freight vehicles are diesel powered and these engines result in emissions of particulates that can damage human health; due to the direct impact on human health and the threat of fines from the European Commission when EU air quality limits are exceeded, city authorities often regard improving air quality as a high priority. Also, Noise generated by freight vehicles in urban areas during the night is often regarded as a nuisance by residents because it disturbs their sleep (MDS Transmodal Limited, 2012). Future research is needed to incorporate freight flow with passenger flow and conduct the analysis in chapter 2, 3 and 4.

Zonal attractiveness encompasses the amenities of residential locations. It describes residents' valuation of alternative locations, which can be measured by associated attributes. Some attributes are exogenous, such as the natural environment and lot size; others are endogenous within the model, also known as location externalities, resulted from land-use and transport interactions, or other neighborhood interactions, such as traffic noise and segregated neighborhood in residential locations, which will impact residents' location choices (Ma and Lo, 2012). In this study for simplicity, I considered the utility function as a function of zonal attractiveness, which is measured by two terms: first, the zone congestions and second, travel cost. However, other elements such as, safety, security, air pollution, noise pollution, accessibility and affordability can be considered to incorporate sustainability in the utility function. Future studies should be conducted to formulate an improved utility function and analyze the problem addressed in chapter 2 with the new utility function.

In the formulated models for the Istanbul case, I considered environmental aspect of sustainability in our formulation. However incorporation of economic aspects such as travel cost is recommended. In addition, the formulations are focused on transportation network design without considering the land-use system. Despite Istanbul is large size, residential areas are concentrated in small sections, which makes the incorporation of land-use system quite important. Further studies are needed to incorporate the economic aspects and the land-use structure into the formulations.

I assumed travelers choose the shortest path to travel from their origin to destination zones. However it is possible to select paths which are less congested or less expensive to travel. I also assumed travelers will not change their travel behavior. However, it is also possible to change their travel behavior by installing new public transport lines. Further studies are needed to analyze the travel behaviors and evaluate the impact of the shortest path assumption.

The effect of the road slope on emission production is ignored in formulations. However, most of the roads are not smooth in Istanbul because of its geographic location. Steep hills in Istanbul contribute to high grade slopes which further impact emission production. Future studies should incorporate the effect of road slops on emission productions.

The modeling framework, presented in chapter 4, provides a pioneer perspective to combine modeling of emission generated by transportation for mega cities. This perspective would be developed further with a micro analysis for each district as well as with the micro scale analysis done in this study for a city.

Environmental Impact Assessment (EIA) Directive (85/337/EEC) of the EC has been in force since 1985 and applies to a wide range of defined public and private projects. The optimization model developed and tested for Istanbul has a strong potential to contribute the efficiency of the implementation of the directive addressing to emissions caused by urban transport and logistics activities. Specially, since the number of large scale transportation and infrastructure projects have been carrying on, the framework developed in this study for emission calculation would be useful for taking measures and for providing feedback for a diverse policy related to urban management. The third airport, two intercontinental transits (new underground motor vehicle tunnel and the bridge for both rail and motor vehicle systems), a new highway and its connections, the Izmit Bay Area Transit Bridge with another highway that will have a regional impact are some of these mega projects which have been developed simultaneously.

Furthermore, another dimension is the area based urban management, especially for historic sites that have special regulations, planning framework and management. For instance the Historical Peninsula Site Management Plan for UNESCO World Heritage Sites has a clear direction on minimizing emissions generated by motor vehicles. The impact of the new transport network would need optimization approaches that enable testing several scenarios to provide feedback for urban management in the historical setting. The impact of transportation structures on the quality of life for citizens and tourists but also on the physical conditions of cultural heritage plays a key role for effectiveness of urban preservation and conservation studies.

Another future direction is to develop user-friendly software based on developed optimization framework for Istanbul, integrated to the existing transport model of the city that is built with special software like TransCAD. That could provide feedback for transport planning, transport management and interaction with urban planning at metropolitan and district scales.

Electric cars have just been introduced to the market in Turkey. Therefore the usage rate is quite low, but for future research the optimization model could take in to account the potential decrease of the motor vehicles use LPG, diesel and gasoline.

While the proposed model in chapter 5 has the merit of incorporating real world vehicle travel behavior to better estimate public charging demand, a key assumption is that the drivers will not change their behavior when they switch from conventional gasoline vehicles to PHEVs. This assumption is made under the consideration that, if the drivers do not change their travel patterns, they are more likely to adopt using gas stations to charge their EVs. However, it is possible that PHEV drivers may modify their behavior to actively seek charging opportunities, because electricity is cheaper than gasoline on a per mile basis. Future studies to compare travel behavior before and after EV adoption will be needed to evaluate the impact of this assumption.

The case study of taxi fleet in Beijing, China demonstrates that real world vehicle trajectories can be used in optimization models to estimate charging demand. However, the results of the case study need to be used carefully for policy recommendations. First of all, the case study assumes that the public charging infrastructure only serves the taxi fleet. The charging demand of other vehicles (e.g. private vehicles, public service vehicles, buses) is not considered. Future research incorporating data of different fleets will be needed to better reflect city level public charging infrastructure for mixed uses. In addition, this model does not take into consideration the space constraints and the capacity limits of the charging stations. Depending on the location of the existing gas stations, certain stations may be constrained by space, the number of charging posts, and the associated parking space it can accommodate. If all charging posts are occupied at a given time, nearby vehicles with charging needs will not be able to charge at this station. Furthermore, the candidate locations in this case study are limited to existing gas stations only. When modeling private vehicles, existing parking lots may be better candidates for charging stations.

Lastly, the maximized electrified fleet VMT does not guarantee maximized environmental benefits. Higher electrified fleet VMT displaces more fossil-based liquid fuels (e.g., gasoline). However, the environmental impacts of fleet electrification depend on the grid fuel mix, charging time (base load versus peak load), and individual driving conditions (variations of fuel economy). Future studies can expand the model to optimize environmental benefits.

REFERENCES

A Krieger, L Wang, P Radtke, C.M., 2012. Recharging China’s electric vehicle aspirations: A perspective on revitalizing China's electric vehicle industry. McKinsey Co. China Auto Hub.

AASHTO, 2015. Sustainability.

Abbaspour, M., Soltaninejad, a, 2004. Design of an environmental assessment model on the effect of vehicle emission in greater Tehran on air pollution with economic sensitivity 1, 27–38.

Affum, J.K., Brown, A.L., Chan, Y.C., 2003. Integrating air pollution modelling with scenario testing in road transport planning: the TRAEMS approach. Sci. Total Environ. 312, 1–14. doi:10.1016/S0048-9697(03)00192-X

Aggarwal, P., Jain, S., 2014. Energy demand and CO2 emissions from urban on-road transport in Delhi: current and future projections under various policy measures. J. Clean. Prod. 2040. doi:10.1016/j.jclepro.2014.12.012

Anas, A., 2013. Modelling in Urban and Regional Economics. Taylor & Francis.

Anderstig, C., Mattsson, L., 1998. Modelling land-use and transport interaction: evaluations and policy analysis. Netw. Infrastruct. Urban Environ. ….

Ban, J.X., Liu, H.X., Ferris, M.C., Ran, B., 2006. A general MPCC model and its solution algorithm for continuous network design problem. Math. Comput. Model. 43, 493–505. doi:10.1016/j.mcm.2005.11.001

Barra, T.D. La, Pérez, B., Vera, N., 1984. TRANUS-J: putting large models into small computers. … Plan. B Plan. Des.

BATTY, M., 1985. INTEGRATED URBAN MODELS-POLICY ANALYSIS OF TRANSPORTATION AND LAND-USE-PUTNAM, SH.

Boyce, D.E., Janson, B.N., 1980. A discrete transportation network design problem with combined trip distribution and assignment. Transp. Res. Part B Methodol. 14, 147–154. doi:10.1016/0191-2615(80)90040-5

Bravo, M., Briceño, L., Cominetti, R., Cortés, C.E., Martínez, F., 2010. An integrated behavioral model of the land-use and transport systems with network congestion and location externalities. Transp. Res. Part B Methodol. 44, 584–596. doi:10.1016/j.trb.2009.08.002

Cai, H., Jia, X., Chiu, A.S.F., Hu, X., Xu, M., 2014. Siting public electric vehicle charging stations in Beijing using big-data informed travel patterns of the taxi fleet. Transp. Res. Part D Transp. Environ. 33, 39–46. doi:10.1016/j.trd.2014.09.003

Cai, H., Xu, M., 2013. Greenhouse gas implications of fleet electrification based on big data-informed individual travel patterns. Environ. Sci. Technol. 47, 9035–43. doi:10.1021/es401008f

Chang, J.S., Mackett, R.L., 2006. A bi-level model of the relationship between transport and residential location. Transp. Res. Part B Methodol. 40, 123–146. doi:10.1016/j.trb.2005.02.002

Chen, A., Kim, J., Lee, S., Kim, Y., 2010a. Stochastic multi-objective models for network design problem. Expert Syst. Appl. 37, 1608–1619. doi:10.1016/j.eswa.2009.06.048

Chen, A., Pravinvongvuth, S., Chootinan, P., 2010b. Scenario-based multi-objective AVI reader location models under different travel demand patterns. Transportmetrica 6, 53–78. doi:10.1080/18128600902929617

Chen, A., Subprasom, K., Ji, Z., 2006. A simulation-based multi-objective genetic algorithm (SMOGA) procedure for BOT network design problem. Optim. Eng. 7, 225–247. doi:10.1007/s11081-006-9970-y

Cheng, Y.-H., Chang, Y.-H., Lu, I.J., 2015. Urban transportation energy and carbon dioxide emission reduction strategies. Appl. Energy. doi:10.1016/j.apenergy.2015.01.126

Chiou, S.-W., 2009. A subgradient optimization model for continuous road network design problem. Appl. Math. Model. 33, 1386–1396. doi:10.1016/j.apm.2008.01.020

City of Surrey, 2012. Electric Vehicles [WWW Document]. URL http://www.surrey.ca/community/12250.aspx (accessed 8.27.14).

Davis, G.A., 1994. Exact local solution of the continuous network design problem via stochastic user equilibrium assignment. Transp. Res. Part B Methodol. 28, 61–75. doi:10.1016/0191-2615(94)90031-0

Davis, S.C., Diegel, S.W., Boundy, R.G., 2011. Data Book 30.

Deb, K., 2001. Multi-objective optimization using evolutionary algorithms.

Demirel, H., Sertel, E., Kaya, S., Zafer Seker, D., 2008. Exploring impacts of road transportation on environment: a spatial approach. Desalination 226, 279–288. doi:10.1016/j.desal.2007.02.111

Dempe, S., 2002. Foundations of Bilevel Programming. Springer.

Dong, J., Liu, C., Lin, Z., 2014. Charging infrastructure planning for promoting battery electric vehicles: An activity-based approach using multiday travel data. Transp. Res. Part C Emerg. Technol. 38, 44–55. doi:10.1016/j.trc.2013.11.001

Dowling, R., 2005. Predicting air quality effects of traffic-flow improvements: final report and user's guide.

Drud, A., 1994. CONOPT—A Large-Scale GRG Code. ORSA J. Comput. 6, 207–216.

Duran, M.A., Grossmann, I.E., 1986. An outer-approximation algorithm for a class of mixed-integer nonlinear programs. Math. Program. 36, 307–339. doi:10.1007/BF02592064

Echenique, M., Crowther, D., Lindsay, W., 1969. A spatial model of urban stock and activity. Reg. Stud.

Environmental Protection Agency, 2000. Projecting Land-Use Change: A Summary of Models for Assessing the Effects of Community Growth and Change on Land-Use Patterns [WWW Document]. URL http://www.epa.gov/reva/docs/ProjectingLandUseChange.pdf (accessed 4.26.15).

European Commission, 2015a. Road transport: Reducing CO2 emissions from vehicles [WWW Document]. URL http://ec.europa.eu/clima/policies/transport/vehicles/index_en.htm (accessed 4.20.15).

European Commission, 2015b. Reducing CO2 emissions from passenger cars [WWW Document]. URL http://ec.europa.eu/clima/policies/transport/vehicles/cars/index_en.htm (accessed 4.20.15).

Farahani, R.Z., Miandoabchi, E., Szeto, W.Y., Rashidi, H., 2013. A review of urban transportation network design problems. Eur. J. Oper. Res. 229, 281–302. doi:10.1016/j.ejor.2013.01.001

Farvaresh, H., Sepehri, M.M., 2012. A Branch and Bound Algorithm for Bi-level Discrete Network Design Problem, Networks and Spatial Economics. doi:10.1007/s11067-012-9173-3

Federal Highway Administration (FHWA), 2006. Multi-Pollutant Emissions Benefits of Transportation Strategies [WWW Document]. URL http://www.fhwa.dot.gov/environment/air_quality/publications/fact_book/index.cfm (accessed 5.22.14).

Ferguson, E.M., Duthie, J., Waller, S.T., 2010. Network methods for project selection based on optimizing environmental impact.

Fletcher, R., Leyffer, S., 1994. Solving mixed integer nonlinear programs by outer approximation. Math. Program. 66, 327–349. doi:10.1007/BF01581153

Friesz, T.L., Anandalingam, G., Mehta, N.J., Nam, K., Shah, S.J., Tobin, R.L., 1993. The multiobjective equilibrium network design problem revisited: A simulated annealing approach. Eur. J. Oper. Res. 65, 44–57. doi:10.1016/0377-2217(93)90143-B

Garrett, M., Wachs, M., 1996. Transportation planning on trial: The Clean Air Act and travel forecasting.

Genz, A., 1992. Numerical Computation of Multivariate Normal Probabilities. J. Comput. Graph. Stat. 1, 141–149. doi:10.1080/10618600.1992.10477010

Geoffrion, A.M., 1972. Generalized Benders decomposition. J. Optim. Theory Appl. 10, 237–260. doi:10.1007/BF00934810

Hall, P., 1998. Cities in Civilization. New York: Pantheon.

Hao, H., Geng, Y., Wang, H., Ouyang, M., 2014. Regional disparity of urban passenger transport associated GHG (greenhouse gas) emissions in China: A review. Energy 68, 783–793. doi:10.1016/j.energy.2014.01.008

He, D., Liu, H., He, K., Meng, F., Jiang, Y., Wang, M., Zhou, J., Calthorpe, P., Guo, J., Yao, Z., Wang, Q., 2013. Energy use of, and CO2 emissions from China's urban passenger transportation sector - Carbon mitigation scenarios upon the transportation mode choices. Transp. Res. Part A Policy Pract. 53, 53–67. doi:10.1016/j.tra.2013.06.004

He, F., Wu, D., Yin, Y., Guan, Y., 2013. Optimal deployment of public charging stations for plug-in hybrid electric vehicles. Transp. Res. Part B Methodol. 47, 87–101. doi:10.1016/j.trb.2012.09.007

Hickman, J., Hassel, D., Joumard, R., Samaras, Z., Sorenson, S., 1999. Methodology for calculating transport emissions and energy consumption.

Ho, H., Wong, S., 2007. Housing allocation problem in a continuum transportation system. Transportmetrica.

Hoogma, R., Kemp, R., Schot, J., Truffer, B., 2005. Experimenting for Sustainable Transport: The Approach of Strategic Niche Management. Routledge.

Huang, Ke, Jin Zhang, Meiling He, and W.L., 2010. An Optimal Model and Solution Algorithm of Urban Traffic Network Considering Exhaust Emission Control, in: ICLEM. pp. 526–532.

Hui, X., Kefei, Y., 2009. A bi-level programming model of urban land use and network design problem. (PEITS), 2009 2nd Int. Conf.

Ibeas, Á., Cordera, R., Dell'Olio, L., Coppola, P., 2013. Modelling the spatial interactions between workplace and residential location. Transp. Res. Part A Policy Pract.

IMM, 2009. İstanbul Air Quality Strategy-Istanbul Metropolitan Municipality.

IMM, 2011. Istanbul Metropolitan Area Integrated Urban Transportation Master Plan Summary Report-Istanbul Metropolitan Municipality.

IMM, 2014. Strategic Plan 2015-2019-Istanbul Metropolitan Municipality.

J. Javid, R., Nejat, A., Hayhoe, K., 2014. Selection of CO2 mitigation strategies for road transportation in the United States using a multi-criteria approach. Renew. Sustain. Energy Rev. 38, 960–972. doi:10.1016/j.rser.2014.07.005

JR, E.G.B., 2012. $120 Million Settlement to Fund Electric Car Charging Stations Across California [WWW Document]. URL http://gov.ca.gov/news.php?id=17463 (accessed 8.27.14).

Kanakidou, M., Mihalopoulos, N., Kindap, T., 2011. Megacities as hot spots of air pollution in the East Mediterranean. Atmos. Environ. 45.

Kanaroglou, P., Scott, D., 2002. Integrated urban transportation and land-use models for policy analysis. Gov. Cities Move Funct. Manag. Perspect. Transform. Eur. Urban Infrastructures. Ed. by M. Dijst, W. Schenkel, I. Thomas. Ashgate, Aldershot, UK.

Kelly, J.C., MacDonald, J.S., Keoleian, G.A., 2012. Time-dependent plug-in hybrid electric vehicle charging based on national driving patterns and demographics. Appl. Energy 94, 395–405. doi:10.1016/j.apenergy.2012.02.001

Khanna, P., Jain, S., Sharma, P., Mishra, S., 2011. Impact of increasing mass transit share on energy use and emissions from transport sector for National Capital Territory of Delhi. Transp. Res. Part D Transp. Environ. 16, 65–72. doi:10.1016/j.trd.2010.08.005

Kim, B., Kim, W., Song, B., 2008. Sequencing and scheduling highway network expansion using a discrete network design model. Ann. Reg. Sci.

Kim, B.J., Kim, W., Song, B.H., 2007. Sequencing and scheduling highway network expansion using a discrete network design model. Ann. Reg. Sci. 42, 621–642. doi:10.1007/s00168-007-0170-2

Kitamura, R., Susilo, Y.O., 2005. is travel demand insatiable? a study of changes in structural relationships underlying travel. Transportmetrica 1, 23–45. doi:10.1080/18128600508685640

Kumares C. Sinha, S.L., 2007. Transportation Decision Making: Principles of Project Evaluation and Programming -. John Wiley & Sons.

Leblanc, L.J., 1975. An Algorithm for the Discrete Network Design Problem. Transp. Sci. 9, 183–199.

Lents, J., Nickila, N., Davis, N., Canada, M., Martinez, H., Osses, M., Tolvett, S., 2007. A Study of the Emissions from Diesel Vehicles Operating in Istanbul, Turkey 36.

Li, Z.-C., Lam, W.H.K., Wong, S.C., 2012a. Modeling intermodal equilibrium for bimodal transportation system design problems in a linear monocentric city. Transp. Res. Part B Methodol. 46, 30–49. doi:10.1016/j.trb.2011.08.002

Li, Z.-C., Lam, W.H.K., Wong, S.C., Sumalee, a., 2012b. Environmentally Sustainable Toll Design for Congested Road Networks with Uncertain Demand. Int. J. Sustain. Transp. 6, 127–155. doi:10.1080/15568318.2011.570101

Li, Z.-C., Lam, W.H.K., Wong, S.C., Sumalee, a., 2012c. Environmentally Sustainable Toll Design for Congested Road Networks with Uncertain Demand. Int. J. Sustain. Transp. 6, 127–155. doi:10.1080/15568318.2011.570101

Lin, D.-Y., Xie, C., 2010. The Pareto-optimal Solution Set of the Equilibrium Network Design Problem with Multiple Commensurate Objectives. Networks Spat. Econ. 11, 727–751. doi:10.1007/s11067-010-9146-3

Lin, J.-J., Feng, C.-M., 2003. A bi-level programming model for the land use - network design problem. Ann. Reg. Sci. 37, 93–105. doi:10.1007/s001680200112

Liu, L., Yang, J., Mu, H., Li, X., Wu, F., 2014. Exact algorithms for multi-criteria multi-modal shortest path with transfer delaying and arriving time-window in urban transit network. Appl. Math. Model. 38, 2613–2629. doi:10.1016/j.apm.2013.10.059

Lo, H.K., Szeto, W.Y., 2009. Time-dependent transport network design under cost-recovery. Transp. Res. Part B Methodol. 43, 142–158. doi:10.1016/j.trb.2008.06.005

Long, J., Gao, Z., Zhang, H., Szeto, W.Y., 2010. A turning restriction design problem in urban road networks. Eur. J. Oper. Res. 206, 569–578. doi:10.1016/j.ejor.2010.03.013

Lowty, I.S., 1964. A model of metropolis. Rand Corporation, Santa Monica, CA, USA.

Ma, X., Lo, H.K., 2012. Modeling transport management and land use over time. Transp. Res. Part B Methodol. 46, 687–709. doi:10.1016/j.trb.2012.01.010

Mackett, R., 1983. LEEDS INTEGRATED LAND-USE TRANSPORT MODEL (LILT). TRRL Suppl. Rep. (Transport Road Res. Lab. Gt. Britain).

Marcotte, P., 1986. Network design problem with congestion effects: A case of bilevel programming. Math. Program. 34, 142–162. doi:10.1007/BF01580580

Markel, T., 2010. Plug-in Electric Vehicle Infrastructure : A Foundation for Electrified Transportation Preprint.

Martinez, F., 1992. The bid-choice land-use model: an integrated economic framework. Environ. Plan. A.

Martinez, F., 1996. MUSSA: land use model for Santiago city. Transp. Res. Rec. J. Transp. Res. Board 1552, 126–134.

MDS Transmodal Limited, 2012. Study on Urban Freight Transport.

Melo, P.C., Ramli, A.R., 2014. Estimating fuel demand elasticities to evaluate CO2 emissions: Panel data evidence for the Lisbon Metropolitan Area. Transp. Res. Part A Policy Pract. 67, 30–46. doi:10.1016/j.tra.2014.06.001

Meng, Q., Yang, H., Bell, M.G.H., 2001. An equivalent continuously differentiable model and a locally convergent algorithm for the continuous network design problem. Transp. Res. Part B Methodol. 35, 83–105. doi:10.1016/S0191-2615(00)00016-3

Miandoabchi, E., Daneshzand, F., Szeto, W.Y., Zanjirani Farahani, R., 2013. Multi-objective discrete urban road network design. Comput. Oper. Res. 40, 2429–2449. doi:10.1016/j.cor.2013.03.016

Miandoabchi, E., Farahani, R., 2012. Hybrid evolutionary metaheuristics for concurrent multi-objective design of urban road and public transit networks. Networks Spat. Econ. 12, 441–480.

Miandoabchi, E., Farahani, R., Szeto, W., 2012. Bi-objective bimodal urban road network design using hybrid metaheuristics. Cent. Eur. J. Oper. Res. 20, 583–621.

Miandoabchi, E., Farahani, R.Z., Szeto, W.Y., 2011. Bi-objective bimodal urban road network design using hybrid metaheuristics. Cent. Eur. J. Oper. Res. 20, 583–621. doi:10.1007/s10100-011-0189-4

Miller, E., Kriger, D., Hunt, J., 1998. Integrated urban models for simulation of transit and land-use policies.

Morrow, K., 2008. U . S . Department of Energy Vehicle Technologies Program – Advanced Vehicle Testing Activity Plug-in Hybrid Electric Vehicle Charging Infrastructure Review.

Muneer, T., Celik, a. N., Caliskan, N., 2011. Sustainable transport solution for a medium-sized town in Turkey - A case study. Sustain. Cities Soc. 1, 29–37. doi:10.1016/j.scs.2010.08.004

Murphy, C., 2014. Electric Cars Get a Needed Jolt in China - WSJ [WWW Document]. URL http://online.wsj.com/news/articles/SB10001424052702304071004579406791647975728 (accessed 8.27.14).

Nejadkoorki, F., Nicholson, K., Lake, I., Davies, T., 2008. An approach for modelling CO2 emissions from road traffic in urban areas. Sci. Total Environ. 406, 269–278. doi:10.1016/j.scitotenv.2008.07.055

Newman, P., Kenworthy, J., 1989. Cities and Automobile Dépendance: a sourcebook.

Ng, M., Lo, H.K., 2013. Regional Air Quality Conformity in Transportation Networks with Stochastic Dependencies: A Theoretical Copula-Based Model. Networks Spat. Econ. 13, 373–397. doi:10.1007/s11067-013-9185-7

Paulley, N., Webster, F., 1991. Overview of an international study to compare models and evaluate land- use and transport policies. Transp. Rev.

Peng, B., Du, H., Ma, S., Fan, Y., Broadstock, D.C., 2015. Urban passenger transport energy saving and emission reduction potential: A case study for Tianjin, China. Energy Convers. Manag. doi:10.1016/j.enconman.2015.01.017

Qiu Yuzhuo, Chen Senfa, 2007. Bi-level programming for continuous network design of comprehensive transportation system based on external optimization, in: 2007 IEEE International Conference on Grey Systems and Intelligent Services. IEEE, pp. 1186–1190. doi:10.1109/GSIS.2007.4443459

Rijn, J. van, 2004. Road capacities.

Rodrigue, J., 2004. REGIONS : THE LOGISTICAL INTEGRATION OF 95, 147–161.

Rosenthal, R., 2012. GAMS: A user's guide.

Ryu, B.Y., Jung, H.J., Bae, S.H., Choi, C.U., 2013. Estimation of carbon dioxide emissions per urban center link unit using data collected by the Advanced Traffic Information System in Daejeon, Korea. Atmos. Environ. 81, 433–442. doi:10.1016/j.atmosenv.2013.09.027

Sadeghi-Barzani, P., Rajabi-Ghahnavieh, A., Kazemi-Karegar, H., 2014. Optimal fast charging station placing and sizing. Appl. Energy 125, 289–299. doi:10.1016/j.apenergy.2014.03.077

Shahraki, N., Turkay, M., 2014. Analysis of interaction among land use, transportation network and air pollution using stochastic nonlinear programming. Int. J. Environ. Sci. Technol. doi:10.1007/s13762-014-0566-3

Sharma, S., Mathew, T. V., 2011. Multiobjective network design for emission and travel-time trade-off for a sustainable large urban transportation network. Environ. Plan. B Plan. Des. 38, 520–538. doi:10.1068/b37018

Sheffi, Y., 1985. urban transportation networks: equilibrium analysis with mathematical programming methods. Prentice-Hall, Inc.

Shuwen, Q., 2011. Electric vehicles in Beijing will face more charging stations - People's Daily Online [WWW Document]. URL http://english.peopledaily.com.cn/90001/90776/90882/7419252.html (accessed 8.29.14).

Siemens, 2009. European Green City Index: Assessing the environmental impact of Europe's major cities.

Simmonds, D., Still, B., 1999. DELTA/START: adding land use analysis to integrated transport models. World Transp. Res. Sel. Proc. 8th World Conf. Transp. Res. 4.

Solutions, K.M., Remote, C., Server, O., 2012. Cplex 12.

Sookun, A., Boojhawon, R., Rughooputh, S.D.D. V, 2014. Assessing greenhouse gas and related air pollutant emissions from road traffic counts: A case study for Mauritius. Transp. Res. Part D Transp. Environ. 32, 35–47. doi:10.1016/j.trd.2014.06.005

Southworth, F., 1995. A Technical Review of Urban Land Use--Transportation Models as Tools for Evaluating Vehicle Travel Reduction Strategies.

Soylu, S., 2007. Estimation of Turkish road transport emissions. Energy Policy 35, 4088–4094. doi:10.1016/j.enpol.2007.02.015

State Grid Corporation of China, 2010. Technical specification for electric vehicle charging spot (in Chinese), 2010th ed.

Stubbs, R.A., Mehrotra, S., 1999. A branch-and-cut method for 0-1 mixed convex programming. Math. Program. 86, 515–532. doi:10.1007/s101070050103

Szeto, W., Jaber, X., O'Mahony, M., 2010. Time- Dependent Discrete Network Design Frameworks Considering Land Use. Comput. Civ. ….

Szeto, W.Y., Jaber, X., O'Mahony, M., 2010. Time-dependent discrete network design frameworks considering land use. Comput. Civ. Infrastruct. Eng. 25, 411–426. doi:10.1111/j.1467-8667.2010.00654.x

Szeto, W.Y., Jaber, X., Wong, S.C., 2012. Road Network Equilibrium Approaches to Environmental Sustainability. Transp. Rev. 32, 491–518. doi:10.1080/01441647.2012.690000

Szeto, W.Y., Jiang, Y., Wang, D.Z.W., Sumalee, a., 2013. A Sustainable Road Network Design Problem with Land Use Transportation Interaction over Time. Networks Spat. Econ. doi:10.1007/s11067-013-9191-9

Timmermans, H., 2003. The saga of integrated land use-transport modeling: how many more dreams before we wake up? Keynote Pap. Mov. through nets Phys. Soc. Dimens. Travel. 10th Int. Conf. Travel Behav. Res. Lucerna, www. ivt. baug. ethz. ch/allgemein/pdf/timmermans. pdf.

Tong, S., 2014. Beijing: New Energy Vehicles Have Seperate Quota Starting in Feburary 2014 [WWW Document]. URL http://news.xinhuanet.com/politics/2014-01/29/c_126076733.htm

Tongwane, M., Piketh, S., Stevens, L., Ramotubei, T., 2015. Greenhouse gas emissions from road transport in South Africa and Lesotho between 2000 and 2009. Transp. Res. Part D Transp. Environ. 37, 1–13. doi:10.1016/j.trd.2015.02.017

Torchio, M.F., Santarelli, M.G., 2010. Energy, environmental and economic comparison of different powertrain/fuel options using well-to-wheels assessment, energy and external costs – European market analysis. Energy 35, 4156–4171. doi:10.1016/j.energy.2010.06.037

TurkStat, 2011. Greenhouse Gas Emissions Inventory, 1990-2011 [WWW Document]. URL http://www.turkstat.gov.tr/PreHaberBultenleri.do?id=13482 (accessed 5.12.15).

TurkStat, 2015. Road Motor Vehicles [WWW Document]. URL http://www.turkstat.gov.tr/PreHaberBultenleri.do?id=18763 (accessed 4.8.15).

U.S. Department of Energy, 2008. One Million Electric Vehicles By 2015.

U.S. Dept. of Energy, E.I.A., 2012. Annual Energy Review.

Uchida, K., Sumalee, A., Watling, D., Connors, R., 2006. A Study on Network Design Problems for Multi-modal Networks by Probit-based Stochastic User Equilibrium. Networks Spat. Econ. 7, 213–240. doi:10.1007/s11067-006-9010-7

Ukkusuri, S. V., Mathew, T. V., Waller, S.T., 2007. Robust Transportation Network Design Under Demand Uncertainty. Comput. Civ. Infrastruct. Eng. 22, 6–18. doi:10.1111/j.1467-8667.2006.00465.x

US Environmental Protection Agency (EPA), 2010. Carbon Monoxide Implementation.

USA.gov, 2013. New Plug-in Hybrids [WWW Document]. URL http://www.fueleconomy.gov/feg/phevtech.shtml (accessed 8.28.14).

Waddell, P., Ulfarsson, G., Franklin, J., Lobb, J., 2007. Incorporating land use in metropolitan transportation planning. Transp. Res. Part A Policy Pract. 41, 382–410.

Wegener, M., 1995. Current and future land use models, in: Travel Model Improvement Program Land Use Model Conference. Dallas, Texas.

Wegener, M., 1998. The IRPUD model: overview. Website Inst. Spat. planning, Univ. Dortmund.

Wegener, M., 2004. Overview of land-use transport models, Handbook of transport geography and spatial systems.

Westerlund, T., Pettersson, F., 1995. An extended cutting plane method for solving convex MINLP problems. Comput. Chem. Eng. 19, 131–136. doi:10.1016/0098-1354(95)87027-X

World Bank, 2002. Cities on the move: a World Bank urban transport strategy review. World Bank Publications.

Xi, X., Sioshansi, R., Marano, V., 2013. Simulation–optimization model for location of a public electric vehicle charging infrastructure. Transp. Res. Part D Transp. Environ. 22, 60–69. doi:10.1016/j.trd.2013.02.014

Yang, H., Xu, W., He, B., Meng, Q., 2010. Road pricing for congestion control with unknown demand and cost functions. Transp. Res. Part C Emerg. Technol. 18, 157–175. doi:10.1016/j.trc.2009.05.009

Yim, K.K.W., Wong, S.C., Chen, A., Wong, C.K., Lam, W.H.K., 2011. A reliability-based land use and transportation optimization model. Transp. Res. Part C Emerg. Technol. 19, 351–362. doi:10.1016/j.trc.2010.05.019

Yin, Y., Lawphongpanich, S., 2006a. Internalizing emission externality on road networks. Transp. Res. Part D Transp. Environ. 11, 292–301. doi:10.1016/j.trd.2006.05.003

Yin, Y., Lawphongpanich, S., 2006b. Internalizing emission externality on road networks. Transp. Res. Part D Transp. Environ. 11, 292–301. doi:10.1016/j.trd.2006.05.003

Yin, Y., Lu, H., 1999. Traffic equilibrium problems with environmental concerns. ournal East. Asia Soc. Transp. Stud. 3.6.

Zhong, R., Sumalee, A., Maruyama, T., 2012. Dynamic marginal cost , access control , and pollution charge : a comparison of bottleneck and whole link models 191–221. doi:10.1002/atr

Zhou, S., Yan, X., Wu, C., 2008. Optimization Model for Traffic Signal Control with Environmental Objectives, in: 2008 Fourth International Conference on Natural Computation. IEEE, pp. 530–534. doi:10.1109/ICNC.2008.494

ANNEX

Annex I. Appendixes for Chapter II

Annex II. Appendixes for Chapter III

Annex II. Appendixes for Chapter V

Annex I. Appendixes for Chapter II

The detail results of the sensitivity analysis part are summarized in Table A. 1, Table A. 2, Table A. 3, and Table A. 4. In addition, the efficient frontiers of the solutions of the ten problems listed in Tables 4 and the layout structures of these problems are presented in this Appendix.

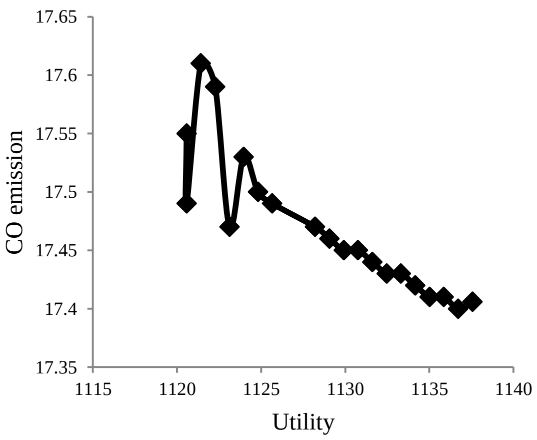

Figure A. 1. Relation between CO emission and utility

Table A. 1. Solutions of the illustrative example by changing the budget value for model I

Allocated budget		300		350		400		450		500	
Emission index		17.440	17.759	17.416	17.656	17.409	17.562	17.406	17.550	17.405	17.493
Reliability index		0.920964	0.99033	0.937099	0.990333	0.944738	0.992002	0.9484843	0.99239362	0.949498	0.992431
Utility value		1134.558	1103.268	1136.564	1113.060	1137.233	1122.479	1137.565	1120.572	1137.701	1123.724
Total travel cost		846.99	878.28	844.99	868.49	844.32	859.07	843.985	860.978	843.85	857.83
Total budget used		300.00	300.00	350.00	350.00	400.00	395.24	450.000	387.069	500.00	442.79
Budget used for network enhancement		50.000	50.000	100.00	100.00	150.00	145.24	200.000	137.069	250.00	192.79
Budget used for land development		250.00	250.00	250.00	250.00	250.00	250.00	250.000	250.000	250.00	250.00
Capacity expansion	1	2.933	11.705	11.265	15.600	15.600	15.600	15.600	15.600	15.600	15.600
	2	0.591	4.600	1.710	4.600	2.331	4.600	4.600	4.600	4.600	4.600
	3	4.600	2.054	4.600	3.255	4.600	4.600	4.600	4.600	4.600	4.600
	4	7.798	0	8.600	5.486	8.600	8.600	8.600	8.600	8.600	8.600
	5	1.337	0	5.868	0	9.062	5.247	15.267	0	18.600	14.458
	6	0.001	0	0.002	2.645	0.001	4.798	0.022	4.827	7.333	0
	7	8.600	2.068	8.600	4.596	8.600	8.600	8.600	8.600	8.600	8.600
Residential development for high income group	1	6.000	1.000	6.000	1.000	6.000	1.000	6.000	1.000	6.000	1.009
	2	0	5.000	0	5.000	0	5.000	0	5.000	0	4.991
Residential development for low income	1	9.000	14.000	9.000	14.000	9.000	14.000	9.000	14.000	9.000	13.991
	2	5.000	0	5.000	0	5.000	0	5.000	0	5.000	0.009

group											
Link flow	1	57.334	38.225	58.309	38.426	58.651	38.426	57.411	38.435	57.072	38.409
	2	7.666	26.775	6.691	26.574	6.349	26.574	7.589	26.565	7.928	26.591
	3	22.095	24.897	21.846	25.300	21.784	22.993	21.724	24.796	21.691	21.402
	4	42.905	40.103	43.154	39.700	43.216	42.007	43.276	40.204	43.309	43.598
	5	50.571	66.877	49.845	66.274	49.565	68.581	50.865	66.769	51.237	70.189
	6	2.666	21.775	1.691	21.574	1.349	21.574	2.589	21.565	2.928	21.591
	7	47.905	45.103	48.154	44.700	48.216	47.007	48.276	45.204	48.309	48.598
O-D mean demand	Zone 1- Zone 3	58.562	58.562	58.562	58.562	58.651	58.562	57.411	58.562	58.562	58.562
	Zone 1- Zone 4	6.438	6.438	6.438	6.438	6.349	6.438	7.589	6.438	6.438	6.438
	Zone 2- Zone 3	1.438	1.438	1.438	1.438	1.349	1.438	2.589	1.438	1.438	1.438
	Zone 2- Zone 4	63.562	63.562	63.562	63.562	63.651	63.562	62.411	63.562	63.562	63.562
Optimal route choice	Zone 1- Zone 3	97.9% from route1 2.1% from route2	65.3% from route1 34.7% from route2	99.6% from route1 0.4% from route2	65.6% from route1 34.4% from route2	100% from route1	65.6% from route1 34.4% from route2	100% from route1	65.6% from route1 34.4% from route2	97.5% from route1 0.25% from	65.6% from route1 34.4% from route2
	Zone 1- Zone 4	100% from route 1	100% from route 1	100% from route 1	100% from route 1	100% from route 1	100% from route 1	100% from route 1	100% from route 1	100% from route 1	100% from route 1
	Zone 2- Zone 3	100% from route 1	100% from route 1	100% from route 1	100% from route 1	100% from route 1	100% from route 1	100% from route 1	100% from route 1	100% from route 1	100% from route 1
	Zone 2- Zone 4	65.2% from route1 34.8% from route2	60.8% from route1 39.2% from route2	65.6% from route1 34.4% from route2	60.2% from route1 39.8% from route2	65.8% from route1 34.2% from route2	63.8% from route1 36.2% from route2	65.2% from route1 34.8% from route2	61% from route1 39% from route2	65.9% from route1 34.1% from route2	66.3% from route1 33.7% from route2

Table A. 2. Solutions of the illustrative example by changing the budget value for model II

Allocated budget		300		350		400		450		500	
Emission index		17.440	17.392	17.416	17.369	17.409	17.365	17.406	17.365	17.405	17.365
Reliability index		0.920964	0.942	0.937099	0.960	0.944738	0.965	0.948	0.965	0.949498	0.992431
Utility value		1134.558	1130.221	1136.564	1132.011	1137.233	1132.422	1137.565	1132.421	1137.701	1132.421
Total travel cost		846.99	851.329	844.99	849.539	844.32	849.128	843.985	849.129	843.85	849.129
Total budget used		300.00	300.00	350.00	350.00	400.00	400.00	450.000	402.268	500.00	402.268
Budget used for network enhancement		50.000	50.000	100.00	100.00	150.00	150.00	200.000	152.268	250.00	152.268
Budget used for land development		250.00	250.00	250.00	250.00	250.00	250.00	250.000	250.000	250.00	250.00
Capacity expansion	1	2.933	2.328	11.265	11.957	15.600	15.600	15.600	15.600	15.600	15.600
	2	0.591	2.553	1.710	4.600	2.331	4.600	4.600	4.600	4.600	4.600
	3	4.600	4.600	4.600	4.600	4.600	4.600	4.600	4.600	4.600	4.600
	4	7.798	7.789	8.600	8.600	8.600	8.600	8.600	8.600	8.600	8.600
	5	1.337	0	5.868	0	9.062	0	15.267	0	18.600	0
	6	0.001	0.044	0.002	0.349	0.001	8.149	0.022	8.600	7.333	8.600
	7	8.600	8.538	8.600	8.600	8.600	8.600	8.600	8.600	8.600	8.600
Residential development for high income group	1	1.000	1.000	6.000	1.000	6.000	1.000	6.000	1.000	6.000	1.009
	2	5.000	5.000	0	5.000	0	5.000	0	5.000	0	4.991
Residential development for low income group	1	14.000	14.000	9.000	14.000	9.000	14.000	9.000	14.000	9.000	13.991
	2	0	0	5.000	0	5.000	0	5.000	0	5.000	0.009
Link flow	1	57.334	51.131	58.309	51.333	58.651	51.692	57.411	51.688	57.072	51.688
	2	7.666	13.869	6.691	13.667	6.349	13.308	7.589	13.312	7.928	13.312
	3	22.095	17.562	21.846	17.402	21.784	17.405	21.724	17.405	21.691	17.405
	4	42.905	47.438	43.154	47.598	43.216	47.595	43.276	47.595	43.309	47.595

	5	50.571	61.307	49.845	61.266	49.565	60.903	50.865	60.907	51.237	60.907
	6	2.666	8.869	1.691	8.667	1.349	8.308	2.589	8.312	2.928	8.312
	7	47.905	52.438	48.154	52.598	48.216	52.595	48.276	52.595	48.309	52.595
O-D mean demand	Zone 1- Zone 3	58.562	58.572	58.562	58.562	58.651	58.562	57.411	58.562	58.562	58.562
	Zone 1- Zone 4	6.438	6.428	6.438	6.438	6.349	6.438	7.589	6.438	6.438	6.438
	Zone 2- Zone 3	1.438	1.428	1.438	1.438	1.349	1.438	2.589	1.438	1.438	1.438
	Zone 2- Zone 4	63.562	63.572	63.562	63.562	63.651	63.562	62.411	63.562	63.562	63.562
Optimal route choice	Zone 1- Zone 3	97.9% from route1 2.1% from route2	87.3% from route1 12.7% from route2	99.6% from route1 0.4% from route2	87.7% from route1 12.3% from route2	100% from route1	88.3% from route1 11.7% from route2	100% from route1	88.3% from route1 11.7% from route2	97.5% from route1 0.25% from	88.3% from route1 11.7% from route2
	Zone 1- Zone 4	100% from route 1	100% from route 1	100% from route 1	100% from route 1	100% from route 1	100% from route 1	100% from route 1	100% from route 1	100% from route 1	100% from route 1
	Zone 2- Zone 3	100% from route 1	100% from route 1	100% from route 1	100% from route 1	100% from route 1	100% from route 1	100% from route 1	100% from route 1	100% from route 1	100% from route 1
	Zone 2- Zone 4	65.2% from route1 34.8% from route2	72.4% from route1 27.6% from route2	65.6% from route1 34.4% from route2	72.6% from route1 27.4% from route2	65.8% from route1 34.2% from route2	72.6% from route1 27.4% from route2	65.2% from route1 34.8% from route2	72.6% from route1 27.4% from route2	65.9% from route1 34.1% from route2	72.6% from route1 27.4% from route2

Table A. 3. Solutions of the illustrative example by changing the zonal existing population for model I

Zonal population		60-50		50-60		55-55		45-65	
Emission index		17.406	17.540	17.406	17.550	17.405	17.523	17.440	17.752
Reliability index		0.94848	0.992406	0.9484843	0.99239362	0.949498	0.992406	0.920964	0.990121
Utility value		1137.565	1124.221	1137.565	1120.572	1137.701	1123.996	1134.558	1103.843
Total travel cost		843.985	857.329	843.985	860.978	843.849	857.554	846.992	877.707
Total budget used		450.000	448.924	450.000	387.069	450.000	396.347	450.000	450.000
Budget used for network enhancement		200.000	198.924	200.000	137.069	200.000	196.347	50.000	50.000
Budget used for land development		250.000	250.000	250.000	250.000	250.000	200.000	400.000	400.000
Capacity expansion	1	15.600	15.600	15.600	15.600	15.600	15.600	2.933	11.675
	2	4.600	4.600	4.600	4.600	4.600	4.600	0.591	4.600
	3	4.600	4.600	4.600	4.600	4.600	4.600	4.600	2.136
	4	8.600	8.600	8.600	8.600	8.600	8.600	7.798	0
	5	15.267	14.347	15.267	0	18.600	14.458	1.337	0
	6	0.022	4.863	0.022	4.827	7.333	3.443	0.001	0
	7	8.600	8.600	8.600	8.600	8.600	8.600	8.600	2.151
Residential development for high income group	1	0	1.053	6.000	1.000	6.000	1.009	6.000	6.000
	2	6.000	4.947	0	5.000	0	4.991	0	0
Residential development for low income group	1	5.000	3.947	9.000	14.000	4.000	8.991	14.000	14.000
	2	9.000	10.053	5.000	0	10.000	5.009	0	0
Link flow	1	57.411	38.426	57.411	38.435	57.072	38.426	57.334	38.334
	2	7.589	26.574	7.589	26.565	7.928	26.574	7.666	26.666
	3	21.724	22.101	21.724	24.796	21.691	23.294	22.095	24.906
	4	43.276	42.899	43.276	40.204	43.309	41.706	42.905	40.094
	5	50.865	69.472	50.865	66.769	51.237	68.280	50.571	66.760
	6	2.589	21.574	2.589	21.565	2.928	21.574	2.666	21.666
	7	48.276	47.899	48.276	45.204	48.309	46.706	47.905	45.094

O-D mean demand	Zone 1-Zone 3	58.565	58.564	57.411	58.562	58.568	59.459	60.000	58.562
	Zone 1-Zone 4	6.435	6.436	7.589	6.438	6.432	5.541	5.000	6.438
	Zone 2-Zone 3	1.435	1.436	2.589	1.438	1.432	0.541	0	1.438
	Zone 2-Zone 4	63.565	63.564	62.411	63.562	63.568	64.459	65.000	63.562
Optimal route choice	Zone 1-Zone 3	98% from route1 2% from route2	65.6% from route1 34.4% from route2	100% from route1	65.6% from route1 34.4% from route2	97.4% from route1 26% from route2	64.6% from route1 35.4% from route2	95.6% from route1 4.4% from route2	65.5% from route1 34.5% from route2
	Zone 1-Zone 4	100% from route 1	100% from route 1	100% from route 1	100% from route 1	100% from route 1	100% from route 1	100% from route 1	100% from route 1
	Zone 2-Zone 3	100% from route 1	100% from route 1	100% from route 1	100% from route 1	100% from route 1	100% from route 1	100% from route 1	100% from route 1
	Zone 2-Zone 4	65.8% from route1 34.2% from route2	65.2% from route1 34.8% from route2	65.2% from route1 34.8% from route2	61% from route1 39% from route2	65.9% from route1 34.1% from route2	63.9% from route1 36.1% from route2	66% from route1 34% from route2	60.8% from route1 39.2% from route2

Table A. 4. Solutions of the illustrative example by changing the zonal existing population for model II

Zonal population		60-50		50-60		55-55		45-65	
Emission index		17.406	17.365	17.406	17.365	17.405	17.365	17.440	17.392
Reliability index		0.94848	0.965	0.948	0.965	0.949498	0.965	0.920964	0.942
Utility value		1137.565	1132.421	1137.565	1132.421	1137.701	1132.421	1134.558	1130.221
Total travel cost		843.985	849.129	843.985	849.129	843.849	849.129	846.992	851.329
Total budget used		450.000	402.268	450.000	402.268	450.000	352.268	450.000	450.000
Budget used for network enhancement		200.000	152.268	200.000	152.268	200.000	152.268	50.000	50.000
Budget used for land development		250.000	250.000	250.000	250.000	250.000	200.000	400.000	400.000
Capacity expansion	1	15.600	15.600	15.600	15.600	15.600	15.600	2.933	2.328
	2	4.600	4.600	4.600	4.600	4.600	4.600	0.591	2.553
	3	4.600	4.600	4.600	4.600	4.600	4.600	4.600	4.600
	4	8.600	8.600	8.600	8.600	8.600	8.600	7.798	7.789
	5	15.267	0	0	0	18.600	0	1.337	0
	6	0.022	8.600	8.600	4.827	7.333	8.600	0.001	0.044
	7	8.600	8.600	8.600	8.600	8.600	8.600	8.600	8.538
Residential development for high income group	1	0	1.056	6.000	1.000	6.000	1.009	6.000	6.000
	2	6.000	4.944	0	5.000	0	4.991	0	0
Residential	1	5.000	3.944	9.000	14.000	4.000	8.991	14.000	14.000

development for low income group	2	9.000	10.056	5.000	0	10.000	5.009	0	0
Link flow	1	57.411	51.688	58.651	51.692	57.072	51.688	57.334	51.131
	2	7.589	13.312	6.349	13.308	7.928	13.312	7.666	13.869
	3	21.724	17.405	21.784	17.405	21.691	17.405	22.095	17.562
	4	43.276	47.595	43.216	47.595	43.309	47.595	42.905	47.438
	5	50.865	60.907	49.565	60.903	51.237	60.907	50.571	61.307
	6	2.589	8.312	1.349	8.308	2.928	8.312	2.666	8.869
	7	48.276	52.595	48.216	52.595	48.309	52.595	47.905	52.438
O-D mean demand	Zone 1-Zone 3	58.565	58.562	57.411	58.562	58.568	59.222	60.000	58.562
	Zone 1-Zone 4	6.435	6.438	7.589	6.438	6.432	5.778	5.000	6.438
	Zone 2-Zone 3	1.435	1.438	2.589	1.438	1.432	0.778	0	1.438
	Zone 2-Zone 4	63.565	63.562	62.411	63.562	63.568	64.222	65.000	63.562
Optimal route choice	Zone 1-Zone 3	98% from route1 2% from route2	88.3% from route1 11.7% from route2	100% from route1	88.3% from route1 11.7% from route2	97.4% from route1 26% from route2	87.3% from route1 12.7% from route2	95.6% from route1 4.4% from route2	87.3% from route1 12.7% from route2
	Zone 1-Zone 4	100% from route 1	100% from route 1	100% from route 1	100% from route 1	100% from route 1	100% from route 1	100% from route 1	100% from route 1
	Zone 2-Zone 3	100% from route 1	100% from route 1	100% from route 1	100% from route 1	100% from route 1	100% from route 1	100% from route 1	100% from route 1
	Zone 2-Zone 4	65.8% from route1 34.2% from route2	72.6% from route1 27.4% from route2	65.2% from route1 34.8% from route2	72.6% from route1 27.4% from route2	65.9% from route1 34.1% from route2	72.9% from route1 27.1% from route2	66% from route1 34% from route2	72.4% from route1 27.6% from route2

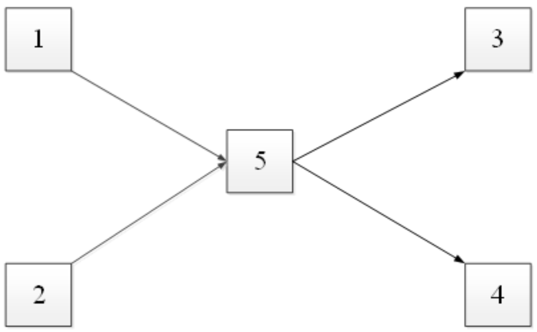

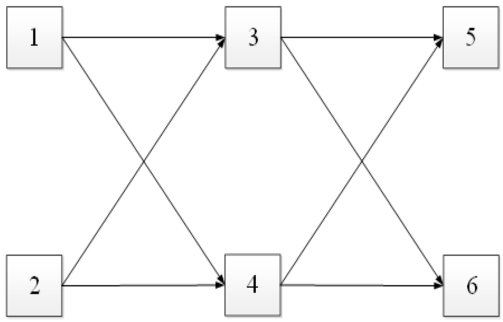

(a) (b)

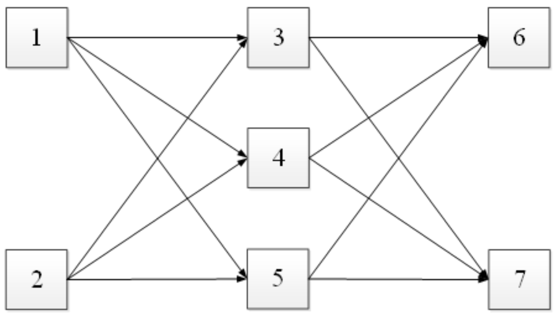

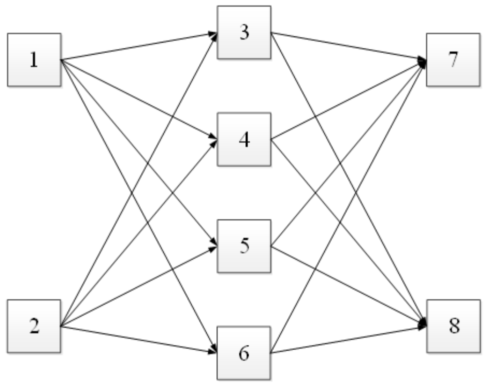

(c) (d)

Figure A. 2. The layout structures of problem (a) “2,2,3,1”, (b) “2,2,3,2”,(c) “2,2,3,3” and (d) “2,2,3,4”

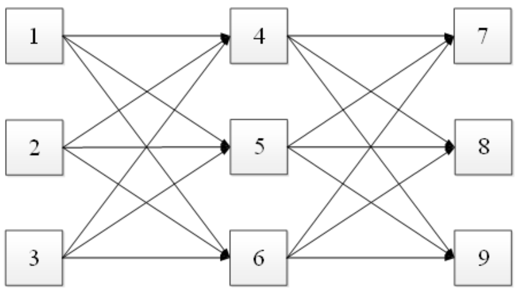

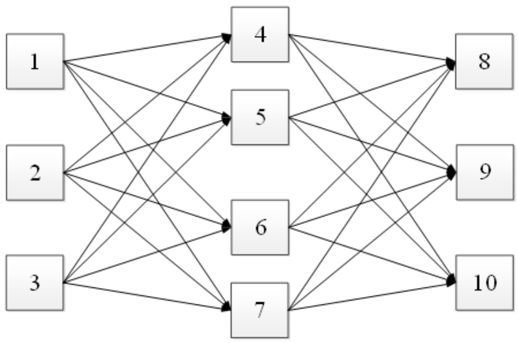

(a) (b)

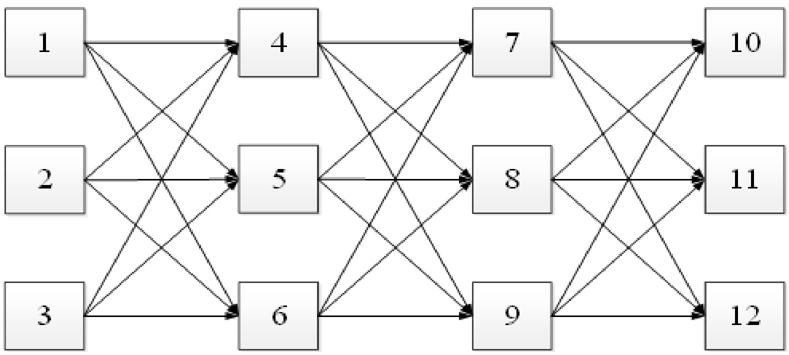

(c)

Figure A. 3. The layout structures of problem (a) “3,3,3,3”, (b) “3,3,3,4” and (c) “3,3,4,3”

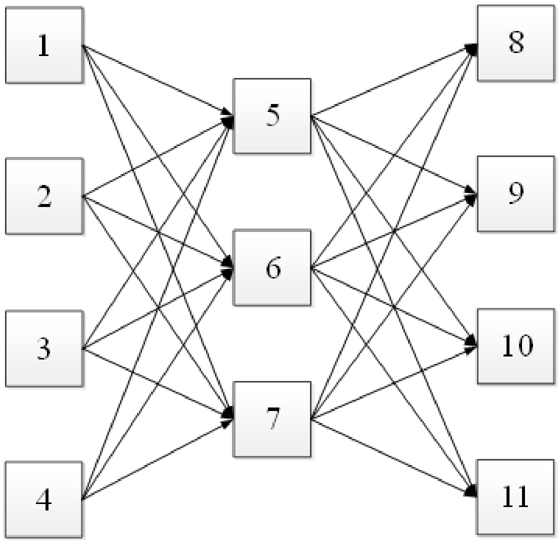

(a)

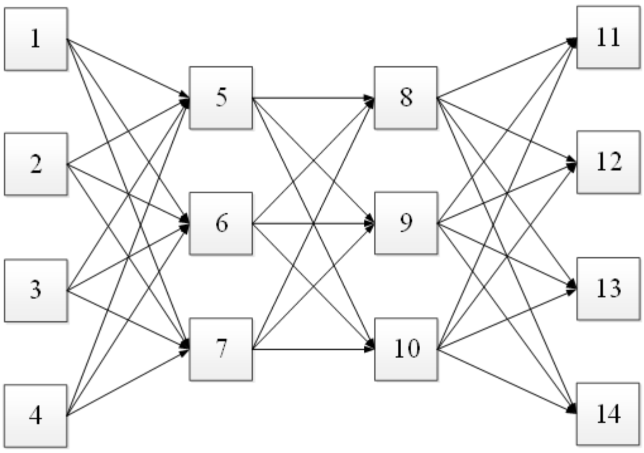

(b)

Figure A. 4. The layout structures of problem (a)“4,4,3,3”and (b) “4,4,4,3”

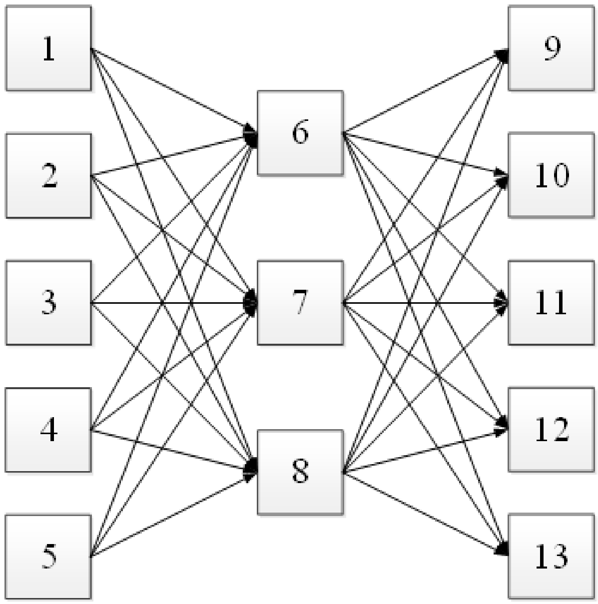

Figure A. 5. The layout structure of problem "5,5,3,3"

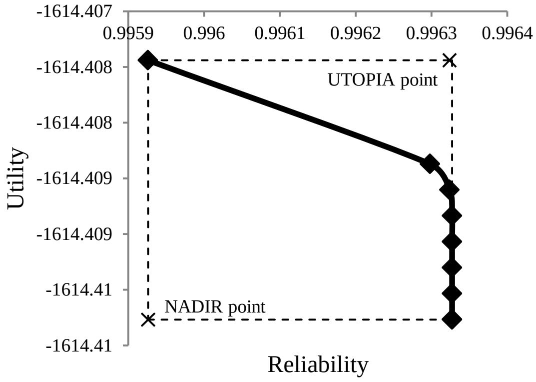

(a)

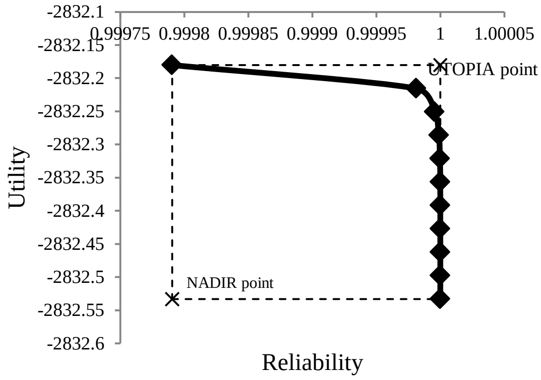

(b)

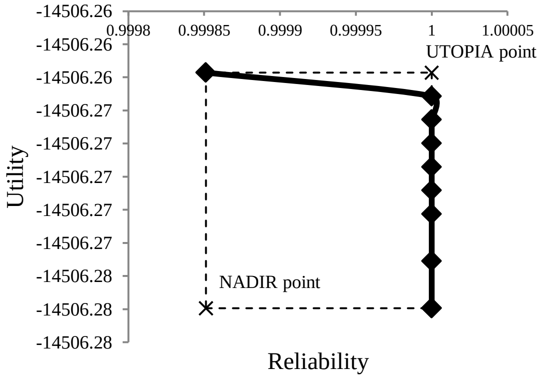

(c)

Figure A. 6. The efficient frontiers of problem (a) “3,3,3,3”, (b) “3,3,3,4” and (c) “3,3,4,3” for model I

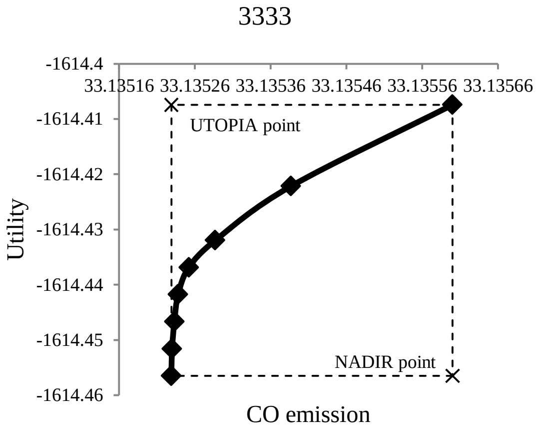

(a)

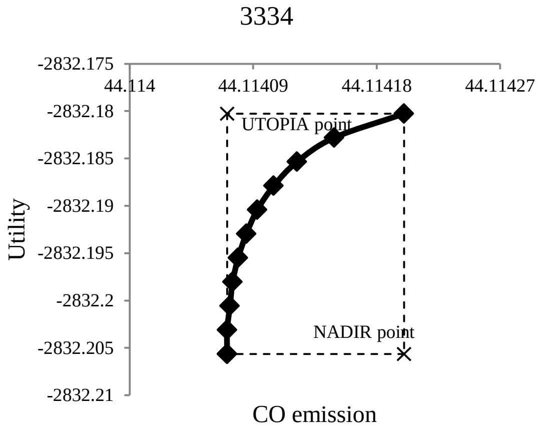

(b)

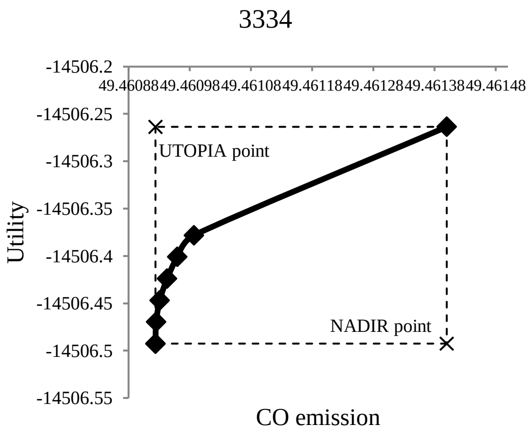

(c)

Figure A. 7. The efficient frontiers of problem (a) “3,3,3,3”, (b) “3,3,3,4” and (c) “3,3,4,3” for model II

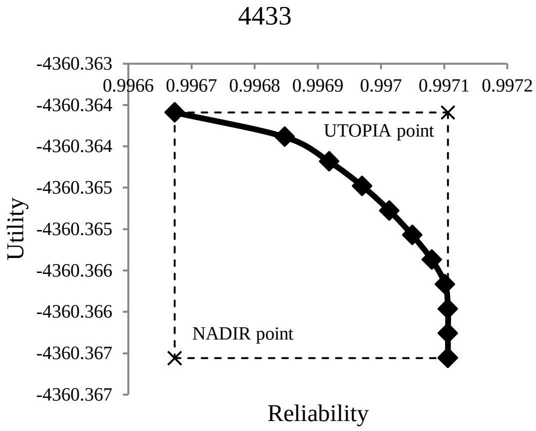

(a)

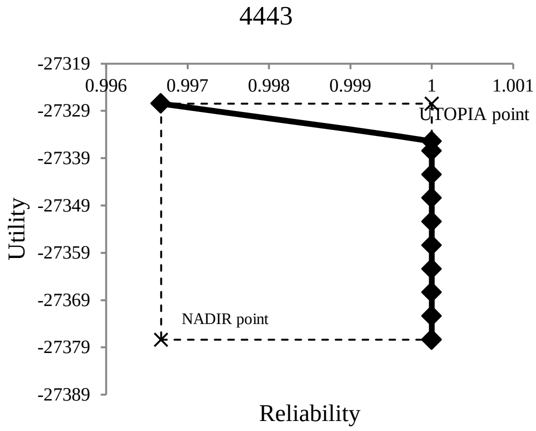

(b)

Figure A. 8. The efficient frontiers of problem (a) “4,4,3,3” and (b) “4,4,4,3” for model I

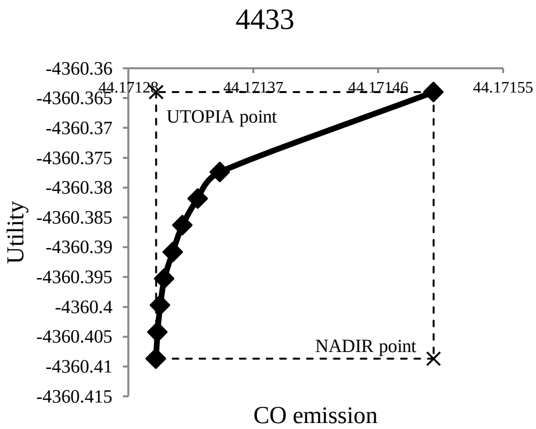

(a)

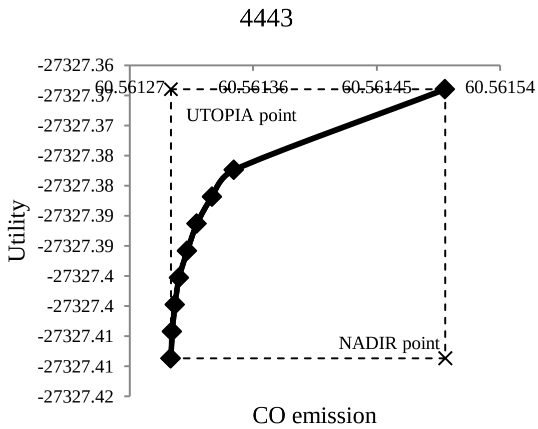

(b)

Figure A. 9. The efficient frontiers of problem (a) “4,4,3,3” and (b) “4,4,4,3” for model II

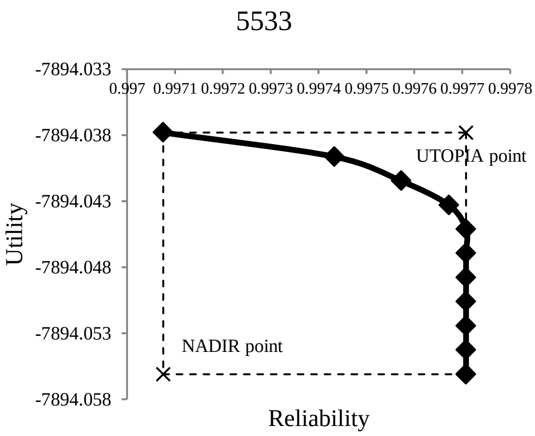

Figure A. 10. The efficient frontiers of problem “5,5,3,3” for model I

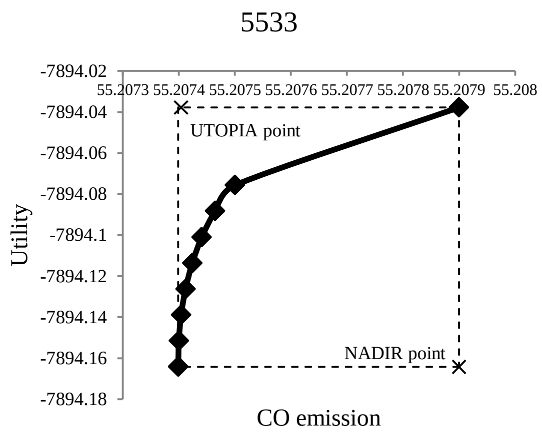

Figure A. 11. The efficient frontiers of problem “5,5,3,3” for model II

Annex II. Appendixes for Chapter III

Appendix A

1. *Lemma 1*. The objective function of lower level problem is convex.

Let's assume H_{AA}, H_{BB} and H_{CC} be the hessian matrix of *AA*, *BB* and *CC* in Eqs. (3-66), (3-67) and (3-68) respectively. Since $\bar{x}_a^{auto}$, σ_a^{auto}, ω, θ and π are positive, $PP = XHX^T$ is greater or equal to zero for the three hessian matrices as shown in Eq. A.1, A.2 and A.3. So we can conclude convexity.

$$PP_{AA} = \left(\frac{\bar{x}_a^{auto}}{\pi}\right)\left(12\left(\frac{\bar{x}_a^{auto}}{\pi}\right)\left(\left(\frac{\bar{x}_a^{auto}}{\pi}\right) + \left(\omega\frac{\bar{x}_a^{bus}}{\theta}\right)\right)^2 + 12\left(\omega\frac{\bar{x}_a^{bus}}{\theta}\right)\left(\left(\frac{\bar{x}_a^{auto}}{\pi}\right) + \left(\omega\frac{\bar{x}_a^{bus}}{\theta}\right)\right)^2\right) + \left(\omega\frac{\bar{x}_a^{bus}}{\theta}\right)\left(12\left(\frac{\bar{x}_a^{auto}}{\pi}\right)\left(\left(\frac{\bar{x}_a^{auto}}{\pi}\right) + \left(\omega\frac{\bar{x}_a^{bus}}{\theta}\right)\right)^2 + 12\left(\omega\frac{\bar{x}_a^{bus}}{\theta}\right)\left(\left(\frac{\bar{x}_a^{auto}}{\pi}\right) + \left(\omega\frac{\bar{x}_a^{bus}}{\theta}\right)\right)^2\right) \tag{A.1}$$

$$PP_{BB} = \left(\frac{\sigma_a^{auto}}{\pi^2}\right)\left(\left(\frac{\bar{x}_a^{auto}}{\pi}\right)\left(12\left(\frac{\bar{x}_a^{auto}}{\pi}\right) + 12\left(\omega\frac{\bar{x}_a^{bus}}{\theta}\right)\right) + \left(\omega\frac{\bar{x}_a^{bus}}{\theta}\right)\left(12\left(\frac{\bar{x}_a^{auto}}{\pi}\right) + 12\left(\omega\frac{\bar{x}_a^{bus}}{\theta}\right)\right)\right) + \left(\omega^2\frac{\sigma_a^{bus}}{\theta^2}\right)\left(\left(\frac{\bar{x}_a^{auto}}{\pi}\right)\left(12\left(\frac{\bar{x}_a^{auto}}{\pi}\right) + 12\left(\omega\frac{\bar{x}_a^{bus}}{\theta}\right)\right) + \left(\omega\frac{\bar{x}_a^{bus}}{\theta}\right)\left(12\left(\frac{\bar{x}_a^{auto}}{\pi}\right) + 12\left(\omega\frac{\bar{x}_a^{bus}}{\theta}\right)\right)\right) + \left(\frac{\bar{x}_a^{auto}}{\pi}\right)\left(\left(\frac{\bar{x}_a^{auto}}{\pi}\right)\left(12\left(\frac{\sigma_a^{auto}}{\pi^2}\right) + 12\left(\omega^2\frac{\sigma_a^{bus}}{\theta^2}\right)\right) + \left(\omega\frac{\bar{x}_a^{bus}}{\theta}\right)\left(12\left(\frac{\sigma_a^{auto}}{\pi^2}\right) + 12\left(\omega^2\frac{\sigma_a^{bus}}{\theta^2}\right)\right) + \left(\frac{\sigma_a^{auto}}{\pi^2}\right)\left(12\left(\frac{\bar{x}_a^{auto}}{\pi}\right) + 12\left(\omega\frac{\bar{x}_a^{bus}}{\theta}\right)\right) + \left(\omega^2\frac{\sigma_a^{bus}}{\theta^2}\right)\left(12\left(\frac{\bar{x}_a^{auto}}{\pi}\right) + 12\left(\omega\frac{\bar{x}_a^{bus}}{\theta}\right)\right)\right) + \left(\omega\frac{\bar{x}_a^{bus}}{\theta}\right)\left(\left(\frac{\bar{x}_a^{auto}}{\pi}\right)\left(12\left(\frac{\sigma_a^{auto}}{\pi^2}\right) + 12\left(\omega^2\frac{\sigma_a^{bus}}{\theta^2}\right)\right) + \left(\omega\frac{\bar{x}_a^{bus}}{\theta}\right)\left(12\left(\frac{\sigma_a^{auto}}{\pi^2}\right) + 12\left(\omega^2\frac{\sigma_a^{bus}}{\theta^2}\right)\right) + \left(\frac{\sigma_a^{auto}}{\pi^2}\right)\left(12\left(\frac{\bar{x}_a^{auto}}{\pi}\right) + 12\left(\omega\frac{\bar{x}_a^{bus}}{\theta}\right)\right) + \left(\omega^2\frac{\sigma_a^{bus}}{\theta^2}\right)\left(12\left(\frac{\bar{x}_a^{auto}}{\pi}\right) + 12\left(\omega\frac{\bar{x}_a^{bus}}{\theta}\right)\right)\right) \tag{A.2}$$

$$PP_{CC} = 6\left(\frac{\sigma_a^{auto}}{\pi^2}\right)\left(\left(\frac{\sigma_a^{auto}}{\pi^2}\right) + \left(\omega^2 \frac{\sigma_a^{bus}}{\theta^2}\right)\right) + 6\left(\omega^2 \frac{\sigma_a^{bus}}{\theta^2}\right)\left(\left(\frac{\sigma_a^{auto}}{\pi^2}\right) + \left(\omega^2 \frac{\sigma_a^{bus}}{\theta^2}\right)\right) \quad \text{(A.3)}$$

2. McCormick Envelopes for bilinear terms

We use McCormick Envelopes to estimate the nonlinear term in the lower level problem by linear terms to make the feasible region convex (McCormick 1976). McCormick (1976) uses Eqs. (A.4)-(A.10) to relax the bilinear term "xy".

$w = xy$ (A.4)

$x^L \leq x \leq x^U$ (A.5)

$y^L \leq y \leq y^U$ (A.6)

$w \geq x^L y + y^L x - x^L y^L$ (A.7)

$w \geq x^U y + y^U x - x^U y^U$ (A.8)

$w \leq x^U y + y^L x - x^U y^L$ (A.9)

$w \leq x^L y + y^U x - x^L y^U$ (A.10)

3. ϵ-Constraint Outer Approximation Algorithm

In general, NLP sub problem can be shown by Eq. (A.11) - (A.15).

$$\min\ z = \acute{f}(x) + f(x) \quad \text{(A.11)}$$

subject to

$$g(x) \leq 0 \quad \text{(A.12)}$$
$$h(x) = 0 \quad \text{(A.13)}$$
$$k_i(x) \leq 0, \qquad if\ y_i = 1 \quad \text{(A.14)}$$
$$x \in \mathbb{R}^n \quad \text{(A.15)}$$

where $f(x)$ is the non-linear term of the objective function and $g(x)$, $h(x)$ and $k_i(x)$ are also non-linear functions.

The solution of NLP sub problem (x^{opt}) is the input of MILP formulation shown in Eq. (A.16) - (A.21).

$$\min\ z = \acute{f}(x) + \alpha \quad \text{(A.16)}$$

subject to

$$f(x^{opt}) + \nabla f(x^{opt})(x - x^{opt}) \leq \alpha \quad \text{(A.17)}$$
$$g(x^{opt}) + \nabla g(x^{opt})(x - x^{opt}) \leq 0 \quad \text{(A.18)}$$
$$T^{opt}\ h(x^{opt}) + \nabla h(x^{opt})(x - x^{opt}) \leq 0 \quad \text{(A.19)}$$
$$\nabla k_i(x^{opt})^T x \leq (-k_i(x^{opt}) + \nabla k_i(x^{opt})^T x^{opt}) y_i \quad \text{(A.20)}$$
$$x \in \mathbb{R}^n, y \in \{0,1\} \quad \text{(A.21)}$$

where T^{opt} is the sign of Lagrange multiplier of equality constraints in Eq. (A.19).

Appendix B

The layout structures of the ten benchmark problems listed in Table 10 are shown in Figure B. 1., Figure B. 2., Figure B. 3., and **Error! Reference source not found.**

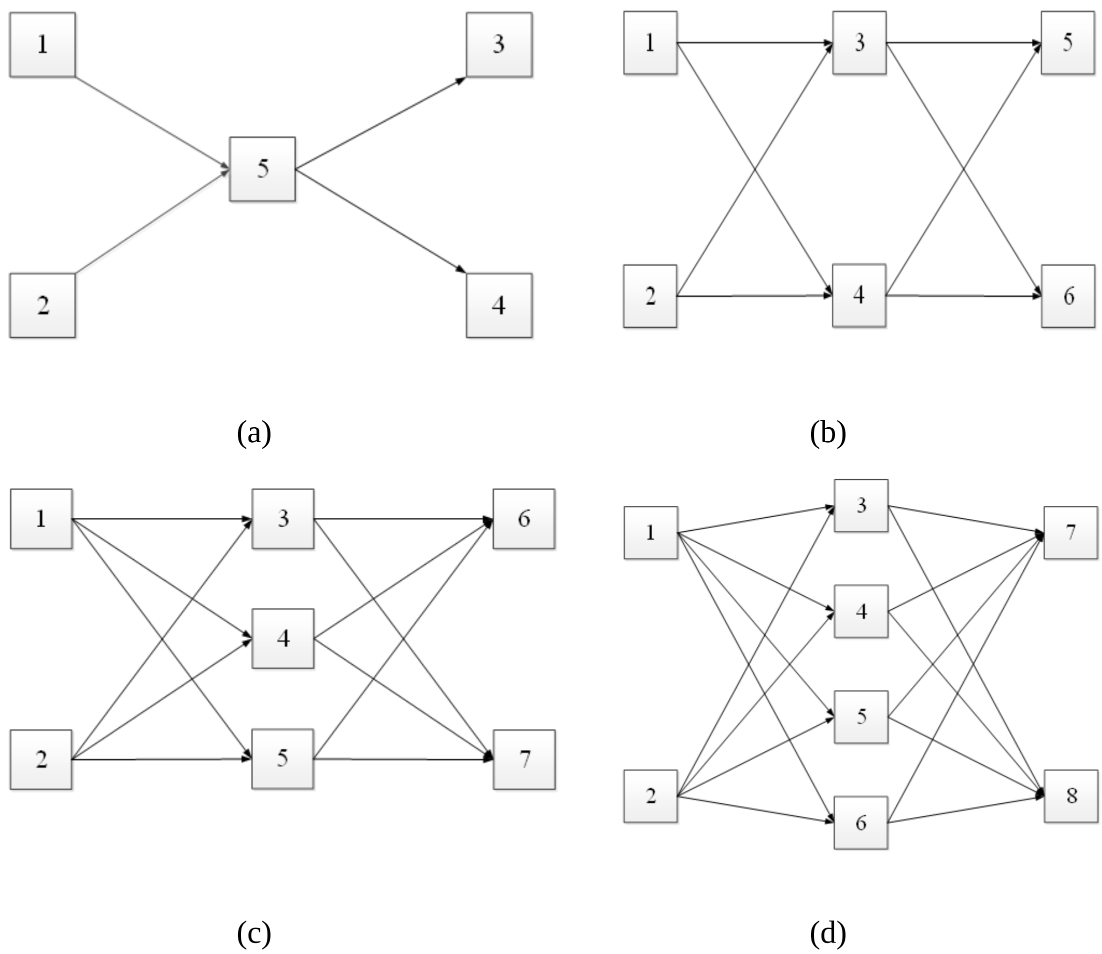

Figure B. 1. The layout structures of problem (a) “2,2,3,1”, (b) “2,2,3,2”,(c) “2,2,3,3” and (d) “2,2,3,4”

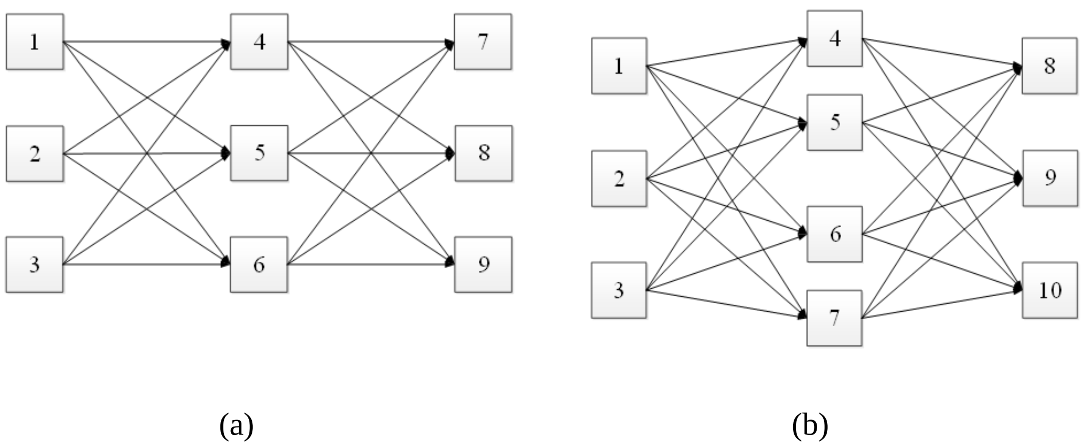

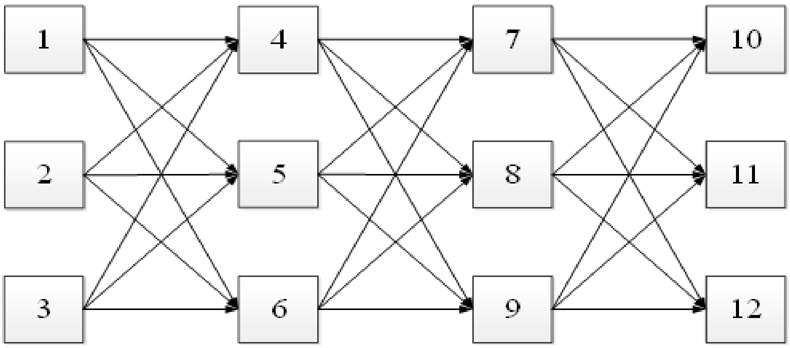

(c)

Figure B. 2. The layout structures of problem (a) “3,3,3,3”, (b) “3,3,3,4” and (c) “3,3,4,3”

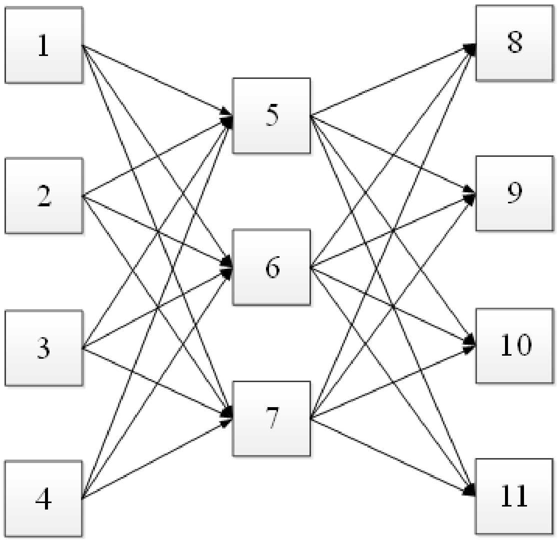

(a)

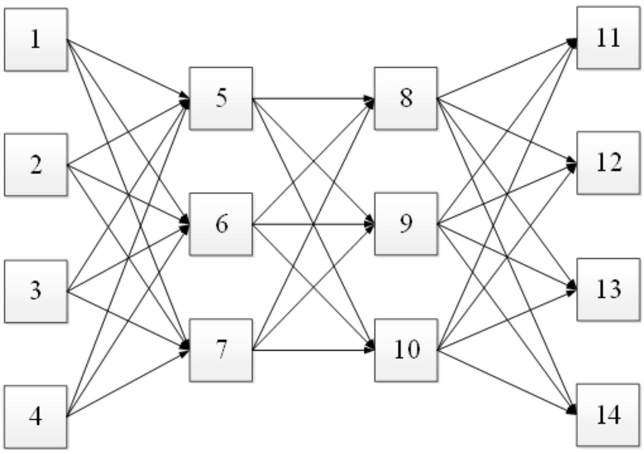

(b)

Figure B. 3. The layout structures of problem (a) “4,4,3,3” and (b) “4,4,4,3”

Appendix C

Non-linear terms and closed form expressions of the derivatives of the integrated model are listed in Table C. 1.

Table C. 1. Closed form expression of the derivatives

Non-linear term	Derivative respect to	Derivative
$t_a^{car} = \check{t}_0^a \left(\frac{0.15({\bar{x}_a}^4+6\sigma_a{\bar{x}_a}^2+3\sigma_a^2)}{(Ca_a+e_a)^4}\right)$	$\bar{x}_a$ σ_a e_a	$\check{t}_0^a \left(\frac{0.15(4{\bar{x}_a}^3+12\sigma_a\bar{x}_a)}{(Ca_a+e_a)^4}\right) \quad \forall a \in A$ $\check{t}_0^a \left(\frac{0.15(6{\bar{x}_a}^2+6\sigma_a)}{(Ca_a+e_a)^4}\right) \quad \forall a \in A$ $\check{t}_0^a \left(\frac{-4({\bar{x}_a}^4+6\sigma_a{\bar{x}_a}^2+3\sigma_a^2)}{(Ca_a+e_a)^5}\right) \quad \forall a \in A$
$t_a^{bus} = y_a^{bus} \left(\hat{t}_0^a \left(1 + \frac{0.15({\bar{x}_a}^4+6\sigma_a{\bar{x}_a}^2+3\sigma_a^2)}{(Ca_a+e_a)^4}\right)\right)$	$\bar{x}_a$ σ_a e_a	$\hat{t}_0^a \left(\frac{0.15(4{\bar{x}_a}^3+12\sigma_a\bar{x}_a)y_a^{bus}}{(Ca_a+e_a)^4}\right) \quad \forall a \in A$ $\hat{t}_0^a \left(\frac{0.15(6{\bar{x}_a}^2+6\sigma_a)y_a^{bus}}{(Ca_a+e_a)^4}\right) \quad \forall a \in A$ $\hat{t}_0^a \left(\frac{-4({\bar{x}_a}^4+6\sigma_a{\bar{x}_a}^2+3\sigma_a^2)y_a^{bus}}{(Ca_a+e_a)^5}\right) \quad \forall a \in A$
$\sum_{a\in A}\sum_{m\in M} 0.2038 t_a^m \exp(0.7962(l_a/t_a^m))$	t_a^m	$0.2038 \exp(0.7962(l_a/t_a^m)) -$ $\frac{0.16226556 l_a \exp(0.7962(l_a/t_a^m))}{t_a^m} \quad \forall m \in M, \forall a \in A$
$\mu_a^1 (\bar{x}_a^{rail} - f_{max}^{rail}\, y_a^{rail}) = 0 \;\; \forall a \in A$	$\bar{x}_a^{rail}$ μ_a^1	$\mu_a^1 \;\; \forall a \in A$ $\bar{x}_a^{rail} - f_{max}^{rail}\, y_a^{rail} \;\; \forall a \in A$
$\mu_a^2(\sigma_a^{rail} - M\, y_a^{rail}) = 0 \;\; \forall a \in A$	σ_a^{rail} μ_a^2	$\mu_a^2 \;\; \forall a \in A$ $\sigma_a^{rail} - M\, y_a^{rail} \quad \forall a \in A$
$\mu_a^3 (\bar{x}_a^{bus} - f_{max}^{bus}\, y_a^{bus}) = 0 \;\; \forall a \in A$	$\bar{x}_a^{bus}$ μ_a^3	$\mu_a^3 \;\; \forall a \in A$ $\bar{x}_a^{bus} - f_{max}^{bus}\, y_a^{bus} \quad \forall a \in A$
$\mu_a^4 (\sigma_a^{bus} - M\, y_a^{bus}) = 0 \;\; \forall a \in A$	σ_a^{bus} μ_a^4	$\mu_a^4 \;\; \forall a \in A$ $\sigma_a^{bus} - M\, y_a^{bus} \quad \forall a \in A$
$\mu_{pqr\acute{r}}^5 (\gamma_{pqr} + \gamma_{pq\acute{r}} - 1 - \Lambda_{pqr\acute{r}}) = 0 \quad \forall p \in P, \forall q \in Q, \forall r \in R_{pq}, \forall \acute{r} \in \acute{R}_{pq}$	$\mu_{pqr\acute{r}}^5$ γ_{pqr} $\Lambda_{pqr\acute{r}}$	$\gamma_{pqr} + \gamma_{pq\acute{r}} - 1 - \Lambda_{pqr\acute{r}} \quad \forall p \in P, \forall q \in Q, \forall r \in R_{pq}, \forall \acute{r} \in \acute{R}_{pq}$ $\mu_{pqr\acute{r}}^5 \quad \forall p \in P, \forall q \in Q, \forall r \in R_{pq}, \forall \acute{r} \in \acute{R}_{pq}$ $-\mu_{pqr\acute{r}}^5 \quad \forall p \in P, \forall q \in Q, \forall r \in R_{pq}, \forall \acute{r} \in \acute{R}_{pq}$
$\mu_{pqr\acute{r}}^6 (\Lambda_{pqr\acute{r}} - \gamma_{pqr}) = 0 \quad \forall p \in P, \forall q \in Q, \forall r \in R_{pq}, \forall \acute{r} \in \acute{R}_{pq}$	$\mu_{pqr\acute{r}}^6$ $\Lambda_{pqr\acute{r}}$ γ_{pqr}	$\Lambda_{pqr\acute{r}} - \gamma_{pqr} \quad \forall p \in P, \forall q \in Q, \forall r \in R_{pq}, \forall \acute{r} \in \acute{R}_{pq}$ $\mu_{pqr\acute{r}}^6 \quad \forall p \in P, \forall q \in Q, \forall r \in R_{pq}, \forall \acute{r} \in \acute{R}_{pq}$ $-\mu_{pqr\acute{r}}^6 \quad \forall p \in P, \forall q \in Q, \forall r \in R_{pq}, \forall \acute{r} \in \acute{R}_{pq}$
$\mu_{pqr\acute{r}}^7 (\Lambda_{pqr\acute{r}} - \gamma_{pq\acute{r}}) = 0 \quad \forall p \in P, \forall q \in Q, \forall r \in R_{pq}, \forall \acute{r} \in \acute{R}_{pq}$	$\mu_{pqr\acute{r}}^7$ $\Lambda_{pqr\acute{r}}$ $\gamma_{pq\acute{r}}$	$\Lambda_{pqr\acute{r}} - \gamma_{pq\acute{r}} \quad \forall p \in P, \forall q \in Q, \forall r \in R_{pq}, \forall \acute{r} \in \acute{R}_{pq}$ $\mu_{pqr\acute{r}}^7 \quad \forall p \in P, \forall q \in Q, \forall r \in R_{pq}, \forall \acute{r} \in \acute{R}_{pq}$ $-\mu_{pqr\acute{r}}^7 \quad \forall p \in P, \forall q \in Q, \forall r \in R_{pq}, \forall \acute{r} \in \acute{R}_{pq}$
$\mu_{a\,m}^8 (\sigma_a^m - \bar{x}_a^m) = 0 \quad \forall a \in A, \forall m \in M$	$\mu_{a\,m}^8$ σ_a^m $\bar{x}_a^m$	$\sigma_a^m - \bar{x}_a^m \quad \forall a \in A, \forall m \in M$ $\mu_{a\,m}^8 \;\; \forall a \in A, \forall m \in M$ $-\mu_{a\,m}^8 \;\; \forall a \in A, \forall m \in M$
$\lambda_a^4 +$ $\sum_{p\in P}\sum_{q\in Q}\sum_{r\in R}\left(\left(\sum_{k\in K} vot^k \left(\frac{0.15\check{t}_a^0(4\bar{x}_a^3+12\bar{x}_a\sigma_a^2)}{(Ca_a+e_a)^4}\right)\delta_{pqra}\right) +\right.$	$\bar{x}_a$	$\sum_{p\in P}\sum_{q\in Q}\sum_{r\in R}\left(\left(\sum_{k\in K} vot^k \left(\frac{0.15\check{t}_a^0(12\bar{x}_a^2+12\sigma_a)}{(Ca_a+e_a)^4}\right)\delta_{pqra}\right) +\right.$ $\left.\left(\sum_{k\in K} vot^k \left(\frac{0.15\hat{t}_a^0(12\bar{x}_a^2+12\sigma_a)y_a^{bus}}{(Ca_a+e_a)^4}\right)\delta_{pqra}\right)\right) \quad \forall a \in A$

$\left(\sum_{k\in K} vot^k\left(\frac{0.15\hat{t}_a^0(4\bar{x}_a^3+12\bar{x}_a\sigma_a)y_a^{bus}}{(Ca_a+e_a)^4}\right)\delta_{pqra}\right)\Big) = 0,\ \forall a \in A$		
	σ_a	$\sum_{p\in P}\sum_{q\in Q}\sum_{r\in R}\Bigg(\left(\sum_{k\in K} vot^k\left(\frac{0.15*12\ \check{t}_a^0\,\bar{x}_a}{(Ca_a+e_a)^4}\right)\delta_{pqra}\right)+ \left(\sum_{k\in K} vot^k\left(\frac{0.15*12\ \check{t}_a^0\,\bar{x}_a\ y_a^{bus}}{(Ca_a+e_a)^4}\right)\delta_{pqra}\right)\Bigg)\quad \forall a \in A$
	e_a	$\sum_{p\in P}\sum_{q\in Q}\sum_{r\in R}\Bigg(\left(\sum_{k\in K} vot^k\left(\frac{-0.15*4\ \check{t}_a^0(4\bar{x}_a^3+12\bar{x}_a\sigma_a)}{(Ca_a+e_a)^5}\right)\delta_{pqra}\right)+ \left(\sum_{k\in K} vot^k\left(\frac{-0.15*4\ \hat{t}_a^0(4\bar{x}_a^3+12\bar{x}_a\sigma_a)y_a^{bus}}{(Ca_a+e_a)^5}\right)\delta_{pqra}\right)\Bigg)\quad \forall a \in A$
	λ_a^4	$1\ \ ,\forall a \in A$
	$\bar{x}_a$	$\sum_{p\in P}\sum_{q\in Q}\sum_{r\in R}\Bigg(\left(\sum_{k\in K} vot^k\left(\frac{0.15*12\ \check{t}_a^0(\bar{x}_a)}{(Ca_a+e_a)^4}\right)\delta_{pqra}\right)+ \left(\sum_{k\in K} vot^k\left(\frac{0.15*12\ \hat{t}_a^0(\bar{x}_a)y_a^{bus}}{(Ca_a+e_a)^4}\right)\delta_{pqra}\right)\Bigg)\quad \forall a \in A$
$\lambda_a^5 + \sum_{p\in P}\sum_{q\in Q}\sum_{r\in R}\Bigg(\left(\sum_{k\in K} vot^k\left(\frac{0.15\check{t}_a^0(6\bar{x}_a^2+6\sigma_a)}{(Ca_a+e_a)^4}\right)\delta_{pqra}\right)+ \left(\sum_{k\in K} vot^k\left(\frac{0.15\hat{t}_a^0(6\bar{x}_a^2+6\sigma_a)y_a^{bus}}{(Ca_a+e_a)^4}\right)\delta_{pqra}\right)\Bigg) = 0,\ \forall a \in A$	σ_a	$\sum_{p\in P}\sum_{q\in Q}\sum_{r\in R}\Bigg(\left(\sum_{k\in K} vot^k\left(\frac{0.15*6\ \check{t}_a^0}{(Ca_a+e_a)^4}\right)\delta_{pqra}\right)+ \left(\sum_{k\in K} vot^k\left(\frac{0.15*6\ \check{t}_a^0\ y_a^{bus}}{(Ca_a+e_a)^4}\right)\delta_{pqra}\right)\Bigg)\quad \forall a \in A$
	y_a	$\sum_{p\in P}\sum_{q\in Q}\sum_{r\in R}\Bigg(\left(\sum_{k\in K} vot^k\left(\frac{-0.15*4\ \check{t}_a^0(6\bar{x}_a^2+6\sigma_a^2)}{(Ca_a+y_a)^5}\right)\delta_{pqra}\right)+ \left(\sum_{k\in K} vot^k\left(\frac{-0.15*4\ \hat{t}_a^0(6\bar{x}_a^2+6\sigma_a^2)y_a^{bus}}{(Ca_a+e_a)^5}\right)\delta_{pqra}\right)\Bigg)\quad \forall a \in A$
	λ_a^5	$1\ \ ,\forall a \in A$
$sq_{a,a} - r_{a,a} + \sum_{i<a} c_{a,i}c_{a,i} = 0\ \ \forall a \in A$ *	$r_{a,a}$	-1
	$c_{a,i}$	$2 * c_{a,i}\ \ \forall a < i, \forall a \in A$
	$sq_{a,a}$	1
$c_{a,a} - \sqrt{sq_{a,a}} = 0\ \forall a \in A$	$c_{a,a}$	1
	$sq_{a,a}$	$\frac{-0.5}{\sqrt{sq_{a,a}}}\ \forall a \in A$
$c_{a,i} - \left(\frac{1}{c_{i,i}} * \left(r_{a,i} - \sum_{j<i} c_{a,j}\ c_{i,j}\right)\right) = 0\ \forall a \in A, \forall i < a$	$r_{a,i}$	$\frac{-1}{c_{i,i}}\ \ \forall a \in A, \forall i < a$
	$c_{i,i}$	$\frac{(r_{a,i} - \sum_{j<i} c_{a,j}\ c_{i,j})}{c_{i,i}{}^2}\ \forall a \in A, \forall i < a$
	$c_{a,j}$	$\frac{c_{i,j}}{c_{i,i}}\ \ \forall a \in A, \forall i < a$
	$c_{i,j}$	$\frac{c_{a,j}}{c_{i,i}}\ \ \forall a \in A, \forall i < a$
	$c_{a,i}$	1
$errorf\left(\frac{al_1}{c_{1,1}}\right) - d_{1,ii} = 0\ \ \forall ii$	al_1	$\frac{2exp(-al_1{}^2)}{c_{1,1}{}^2}/\left(\sqrt{\pi}\ c_{1,1}\ \right)\ \ \forall ii$
	$c_{1,1}$	$\frac{-2\ al_1 exp(-al_1{}^2)}{c_{1,1}{}^2}/\left(\sqrt{\pi}\ c_{1,1}{}^2\ \right)\ \ \forall ii$
	$d_{1,ii}$	-1
$errorf\left(\frac{bl_1}{c_{1,1}}\right) - e_{1,ii} = 0\ \ \forall ii$	bl_1	$\frac{2exp(-bl_1{}^2)}{c_{1,1}{}^2}/\left(\sqrt{\pi}\ c_{1,1}\ \right)\ \ \forall ii$
	$c_{1,1}$	$\frac{-2\ al_1 exp(-bl_1{}^2)}{c_{1,1}{}^2}/\left(\sqrt{\pi}\ c_{1,1}{}^2\ \right)\ \ \forall ii$
	$e_{1,ii}$	-1
$d_{a-1,ii} + ss_{ii}\left(e_{a-1,ii} - d_{a-1,ii}\right) - errorf\left(y_{a-1,ii}\right) = 0\ \ \forall a > 1, \forall ii$	$d_{a-1,ii}$	$1 -\ ss_{ii}$
	$e_{a-1,ii}$	ss_{ii}

	$y_{a-1,ii}$	$\frac{-2exp\left(-y_{a-1,ii}{}^{2}\right)}{\sqrt{\pi}}\ \ \forall a>1,\forall ii$
$errorf\left(\frac{al_a-\sum_{j<a}c_{a,j}\,y_{j,ii}}{c_{a,a}}\right)-d_{a,ii}=0\ \ \forall a>1,\forall ii$	al_a	$\frac{-2exp\left(-\left(al_a-\sum_{j<a}c_{a,j}\,y_{j,ii}\right)^2\right)}{c_{a,a}{}^2}/\left(\sqrt{\pi}\,c_{a,a}\right)\ \ \forall a>1,\forall ii$
	$c_{a,j}$	$\frac{-2\ exp\left(-\left(al_a-\sum_{j<a}c_{a,j}\,y_{j,ii}\right)^2\right)\left(\sum_{j<a}\ c_{a,j}\right)}{c_{a,a}{}^2}/\left(\sqrt{\pi}\,c_{a,a}\right)\ \ \forall a>1,\forall ii$
	$y_{j,ii}$	$\frac{-2\ exp\left(-\left(al_a-\sum_{j<a}c_{a,j}\,y_{j,ii}\right)^2\right)\left(\sum_{j<a}\ y_{j,ii}\right)}{c_{a,a}{}^2}/\left(\sqrt{\pi}\,c_{a,a}\right)\ \ \forall a>1,\forall ii$
	$c_{a,a}$	$\frac{-2exp\left(-\left(al_a-\sum_{j<a}c_{a,j}\,y_{j,ii}\right)^2\right)\left(al_a-\sum_{j<a}c_{a,j}\,y_{j,ii}\right)}{c_{a,a}{}^2}/\left(\sqrt{\pi}\,c_{a,a}\right)\ \ \forall a>1,\forall ii$
	$d_{a,ii}$	$-1\ \forall a>1,\forall ii$

* $r_{i,j}$ and $c_{i,j}$ are elements of matrix of covariance of flow between links and elements of Cholesky factorization matrix respectively. The further equations are nonlinear terms for formulating multivariate normal distribution, for more detail you can refer to Shahraki and Türkay, (2014).

Annex III. Appendixes for Chapter V

1. Calculation of electrification rate

In order to have a unique measure to compare the results of the three weeks, $\Omega^{le}{}_{w}$ is defined in Eq. (A.4). $\Omega^{le}{}_{w}$ calculates the percentage amount of mileage traveled by electricity power in week w, by considering power level type le.

$$\Omega_{w}^{le} = \frac{T_w - obj^{*}{}_{w}^{le}}{T_w} \qquad \forall w \in \{1,2,3\}, \forall le \in \{7.04, 37.5\} \qquad \text{(A.4)}$$

where, T_w calculate the total traveled distances in week w as shown in Eq. (A.5) and $obj^{*le}{}_{w}$ is the best value for the objective function of week w in Eq. (A.6).

$$T_w = \sum_{k \in K} \sum_{j \in J} t_{jk} \qquad \forall w \in \{1,2,3\} \qquad \text{(A.5)}$$

$$obj^{*}{}_{w} = \sum_{k \in K} \sum_{j \in J} \left(\hat{R}^{*}{}_{jk} - R^{*}{}_{jk} \right) \quad \forall w \in \{1,2,3\}, \forall le \in \{7.04, 37.5\} \qquad \text{(A.6)}$$

2. Model statistic

On average it takes 5 hours to run the model to find 40 optimal locations with 100 GB of physical memory. The values of the following Cplex options are changed to improve computational efficiency: reinv, varsel, cuts, nodesel, nodefileind, workmem, memoryemphasis, names, threads, and lpmethod. Justifying these options carefully can have dramatic effects on improving the computing speed and reducing memory usage. We can categorize the contribution of these option adjustments into two groups: speeding up the computation by reducing the number of computational operations and by managing capacity for working files. The reinv, varsel, cuts, nodesel, and lpmethod options can be considered in the first category. And, the nodefileind, workmem, memoryemphasis, names and threads options are in the second one.

The varsel and nodesel options define variable selection strategy at each node and the node selection strategy, respectively. For the varsel option, “strong branching” and for the nodesel option, “best-estimate search” or “depth-first search” are recommended for utilizing less memory for large scale problems. The lpmethod option determines the algorithm to be used for LP problems. Based on the structure of the problem (e.g. the number of equations and variables), a specific method can be chosen to reduce the computational operations. The reinv option can be adjusted to change the number of iterations between refactorizations of the basis matrix. For conserving memory we can increase the refactorization frequency through the reinv option. Using the cuts option, we can turn off the generation of the optional cuts (Solutions et al 2012).

The nodefileind option allows the possibility of changing the location and compressing the working files. Using the workmem option, we can increase the upper limit of memory for storing the working files. Adjusting the memoryemphasis option helps to conserve memory where possible. Using the names option, we can prevent loading

GAMS names into Cplex to reduce memory usage. And the threads option can be adjusted to set the number of cores which can be used parallel (Solutions et al 2012).

3. Locations of selected stations in 40-station scenario

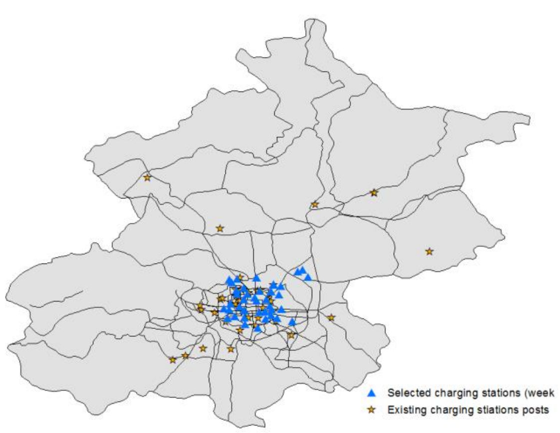

a)

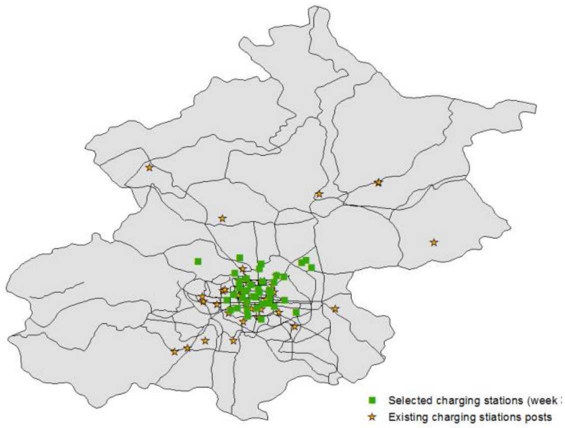

b)

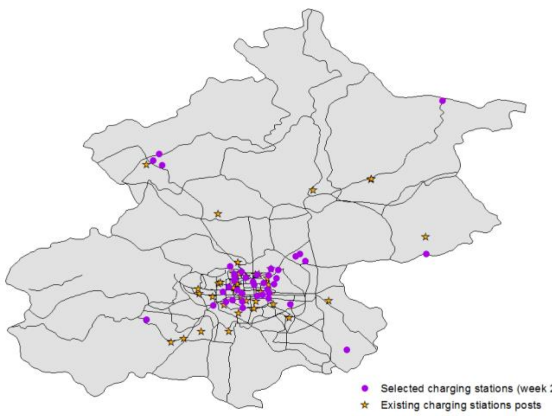

c)

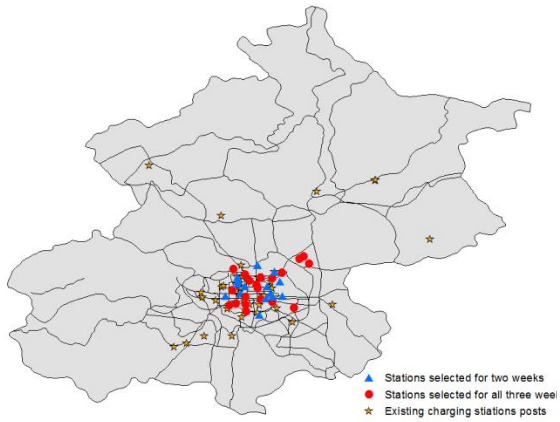

d)

Figure A. 12. Locations of the optimized charging stations in the 40-station scenario using a) data from week 1; b) data from week 2, and c) data from week 3. Charging stations selected as the optimal choices in two or three weeks are highlighted in d) with blue and red color, respectively.

a) b) c) d)

Figure A. 13. Locations of optimized stations in scenarios with different total number of charging stations zoomed into the inner city of Beijing: a) 60 stations, b) 100 stations, c) 200 stations, and d) 500 stations.